10

Stress analysis of aircraft components

In Chapter 9 we established the basic theory for the analysis of open and closed section thin-walled beams subjected to bending, shear and torsional loads. In addition, methods of idealizing stringer stiffened sections into sections more amenable to analysis were presented. We now extend the analysis to actual aircraft components including tapered beams, fuselages, wings, frames and ribs; also included are the effects of cut-outs in wings and fuselages. Finally, an introduction is given to the analysis of components fabricated from composite materials.

Aircraft structural components are, as we saw in Chapter 7, complex, consisting usually of thin sheets of metal stiffened by arrangements of stringers. These structures are highly redundant and require some degree of simplification or idealization before they can be analysed. The analysis presented here is therefore approximate and the degree of accuracy obtained depends on the number of simplifying assumptions made. A further complication arises in that factors such as warping restraint, structural and loading discontinuities and shear lag significantly affect the analysis; we shall investigate these effects in some simple structural components in Chapter 11. Generally, a high degree of accuracy can only be obtained by using computer-based techniques such as the finite element method (see Chapter 12). However, the simpler, quicker and cheaper approximate methods can be used to advantage in the preliminary stages of design when several possible structural alternatives are being investigated; they also provide an insight into the physical behaviour of structures which computer-based techniques do not.

10.1 Tapered beams

Major aircraft structural components such as wings and fuselages are usually tapered along their lengths for greater structural efficiency. Thus, wing sections are reduced both chordwise and in depth along the wing span towards the tip and fuselage sections aft of the passenger cabin taper to provide a more efficient aerodynamic and structural shape.

The analysis of open and closed section beams presented in Chapter 9 assumes that the beam sections are uniform. The effect of taper on the prediction of direct stresses produced by bending is minimal if the taper is small and the section properties are

calculated at the particular section being considered; Eqs (9.6)–(9.10) may therefore be used with reasonable accuracy. On the other hand, the calculation of shear stresses in beam webs can be significantly affected by taper.

10.1.1 Single web beam

Consider first the simple case of a beam positioned in the yz plane and comprising two flanges and a web; an elemental length δz of the beam is shown in Fig. 10.1. At the section z the beam is subjected to a positive bending moment M_x and a positive shear force S_y. The bending moment resultants $P_{z,1}$ and $P_{z,2}$ are parallel to the z axis of the beam. For a beam in which the flanges are assumed to resist all the direct stresses, $P_{z,1} = M_x/h$ and $P_{z,2} = -M_x/h$. In the case where the web is assumed to be fully effective in resisting direct stress, $P_{z,1}$ and $P_{z,2}$ are determined by multiplying the direct stresses $\sigma_{z,1}$ and $\sigma_{z,2}$ found using Eq. (9.6) or Eq. (9.7) by the flange areas B_1 and B_2. $P_{z,1}$ and $P_{z,2}$ are the components in the z direction of the axial loads P_1 and P_2 in the flanges. These have components $P_{y,1}$ and $P_{y,2}$ parallel to the y axis given by

$$P_{y,1} = P_{z,1}\frac{\delta y_1}{\delta z}, \quad P_{y,2} = -P_{z,2}\frac{\delta y_2}{\delta z} \tag{10.1}$$

in which, for the direction of taper shown, δy_2 is negative. The axial load in flange ① is given by

$$P_1 = (P_{z,1}^2 + P_{y,1}^2)^{1/2}$$

Substituting for $P_{y,1}$ from Eqs (10.1) we have

$$P_1 = P_{z,1}\frac{(\delta z^2 + \delta y_1^2)^{1/2}}{\delta z} = \frac{P_{z,1}}{\cos\alpha_1} \tag{10.2}$$

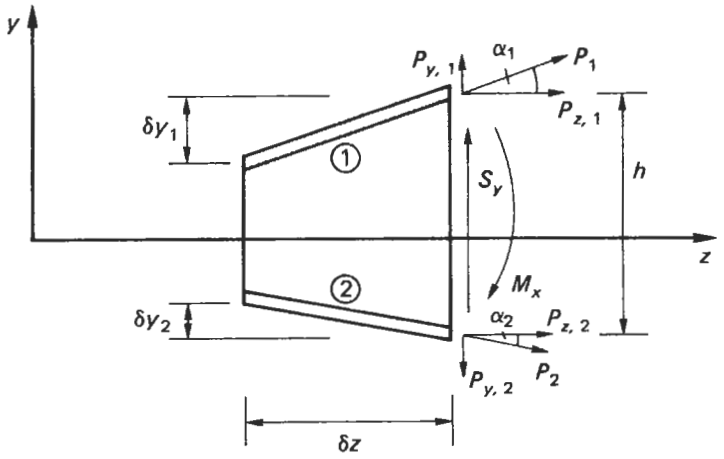

Fig. 10.1 Effect of taper on beam analysis.

Similarly

$$P_2 = \frac{P_{z,2}}{\cos \alpha_2} \tag{10.3}$$

The internal shear force S_y comprises the resultant $S_{y,w}$ of the web shear flows together with the vertical components of P_1 and P_2. Thus

$$S_y = S_{y,w} + P_{y,1} - P_{y,2}$$

or

$$S_y = S_{y,w} + P_{z,1}\frac{\delta y_1}{\delta z} + P_{z,2}\frac{\delta y_2}{\delta z} \tag{10.4}$$

so that

$$S_{y,w} = S_y - P_{z,1}\frac{\delta y_1}{\delta z} - P_{z,2}\frac{\delta y_2}{\delta z} \tag{10.5}$$

Again we note that δy_2 in Eqs (10.4) and (10.5) is negative. Equation (10.5) may be used to determine the shear flow distribution in the web. For a completely idealized beam the web shear flow is constant through the depth and is given by $S_{y,w}/h$. For a beam in which the web is fully effective in resisting direct stresses the web shear flow distribution is found using Eq. (9.75) in which S_y is replaced by $S_{y,w}$ and which, for the beam of Fig. 10.1, would simplify to

$$q_s = -\frac{S_{y,w}}{I_{xx}}\left(\int_0^s t_D y \, ds + B_1 y_1\right) \tag{10.6}$$

or

$$q_s = -\frac{S_{y,w}}{I_{xx}}\left(\int_0^s t_D y \, ds + B_2 y_2\right) \tag{10.7}$$

Example 10.1

Determine the shear flow distribution in the web of the tapered beam shown in Fig. 10.2, at a section midway along its length. The web of the beam has a thickness of

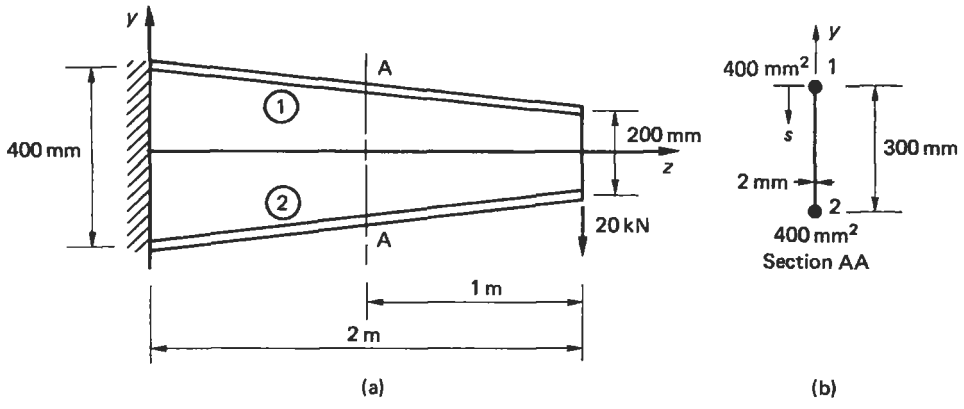

Fig. 10.2 Tapered beam of Example 10.1.

2 mm and is fully effective in resisting direct stress. The beam tapers symmetrically about its horizontal centroidal axis and the cross-sectional area of each flange is $400\,\text{mm}^2$.

The internal bending moment and shear load at the section AA produced by the externally applied load are, respectively

$$M_x = 20 \times 1 = 20\,\text{kN m}, \quad S_y = -20\,\text{kN}$$

The direct stresses parallel to the z axis in the flanges at this section are obtained either from Eq. (9.6) or Eq. (9.7) in which $M_y = 0$ and $I_{xy} = 0$. Thus, from Eq. (9.6)

$$\sigma_z = \frac{M_x y}{I_{xx}} \tag{i}$$

in which

$$I_{xx} = 2 \times 400 \times 150^2 + 2 \times 300^3/12$$

i.e.

$$I_{xx} = 22.5 \times 10^6\,\text{mm}^4$$

Hence

$$\sigma_{z,1} = -\sigma_{z,2} = \frac{20 \times 10^6 \times 150}{22.5 \times 10^6} = 133.3\,\text{N/mm}^2$$

The components parallel to the z axis of the axial loads in the flanges are therefore

$$P_{z,1} = -P_{z,2} = 133.3 \times 400 = 53\,320\,\text{N}$$

The shear load resisted by the beam web is then, from Eq. (10.5)

$$S_{y,w} = -20 \times 10^3 - 53\,320\frac{\delta y_1}{\delta z} + 53\,320\frac{\delta y_2}{\delta z}$$

in which, from Figs 10.1 and 10.2, we see that

$$\frac{\delta y_1}{\delta z} = \frac{-100}{2 \times 10^3} = -0.05, \quad \frac{\delta y_2}{\delta z} = \frac{100}{2 \times 10^3} = 0.05$$

Hence

$$S_{y,w} = -20 \times 10^3 + 53\,320 \times 0.05 + 53\,320 \times 0.05 = -14\,668\,\text{N}$$

The shear flow distribution in the web follows either from Eq. (10.6) or Eq. (10.7) and is (see Fig. 10.2(b))

$$q_{12} = \frac{14\,668}{22.5 \times 10^6}\left(\int_0^s 2(150 - s)\,\text{d}s + 400 \times 150\right)$$

i.e.

$$q_{12} = 6.52 \times 10^{-4}(-s^2 + 300s + 60\,000) \tag{ii}$$

The maximum value of q_{12} occurs when $s = 150\,\text{mm}$ and $q_{12}\,(\text{max}) = 53.8\,\text{N/mm}$. The values of shear flow at points 1 ($s = 0$) and 2 ($s = 300\,\text{mm}$) are $q_1 = 39.1\,\text{N/mm}$ and $q_2 = 39.1\,\text{N/mm}$; the complete distribution is shown in Fig. 10.3.

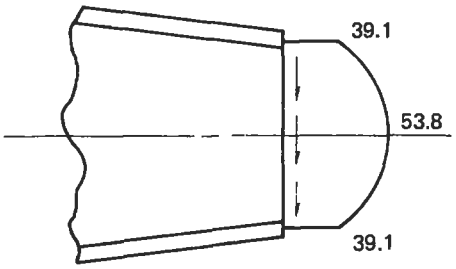

Fig. 10.3 Shear flow (N/mm) distribution at Section AA in Example 10.1.

10.1.2 Open and closed section beams

We shall now consider the more general case of a beam tapered in two directions along its length and comprising an arrangement of booms and skin. Practical examples of such a beam are complete wings and fuselages. The beam may be of open or closed section; the effects of taper are determined in an identical manner in either case.

Figure 10.4(a) shows a short length δz of a beam carrying shear loads S_x and S_y at the section z; S_x and S_y are positive when acting in the directions shown. Note that if the beam were of open cross-section the shear loads would be applied through its shear centre so that no twisting of the beam occurred. In addition to shear loads the beam is subjected to bending moments M_x and M_y which produce direct stresses σ_z in the booms and skin. Suppose that in the rth boom the direct stress in a direction parallel to the z axis is $\sigma_{z,r}$, which may be found using either Eq. (9.6) or Eq. (9.7). The component $P_{z,r}$ of the axial load P_r in the rth boom is then given by

$$P_{z,r} = \sigma_{z,r} B_r \tag{10.8}$$

where B_r is the cross-sectional area of the rth boom.

From Fig. 10.4(b)

$$P_{y,r} = P_{z,r} \frac{\delta y_r}{\delta z} \tag{10.9}$$

Further, from Fig. 10.4(c)

$$P_{x,r} = P_{y,r} \frac{\delta x_r}{\delta y_r}$$

or, substituting for $P_{y,r}$ from Eq. (10.9)

$$P_{x,r} = P_{z,r} \frac{\delta x_r}{\delta z} \tag{10.10}$$

The axial load P_r is then given by

$$P_r = (P_{x,r}^2 + P_{y,r}^2 + P_{z,r}^2)^{1/2} \tag{10.11}$$

or, alternatively

$$P_r = P_{z,r} \frac{(\delta x_r^2 + \delta y_r^2 + \delta z^2)^{1/2}}{\delta z} \tag{10.12}$$

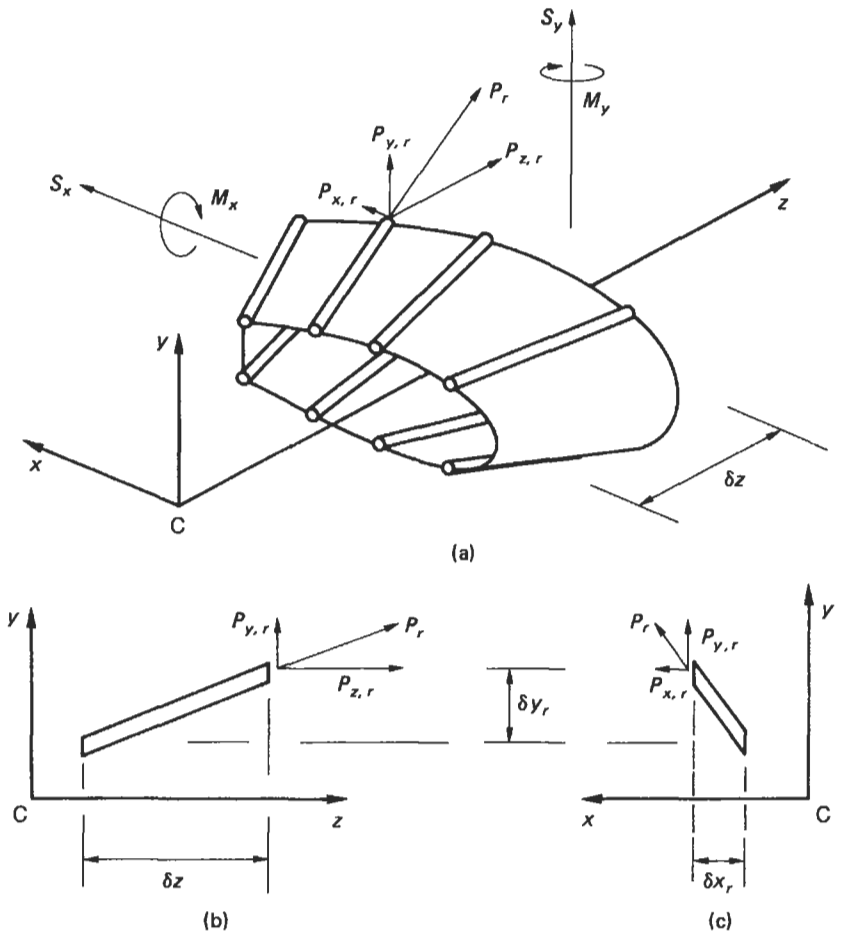

Fig. 10.4 Effect of taper on the analysis of open and closed section beams.

The applied shear loads S_x and S_y are reacted by the resultants of the shear flows in the skin panels and webs, together with the components $P_{x,r}$ and $P_{y,r}$ of the axial loads in the booms. Therefore, if $S_{x,w}$ and $S_{y,w}$ are the resultants of the skin and web shear flows and there is a total of m booms in the section

$$S_x = S_{x,w} + \sum_{r=1}^{m} P_{x,r}, \quad S_y = S_{y,w} + \sum_{r=1}^{m} P_{y,r} \tag{10.13}$$

Substituting in Eqs (10.13) for $P_{x,r}$ and $P_{y,r}$ from Eqs (10.10) and (10.9) we have

$$S_x = S_{x,w} + \sum_{r=1}^{m} P_{z,r}\frac{\delta x_r}{\delta z}, \quad S_y = S_{y,w} + \sum_{r=1}^{m} P_{z,r}\frac{\delta y_r}{\delta z} \tag{10.14}$$

Hence

$$S_{x,w} = S_x - \sum_{r=1}^{m} P_{z,r}\frac{\delta x_r}{\delta z}, \quad S_{y,w} = S_y - \sum_{r=1}^{m} P_{z,r}\frac{\delta y_r}{\delta z} \tag{10.15}$$

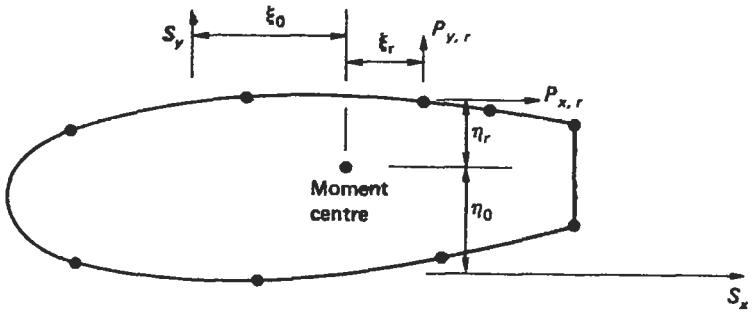

Fig. 10.5 Modification of moment equation in shear of closed section beams due to boom load.

The shear flow distribution in an open section beam is now obtained using Eq. (9.75) in which S_x is replaced by $S_{x,w}$ and S_y by $S_{y,w}$ from Eqs (10.15). Similarly for a closed section beam, S_x and S_y in Eq. (9.80) are replaced by $S_{x,w}$ and $S_{y,w}$. In the latter case the moment equation (Eq. (9.37)) requires modification due to the presence of the boom load components $P_{x,r}$ and $P_{y,r}$. Thus from Fig. 10.5 we see that Eq. (9.37) becomes

$$S_x\eta_0 - S_y\xi_0 = \oint q_b p \frac{ds}{t} + 2Aq_{s,0} - \sum_{r=1}^{m} P_{x,r}\eta_r + \sum_{r=1}^{m} P_{y,r}\xi_r \qquad (10.16)$$

Equation (10.16) is directly applicable to a tapered beam subjected to forces positioned in relation to the moment centre as shown. Care must be taken in a particular problem to ensure that the moments of the forces are given the correct sign.

Example 10.2

The cantilever beam shown in Fig. 10.6 is uniformly tapered along its length in both x and y directions and carries a load of 100 kN at its free end. Calculate the forces in the

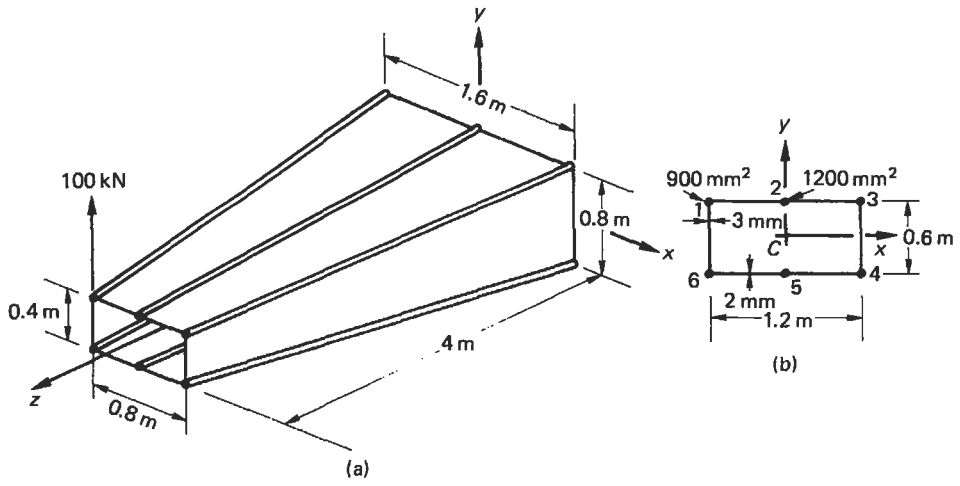

Fig. 10.6 (a) Beam of Example 10.2; (b) section 2 m from built-in end.

booms and the shear flow distribution in the walls at a section 2 m from the built-in end if the booms resist all the direct stresses while the walls are effective only in shear. Each corner boom has a cross-sectional area of 900 mm^2 while both central booms have cross-sectional areas of 1200 mm^2.

The internal force system at a section 2 m from the built-in end of the beam is

$$S_y = 100\,\text{kN}, \quad S_x = 0, \quad M_x = -100 \times 2 = -200\,\text{kN m}, \quad M_y = 0$$

The beam has a doubly symmetrical cross-section so that $I_{xy} = 0$ and Eq. (9.6) reduces to

$$\sigma_z = \frac{M_x y}{I_{xx}} \tag{i}$$

in which, for the beam section shown in Fig. 10.6(b)

$$I_{xx} = 4 \times 900 \times 300^2 + 2 \times 1200 \times 300^2 = 5.4 \times 10^8\,\text{mm}^4$$

Then

$$\sigma_{z,r} = \frac{-200 \times 10^6}{5.4 \times 10^8} y_r$$

or

$$\sigma_{z,r} = -0.37 y_r \tag{ii}$$

Hence

$$P_{z,r} = -0.37 y_r B_r \tag{iii}$$

The value of $P_{z,r}$ is calculated from Eq. (iii) in column ② in Table 10.1; $P_{x,r}$ and $P_{y,r}$ follow from Eqs (10.10) and (10.9) respectively in columns ⑤ and ⑥. The axial load P_r, column ⑦, is given by $[②^2 + ⑤^2 + ⑥^2]^{1/2}$ and has the same sign as $P_{z,r}$ (see Eq. (10.12)). The moments of $P_{x,r}$ and $P_{y,r}$ are calculated for a moment centre at the centre of symmetry with anticlockwise moments taken as positive. Note that in Table 10.1 $P_{x,r}$ and $P_{y,r}$ are positive when they act in the positive directions of the section x and y axes respectively; the distances η_r and ξ_r of the lines of action of $P_{x,r}$ and $P_{y,r}$ from the moment centre are not given signs since it is simpler to determine the sign of each moment, $P_{x,r}\eta_r$ and $P_{y,r}\xi_r$, by referring to the directions of $P_{x,r}$ and $P_{y,r}$ individually.

Table 10.1

① Boom	② $P_{z,r}$ (kN)	③ $\delta x_r/\delta z$	④ $\delta y_r/\delta z$	⑤ $P_{x,r}$ (kN)	⑥ $P_{y,r}$ (kN)	⑦ P_r (kN)	⑧ ξ_r (m)	⑨ η_r (m)	⑩ $P_{x,r}\eta_r$ (kN m)	⑪ $P_{y,r}\xi_r$ (kN m)
1	−100	0.1	−0.05	−10	5	−101.3	0.6	0.3	3	−3
2	−133	0	−0.05	0	6.7	−177.3	0	0.3	0	0
3	−100	−0.1	−0.05	10	5	−101.3	0.6	0.3	−3	3
4	100	−0.1	0.05	−10	5	101.3	0.6	0.3	−3	3
5	133	0	0.05	0	6.7	177.3	0	0.3	0	0
6	100	0.1	0.05	10	5	101.3	0.6	0.3	3	−3

From column ⑥

$$\sum_{r=1}^{6} P_{y,r} = 33.4\,\text{kN}$$

From column ⑩

$$\sum_{r=1}^{6} P_{x,r}\eta_r = 0$$

From column ⑪

$$\sum_{r=1}^{6} P_{y,r}\xi_r = 0$$

From Eqs (10.15)

$$S_{x,w} = 0, \quad S_{y,w} = 100 - 33.4 = 66.6\,\text{kN}$$

The shear flow distribution in the walls of the beam is now found using the method described in Section 9.9. Since, for this beam, $I_{xy} = 0$ and $S_x = S_{x,w} = 0$, Eq. (9.80) reduces to

$$q_s = \frac{-S_{y,w}}{I_{xx}} \sum_{r=1}^{n} B_r y_r + q_{s,0} \tag{iv}$$

We now 'cut' one of the walls, say 16. The resulting 'open section' shear flow is given by

$$q_b = -\frac{66.6 \times 10^3}{5.4 \times 10^8} \sum_{r=1}^{n} B_r y_r$$

or

$$q_b = -1.23 \times 10^{-4} \sum_{r=1}^{n} B_r y_r \tag{v}$$

Thus

$$q_{b,16} = 0$$

$$q_{b,12} = 0 - 1.23 \times 10^{-4} \times 900 \times 300 = -33.2\,\text{N/mm}$$

$$q_{b,23} = -33.2 - 1.23 \times 10^{-4} \times 1200 \times 300 = -77.5\,\text{N/mm}$$

$$q_{b,34} = -77.5 - 1.23 \times 10^{-4} \times 900 \times 300 = -110.7\,\text{N/mm}$$

$$q_{b,45} = -77.5\,\text{N/mm (from symmetry)}$$

$$q_{b,56} = -33.2\,\text{N/mm (from symmetry)}$$

giving the distribution shown in Fig. 10.7. Taking moments about the centre of symmetry we have, from Eq. (10.16)

$$-100 \times 10^3 \times 600 = 2 \times 33.2 \times 600 \times 300 + 2 \times 77.5 \times 600 \times 300 + 110.7 \times 600 \times 600 + 2 \times 1200 \times 600 q_{s,0}$$

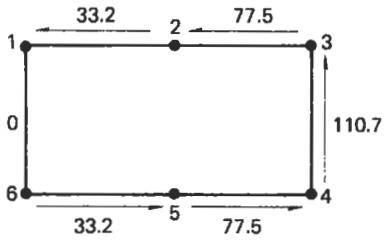

Fig. 10.7 'Open section' shear flow (N/mm) distribution in beam section of Example 10.2.

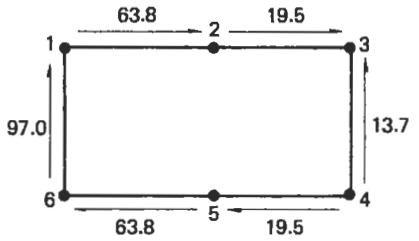

Fig. 10.8 Shear flow (N/mm) distribution in beam section of Example 10.2.

from which $q_{s,0} = -97.0\,\text{N/mm}$ (i.e. clockwise). The complete shear flow distribution is found by adding the value of $q_{s,0}$ to the q_b shear flow distribution of Fig. 10.7 and is shown in Fig. 10.8.

10.1.3 Beams having variable stringer areas

In many aircraft, structural beams, such as wings, have stringers whose cross-sectional areas vary in the spanwise direction. The effects of this variation on the determination of shear flow distribution cannot therefore be found by the methods described in Section 9.9 which assume constant boom areas. In fact, as we noted in Section 9.9, if the stringer stress is made constant by varying the area of cross-section there is no change in shear flow as the stringer/boom is crossed.

The calculation of shear flow distributions in beams having variable stringer areas is based on the alternative method for the calculation of shear flow distributions described in Section 9.9 and illustrated in the alternative solution of Example 9.13. The stringer loads $P_{z,1}$ and $P_{z,2}$ are calculated at two sections z_1 and z_2 of the beam a convenient distance apart. We assume that the stringer load varies linearly along its length so that the change in stringer load per unit length of beam is given by

$$\Delta P = \frac{P_{z,1} - P_{z,2}}{z_1 - z_2}$$

The shear flow distribution follows as previously described.

Example 10.3

Solve Example 10.2 by considering the differences in boom load at sections of the beam either side of the specified section.

In this example the stringer areas do not vary along the length of the beam but the method of solution is identical.

We are required to find the shear flow distribution at a section 2 m from the built-in end of the beam. We therefore calculate the boom loads at sections, say 0.1 m either side of this section. Thus, at a distance 2.1 m from the built-in end

$$M_x = -100 \times 1.9 = -190\,\text{kN m}$$

The dimensions of this section are easily found by proportion and are width = 1.18 m, depth = 0.59 m. Thus the second moment of area is

$$I_{xx} = 4 \times 900 \times 295^2 + 2 \times 1200 \times 295^2 = 5.22 \times 10^8\,\text{mm}^4$$

and

$$\sigma_{z,r} = \frac{-190 \times 10^6}{5.22 \times 10^8} y_r = -0.364 y_r$$

Hence

$$P_1 = P_3 = -P_4 = -P_6 = -0.364 \times 295 \times 900 = -96\,642\,\text{N}$$

and

$$P_2 = -P_5 = -0.364 \times 295 \times 1200 = -128\,856\,\text{N}$$

At a section 1.9 m from the built-in end

$$M_x = -100 \times 2.1 = -210\,\text{kN m}$$

and the section dimensions are width = 1.22 m, depth = 0.61 m so that

$$I_{xx} = 4 \times 900 \times 305^2 + 2 \times 1200 \times 305^2 = 5.58 \times 10^8\,\text{mm}^4$$

and

$$\sigma_{z,r} = \frac{-210 \times 10^6}{5.58 \times 10^8} y_r = -0.376 y_r$$

Hence

$$P_1 = P_3 = -P_4 = -P_6 = -0.376 \times 305 \times 900 = -103\,212\,\text{N}$$

and

$$P_2 = -P_5 = -0.376 \times 305 \times 1200 = -137\,616\,\text{N}$$

Thus, there is an increase in compressive load of 103 212 − 96 642 = 6570 N in booms 1 and 3 and an increase in tensile load of 6570 N in booms 4 and 6 between the two sections. Also, the compressive load in boom 2 increases by 137 616 − 128 856 = 8760 N while the tensile load in boom 5 increases by 8760 N. Therefore, the change in boom load per unit length is given by

$$\Delta P_1 = \Delta P_3 = -\Delta P_4 = -\Delta P_6 = \frac{6570}{200} = 32.85\,\text{N}$$

and

$$\Delta P_2 = -\Delta P_5 = \frac{8760}{200} = 43.8\,\text{N}$$

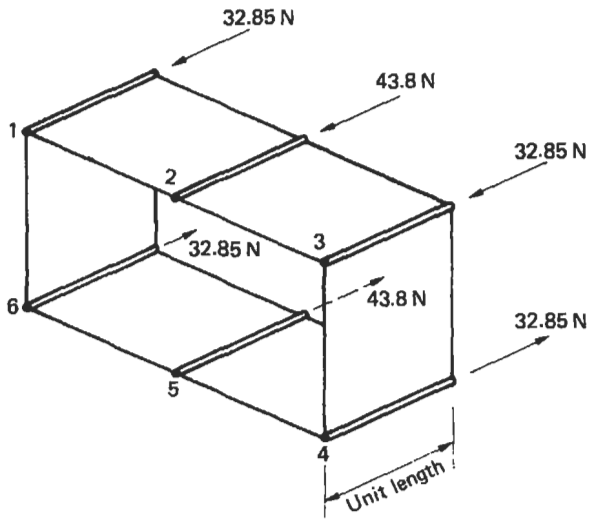

Fig. 10.9 Change in boom loads/unit length of beam.

The situation is illustrated in Fig. 10.9. Suppose now that the shear flows in the panels 12, 23, 24, etc. are q_{12}, q_{23}, q_{34}, etc. and consider the equilibrium of boom 2, as shown in Fig. 10.10, with adjacent portions of the panels 12 and 23. Thus

$$q_{23} + 43.8 - q_{12} = 0$$

or

$$q_{23} = q_{12} - 43.8$$

Similarly

$$q_{34} = q_{23} - 32.85 = q_{12} - 76.65$$

$$q_{45} = q_{34} + 32.85 = q_{12} - 43.8$$

$$q_{56} = q_{45} + 43.8 = q_{12}$$

$$q_{61} = q_{45} + 32.85 = q_{12} + 32.85$$

The moment resultant of the internal shear flows, together with the moments of the components $P_{y,r}$ of the boom loads about any point in the cross-section, is equivalent to the moment of the externally applied load about the same point. We note from

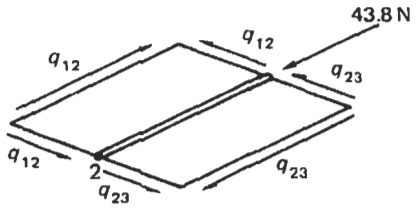

Fig. 10.10 Equilibrium of boom.

Example 10.2 that for moments about the centre of symmetry

$$\sum_{r=1}^{6} P_{x,r}\eta_r = 0, \quad \sum_{r=1}^{6} P_{y,r}\xi_r = 0$$

Therefore, taking moments about the centre of symmetry

$$100 \times 10^3 \times 600 = 2q_{12} \times 600 \times 300 + 2(q_{12} - 43.8)600 \times 300 + (q_{12} - 76.65)600 \times 600 + (q_{12} + 32.85)600 \times 600$$

from which

$$q_{12} = 62.5\,\text{N/mm}$$

whence

$$q_{23} = 19.7\,\text{N/mm}, \quad q_{34} = -13.2\,\text{N/mm}, \quad q_{45} = 19.7\,\text{N/mm}$$
$$q_{56} = 63.5\,\text{N/mm}, \quad q_{61} = 96.4\,\text{N/mm}$$

so that the solution is almost identical to the longer exact solution of Example 10.2.

The shear flows q_{12}, q_{23} etc. induce complementary shear flows q_{12}, q_{23} etc. in the panels in the longitudinal direction of the beam; these are, in fact, the average shear flows between the two sections considered. For a complete beam analysis the above procedure is applied to a series of sections along the span. The distance between adjacent sections may be taken to be any convenient value; for actual wings distances of the order of 350 mm to 700 mm are usually chosen. However, for very small values small percentage errors in $P_{z,1}$ and $P_{z,2}$ result in large percentage errors in ΔP. On the other hand, if the distance is too large the average shear flow between two adjacent sections may not be quite equal to the shear flow midway between the sections.

10.2 Fuselages

Aircraft fuselages consist, as we saw in Chapter 7, of thin sheets of material stiffened by large numbers of longitudinal stringers together with transverse frames. Generally they carry bending moments, shear forces and torsional loads which induce axial stresses in the stringers and skin together with shear stresses in the skin; the resistance of the stringers to shear forces is generally ignored. Also, the distance between adjacent stringers is usually small so that the variation in shear flow in the connecting panel will be small. It is therefore reasonable to assume that the shear flow is constant between adjacent stringers so that the analysis simplifies to the analysis of an idealized section in which the stringers/booms carry all the direct stresses while the skin is effective only in shear. The direct stress carrying capacity of the skin may be allowed for by increasing the stringer/boom areas as described in Section 9.9. The analysis of fuselages therefore involves the calculation of direct stresses in the stringers and the shear stress distributions in the skin; the latter are also required in the analysis of transverse frames, as we shall see in Section 10.4.

10.2.1 Bending

The skin/stringer arrangement is idealized into one comprising booms and skin as described in Section 9.9. The direct stress in each boom is then calculated using either Eq. (9.6) or Eq. (9.7) in which the reference axes and the section properties refer to the direct stress carrying areas of the cross-section.

Example 10.4

The fuselage of a light passenger carrying aircraft has the circular cross-section shown in Fig. 10.11(a). The cross-sectional area of each stringer is $100\,\text{mm}^2$ and the vertical distances given in Fig. 10.11(a) are to the mid-line of the section wall at the corresponding stringer position. If the fuselage is subjected to a bending moment of 200 kN m applied in the vertical plane of symmetry, at this section, calculate the direct stress distribution.

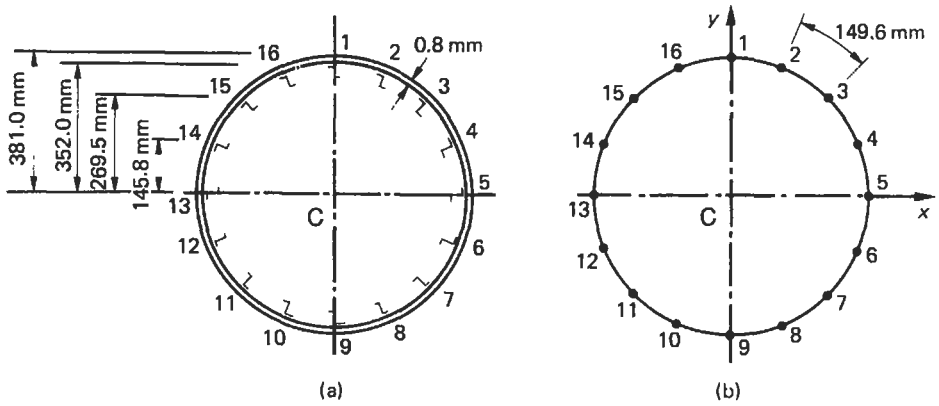

Fig. 10.11 (a) Actual fuselage section; (b) idealized fuselage section.

The section is first idealized using the method described in Section 9.9. As an approximation we shall assume that the skin between adjacent stringers is flat so that we may use either Eq. (9.70) or Eq. (9.71) to determine the boom areas. From symmetry $B_1 = B_9$, $B_2 = B_8 = B_{10} = B_{16}$, $B_3 = B_7 = B_{11} = B_{15}$, $B_4 = B_6 = B_{12} = B_{14}$ and $B_5 = B_{13}$. From Eq. (9.70)

$$B_1 = 100 + \frac{0.8 \times 149.6}{6}\left(2 + \frac{\sigma_2}{\sigma_1}\right) + \frac{0.8 \times 149.6}{6}\left(2 + \frac{\sigma_{16}}{\sigma_1}\right)$$

i.e.

$$B_1 = 100 + \frac{0.8 \times 149.6}{6}\left(2 + \frac{352.0}{381.0}\right) \times 2 = 216.6\,\text{mm}^2$$

Similarly $B_2 = 216.6\,\text{mm}^2$, $B_3 = 216.6\,\text{mm}^2$, $B_4 = 216.7\,\text{mm}^2$. We note that stringers 5 and 13 lie on the neutral axis of the section and are therefore unstressed; the calculation of boom areas B_5 and B_{13} does not then arise.

Table 10.2

Stringer/boom	y (mm)	σ_z (N/mm^2)
1	381.0	302.4
2, 16	352.0	279.4
3, 15	269.5	213.9
4, 14	145.8	115.7
5, 13	0	0
6, 12	−145.8	−115.7
7, 11	−269.5	−213.9
8, 10	−352.0	−279.4
9	−381.0	−302.4

For this particular section $I_{xy} = 0$ since Cx (and Cy) is an axis of symmetry. Further, $M_y = 0$ so that Eq. (9.6) reduces to

$$\sigma_z = \frac{M_x y}{I_{xx}}$$

in which

$$I_{xx} = 2 \times 216.6 \times 381.0^2 + 4 \times 216.6 \times 352.0^2 + 4 \times 216.6 \times 2695^2$$
$$+ 4 \times 216.7 \times 145.8^2 = 2.52 \times 10^8 \text{ mm}^4$$

The solution is completed in Table 10.2.

10.2.2 Shear

For a fuselage having a cross-section of the type shown in Fig. 10.11(a), the determination of the shear flow distribution in the skin produced by shear is basically the analysis of an idealized single cell closed section beam. The shear flow distribution is therefore given by Eq. (9.80) in which the direct stress carrying capacity of the skin is assumed to be zero, i.e. $t_D = 0$, thus

$$q_s = -\left(\frac{S_x I_{xx} - S_y I_{xy}}{I_{xx} I_{yy} - I_{xy}^2}\right) \sum_{r=1}^{n} B_r y_r - \left(\frac{S_y I_{yy} - S_x I_{xy}}{I_{xx} I_{yy} - I_{xy}^2}\right) \sum_{r=1}^{n} B_r x_r + q_{s,0} \qquad (10.17)$$

Equation (10.17) is applicable to loading cases in which the shear loads are not applied through the section shear centre so that the effects of shear and torsion are included simultaneously. Alternatively, if the position of the shear centre is known, the loading system may be replaced by shear loads acting through the shear centre together with a pure torque, and the corresponding shear flow distributions may be calculated separately and then superimposed to obtain the final distribution.

Example 10.5

The fuselage of Example 10.4 is subjected to a vertical shear load of 100 kN applied at a distance of 150 mm from the vertical axis of symmetry as shown, for the idealized section, in Fig. 10.12. Calculate the distribution of shear flow in the section.

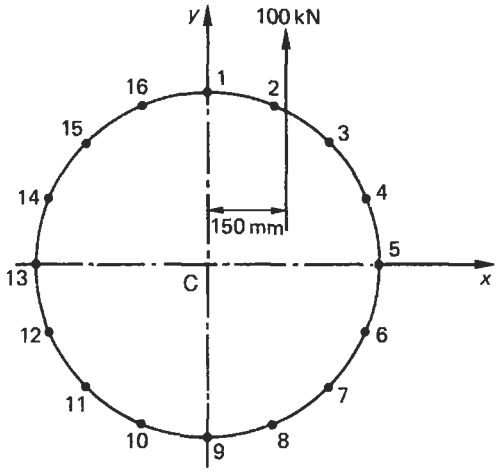

Fig. 10.12 Idealized fuselage section of Example 10.5.

As in Example 10.4, $I_{xy} = 0$ and, since $S_x = 0$, Eq. (10.17) reduces to

$$q_s = -\frac{S_y}{I_{xx}} \sum_{r=1}^{n} B_r y_r + q_{s,0} \tag{i}$$

in which $I_{xx} = 2.52 \times 10^8\ \text{mm}^4$ as before. Thus

$$q_s = \frac{-100 \times 10^3}{2.52 \times 10^8} \sum_{r=1}^{n} B_r y_r + q_{s,0}$$

or

$$q_s = -3.97 \times 10^{-4} \sum_{r=1}^{n} B_r y_r + q_{s,0} \tag{ii}$$

The first term on the right-hand side of Eq. (ii) is the 'open section' shear flow q_b. We therefore 'cut' one of the skin panels, say 12, and calculate q_b. The results are presented in Table 10.3.

Note that in Table 10.3 the column headed Boom indicates the boom that is crossed when the analysis moves from one panel to the next. Note also that, as would be expected, the q_b shear flow distribution is symmetrical about the Cx axis. The shear flow $q_{s,0}$ in the panel 12 is now found by taking moments about a convenient moment centre, say C. Thus from Eq. (9.37)

$$100 \times 10^3 \times 150 = \oint q_b p\, ds + 2Aq_{s,0} \tag{iii}$$

in which $A = \pi \times 381.0^2 = 4.56 \times 10^5\ \text{mm}^2$. Since the q_b shear flows are constant between the booms, Eq. (iii) may be rewritten in the form (see Eq. (9.79))

$$100 \times 10^3 \times 150 = -2A_{12}q_{b,12} - 2A_{23}q_{b,23} - \cdots - 2A_{161}q_{b,161} + 2Aq_{s,0} \tag{iv}$$

in which $A_{12}, A_{23}, \ldots, A_{161}$ are the areas subtended by the skin panels $12, 23, \ldots, 161$ at the centre C of the circular cross-section and anticlockwise moments are taken as

Table 10.3

Skin panel	Boom	B_r (mm^2)	y_r (mm)	q_b (N/mm)
1 2	–	–	–	0
2 3	2	216.6	352.0	−30.3
3 4	3	216.6	269.5	−53.5
4 5	4	216.7	145.8	−66.0
5 6	5	–	0	−66.0
6 7	6	216.7	−145.8	−53.5
7 8	7	216.6	−269.5	−30.3
8 9	8	216.6	−352.0	0
1 16	1	216.6	381.0	−32.8
16 15	16	216.6	352.0	−63.1
15 14	15	216.6	269.5	−86.3
14 13	14	216.6	145.8	−98.8
13 12	13	–	0	−98.8
12 11	12	216.7	−145.8	−86.3
11 10	11	216.6	−269.5	−63.1
10 9	10	216.6	−352.0	−32.8

positive. Clearly $A_{12} = A_{23} = \cdots = A_{161} = 4.56 \times 10^5/16 = 28\,500\,\text{mm}^2$. Equation (iv) then become

$$100 \times 10^3 \times 150 = 2 \times 28\,500(-q_{b_{12}} - q_{b_{23}} - \cdots - q_{b_{161}}) + 2 \times 4.56 \times 10^5 q_{s,0} \quad \text{(v)}$$

Substituting the values of q_b from Table 10.3 in Eq. (v), we obtain

$$100 \times 10^3 \times 150 = 2 \times 28\,500(-262.4) + 2 \times 4.56 \times 10^5 q_{s,0}$$

from which

$$q_{s,0} = 32.8\,\text{N/mm (acting in an anticlockwise sense)}$$

The complete shear flow distribution follows by adding the value of $q_{s,0}$ to the q_b shear flow distribution, giving the final distribution shown in Fig. 10.13. The solution may

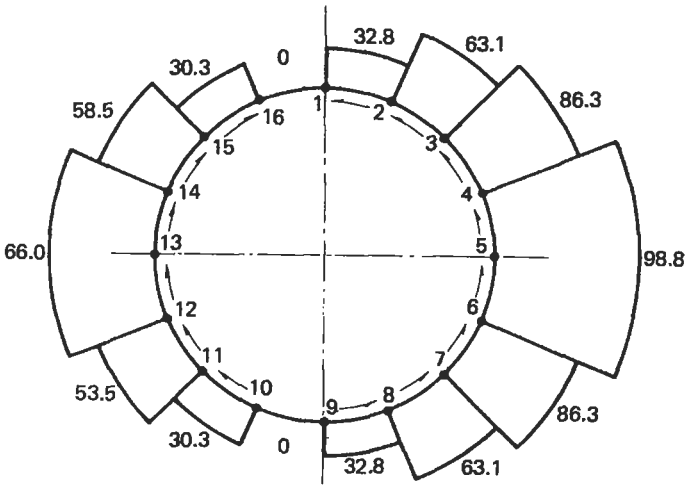

Fig. 10.13 Shear flow (N/mm) distribution in fuselage section of Example 10.5.

be checked by calculating the resultant of the shear flow distribution parallel to the Cy axis. Thus

$$2[(98.8 + 66.0)145.8 + (86.3 + 53.5)123.7 + (63.1 + 30.3)82.5 + (32.8 - 0)29.0] \times 10^{-3} = 99.96\,\text{kN}$$

which agrees with the applied shear load of 100 kN. The analysis of a fuselage which is tapered along its length is carried out using the method described in Section 10.1 and illustrated in Example 10.2.

10.2.3 Torsion

A fuselage section is basically a single cell closed section beam. The shear flow distribution produced by a pure torque is therefore given by Eq. (9.49) and is

$$q = \frac{T}{2A} \tag{10.18}$$

It is immaterial whether or not the section has been idealized since, in both cases, the booms are assumed not to carry shear stresses.

Equation (10.18) provides an alternative approach to that illustrated in Example 10.5 for the solution of shear loaded sections in which the position of the shear centre is known. In Fig. 10.11 the shear centre coincides with the centre of symmetry so that the loading system may be replaced by the shear load of 100 kN acting through the shear centre together with a pure torque equal to $100 \times 10^3 \times 150 = 15 \times 10^6$ N mm as shown in Fig. 10.14. The shear flow distribution due to the shear load may be found using the method of Example 10.5 but with the left-hand side of the moment equation (iii) equal to zero for moments about the centre of symmetry. Alternatively, use may be made of the symmetry of the section and the fact that the shear flow is

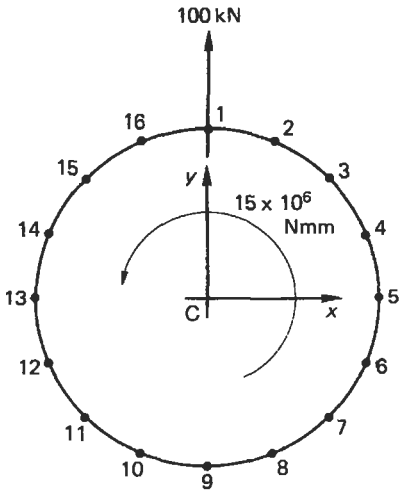

Fig. 10.14 Alternative solution of Example 10.5.

constant between adjacent booms. Suppose that the shear flow in the panel 21 is q_{21}. Then from symmetry and using the results of Table 10.3

$$q_{98} = q_{910} = q_{161} = q_{21}$$

$$q_{32} = q_{87} = q_{1011} = q_{1516} = 30.3 + q_{21}$$

$$q_{43} = q_{76} = q_{1112} = q_{1415} = 53.5 + q_{21}$$

$$q_{54} = q_{65} = q_{1213} = q_{1314} = 66.0 + q_{21}$$

The resultant of these shear flows is statically equivalent to the applied shear load so that

$$4(29.0q_{21} + 82.5q_{32} + 123.7q_{43} + 145.8q_{54}) = 100 \times 10^3$$

Substituting for q_{32}, q_{43} and q_{54} from the above we obtain

$$4(381q_{21} + 18\,740.5) = 100 \times 10^3$$

whence

$$q_{21} = 16.4\,\text{N/mm}$$

and

$$q_{32} = 46.7\,\text{N/mm}, \quad q_{43} = 69.9\,\text{N/mm}, \quad q_{54} = 83.4\,\text{N/mm etc.}$$

The shear flow distribution due to the applied torque is, from Eq. (10.18)

$$q = \frac{15 \times 10^6}{2 \times 4.56 \times 10^5} = 16.4\,\text{N/mm}$$

acting in an anticlockwise sense completely around the section. This value of shear flow is now superimposed on the shear flows produced by the shear load; this gives the solution shown in Fig. 10.13, i.e.

$$q_{21} = 16.4 + 16.4 = 32.8\,\text{N/mm}$$

$$q_{161} = 16.4 - 16.4 = 0 \text{ etc.}$$

10.3 Wings

We have seen in Chapters 7 and 9 that wing sections consist of thin skins stiffened by combinations of stringers, spar webs and caps and ribs. The resulting structure frequently comprises one, two or more cells and is highly redundant. However, as in the case of fuselage sections, the large number of closely spaced stringers allows the assumption of a constant shear flow in the skin between adjacent stringers so that a wing section may be analysed as though it were completely idealized as long as the direct stress carrying capacity of the skin is allowed for by additions to the existing stringer/boom areas. We shall investigate the analysis of multicellular wing sections subjected to bending, torsional and shear loads, although, initially, it will be instructive to examine the special case of an idealized three-boom shell.

The wing section shown in Fig. 10.15 has been idealized into an arrangement of direct-stress carrying booms and shear-stress-only carrying skin panels. The part of

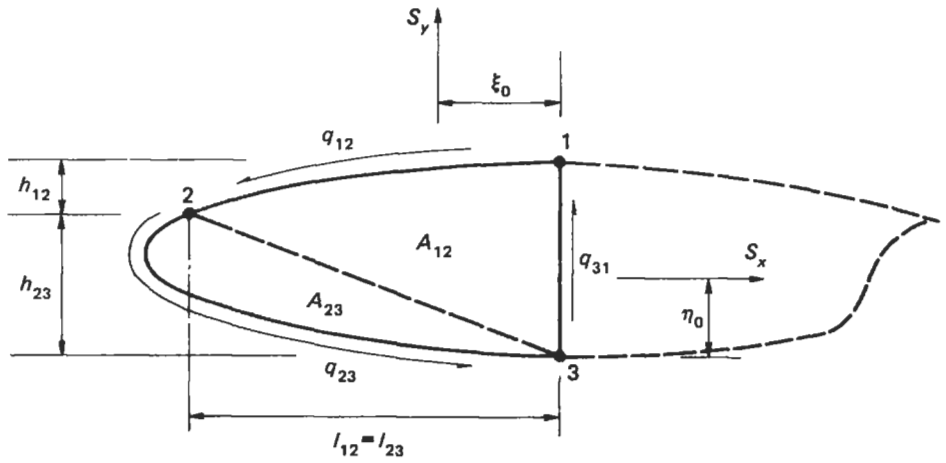

Fig. 10.15 Three-boom wing section.

the wing section aft of the vertical spar 31 performs an aerodynamic role only and is therefore unstressed. Lift and drag loads, S_y and S_x, induce shear flows in the skin panels which are constant between adjacent booms since the section has been completely idealized. Thus, resolving horizontally and noting that the resultant of the internal shear flows is equivalent to the applied load, we have

$$S_x = -q_{12}l_{12} + q_{23}l_{23} \tag{10.19}$$

Now resolving vertically

$$S_y = q_{31}(h_{12} + h_{23}) - q_{12}h_{12} - q_{23}h_{23} \tag{10.20}$$

Finally, taking moments about, say, boom 3

$$S_x\eta_0 + S_y\xi_0 = -2A_{12}q_{12} - 2A_{23}q_{23} \tag{10.21}$$

(see Eqs (9.78) and (9.79)). In the above there are three unknown values of shear flow, q_{12}, q_{23}, q_{31} and three equations of statical equilibrium. We conclude therefore that a three-boom idealized shell is statically determinate.

We shall return to the simple case of a three-boom wing section when we examine the distributions of direct load and shear flows in wing ribs. Meanwhile, we shall consider the bending, torsion and shear of multicellular wing sections.

10.3.1 Bending

Bending moments at any section of a wing are usually produced by shear loads at other sections of the wing. The direct stress system for such a wing section (Fig. 10.16) is given by either Eq. (9.6) or Eq. (9.7) in which the coordinates (x, y) of any point in the cross-section and the sectional properties are referred to axes Cxy in which the origin C coincides with the centroid of the direct stress carrying area.

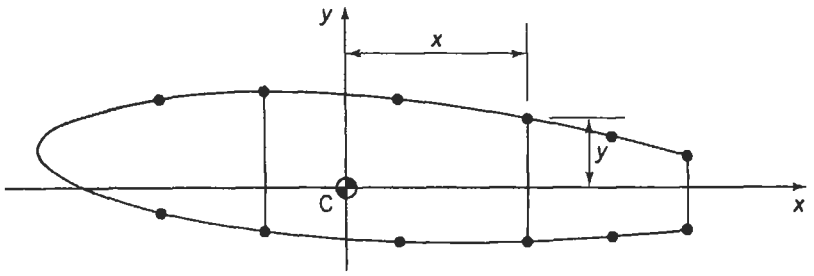

Fig. 10.16 Idealized section of a multicell wing.

Example 10.6

The wing section shown in Fig. 10.17 has been idealized such that the booms carry all the direct stresses. If the wing section is subjected to a bending moment of 300 kN m applied in a vertical plane, calculate the direct stresses in the booms.

Boom areas: $B_1 = B_6 = 2580\,\text{mm}^2$, $B_2 = B_5 = 3880\,\text{mm}^2$, $B_3 = B_4 = 3230\,\text{mm}^2$

We note that the distribution of the boom areas is symmetrical about the horizontal x axis. Hence, in Eq. (9.6), $I_{xy} = 0$. Further, $M_x = 300\,\text{kN m}$ and $M_y = 0$ so that Eq. (9.6) reduces to

$$\sigma_z = \frac{M_x y}{I_{xx}} \tag{i}$$

in which

$$I_{xx} = 2(2580 \times 165^2 + 3880 \times 230^2 + 3230 \times 200^2) = 809 \times 10^6\,\text{mm}^4$$

Hence

$$\sigma_z = \frac{300 \times 10^6}{809 \times 10^6} y = 0.371y \tag{ii}$$

The solution is now completed in Table 10.4 in which positive direct stresses are tensile and negative direct stresses compressive.

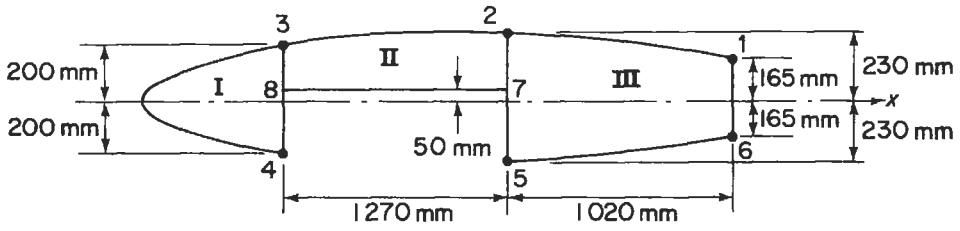

Fig. 10.17 Wing section of Example 10.6.

Table 10.4

Boom	y (mm)	σ_z (N/mm^2)
1	165	61.2
2	230	85.3
3	200	74.2
4	−200	−74.2
5	−230	−85.3
6	−165	−61.2

10.3.2 Torsion

The chordwise pressure distribution on an aerodynamic surface may be represented by shear loads (lift and drag loads) acting through the aerodynamic centre together with a pitching moment M_0 (see Section 7.2). This system of shear loads may be transferred to the shear centre of the section in the form of shear loads S_x and S_y together with a torque T. It is the pure torsion case that is considered here. In the analysis we assume that no axial constraint effects are present and that the shape of the wing section remains unchanged by the load application. In the absence of axial constraint there is no development of direct stress in the wing section so that only shear stresses are present. It follows that the presence of booms does not affect the analysis in the pure torsion case.

The wing section shown in Fig. 10.18 comprises N cells and carries a torque T which generates individual but unknown torques in each of the N cells. Each cell therefore develops a constant shear flow $q_{\mathrm{I}}, q_{\mathrm{II}}, \ldots, q_{\mathrm{R}}, \ldots, q_N$ given by Eq. (9.49).

The total is therefore

$$T = \sum_{R=1}^{N} 2A_R q_R \tag{10.22}$$

Although Eq. (10.22) is sufficient for the solution of the special case of a single cell section, which is therefore statically determinate, additional equations are required for an N-cell section. These are obtained by considering the rate of twist in each cell and the compatibility of displacement condition that all N cells possess the same rate of twist $\mathrm{d}\theta/\mathrm{d}z$; this arises directly from the assumption of an undistorted cross-section.

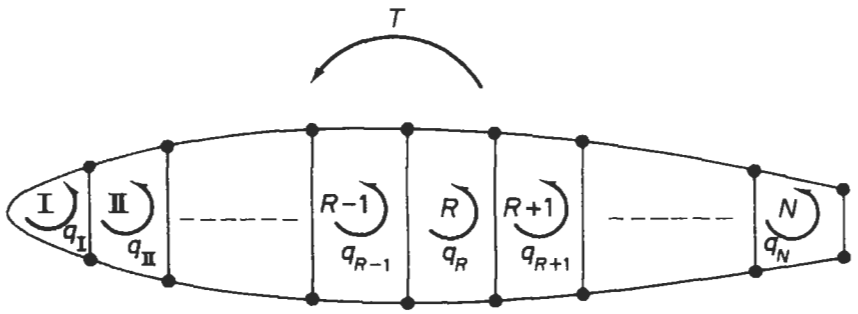

Fig. 10.18 Multicell wing section subjected to torsion.

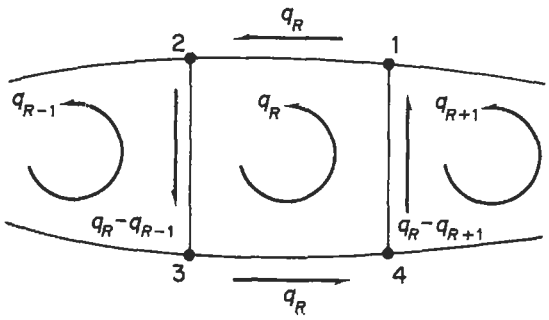

Fig. 10.19 Shear flow distribution in the Rth cell of an N-cell wing section.

Consider the Rth cell of the wing section shown in Fig. 10.18. The rate of twist in the cell is, from Eq. (9.42)

$$\frac{d\theta}{dz} = \frac{1}{2A_R G} \oint_R q \frac{ds}{t} \tag{10.23}$$

The shear flow in Eq. (10.23) is constant along each wall of the cell and has the values shown in Fig. 10.19. Writing $\int ds/t$ for each wall as δ, Eq. (10.23) becomes

$$\frac{d\theta}{dz} = \frac{1}{2A_R G}[q_R\delta_{12} + (q_R - q_{R-1})\delta_{23} + q_R\delta_{34} + (q_R - q_{R+1})\delta_{41}]$$

or, rearranging the terms in square brackets

$$\frac{d\theta}{dz} = \frac{1}{2A_R G}[-q_{R-1}\delta_{23} + q_R(\delta_{12} + \delta_{23} + \delta_{34} + \delta_{41}) - q_{R+1}\delta_{41}]$$

In general terms, this equation may be rewritten in the form

$$\frac{d\theta}{dz} = \frac{1}{2A_R G}(-q_{R-1}\delta_{R-1,R} + q_R\delta_R - q_{R+1}\delta_{R+1,R}) \tag{10.24}$$

in which $\delta_{R-1,R}$ is $\int ds/t$ for the wall common to the Rth and $(R-1)$th cells, δ_R is $\int ds/t$ for all the walls enclosing the Rth cell and $\delta_{R+1,R}$ is $\int ds/t$ for the wall common to the Rth and $(R+1)$th cells.

The general form of Eq. (10.24) is applicable to multicell sections in which the cells are connected consecutively, that is, cell I is connected to cell II, cell II to cells I and III and so on. In some cases, cell I may be connected to cells II and III etc. (see problem P.10.9) so that Eq. (10.24) cannot be used in its general form. For this type of section the term $\oint q(ds/t)$ should be computed by considering $\int q(ds/t)$ for each wall of a particular cell in turn.

There are N equations of the type (10.24) which, with Eq. (10.22), comprise the $N+1$ equations required to solve for the N unknown values of shear flow and the one unknown value of $d\theta/dz$.

Frequently, in practice, the skin panels and spar webs are fabricated from materials possessing different properties such that the shear modulus G is not constant. The analysis of such sections is simplified if the actual thickness t of a wall is converted to a modulus-weighted thickness t^* as follows. For the Rth cell of an N-cell wing

section in which G varies from wall to wall, Eq. (10.23) takes the form

$$\frac{d\theta}{dz} = \frac{1}{2A_R}\oint_R q\frac{ds}{Gt}$$

This equation may be rewritten as

$$\frac{d\theta}{dz} = \frac{1}{2A_R G_{REF}}\oint_R q\frac{ds}{(G/G_{REF})t} \tag{10.25}$$

in which G_{REF} is a convenient reference value of the shear modulus. Equation (10.25) is now rewritten as

$$\frac{d\theta}{dz} = \frac{1}{2A_R G_{REF}}\oint_R q\frac{ds}{t^*} \tag{10.26}$$

in which the modulus-weighted thickness t^* is given by

$$t^* = \frac{G}{G_{REF}}t \tag{10.27}$$

Then, in Eq. (10.24), δ becomes $\int ds/t^*$.

Example 10.7

Calculate the shear stress distribution in the walls of the three-cell wing section shown in Fig. 10.20, when it is subjected to an anticlockwise torque of 11.3 kN m.

Wall	Length (mm)	Thickness (mm)	G (N/mm^2)	Cell area (mm^2)
12^o	1650	1.22	24200	$A_I = 258000$
12^i	508	2.03	27600	$A_{II} = 355000$
13, 24	775	1.22	24200	$A_{III} = 161000$
34	380	1.63	27600	
35, 46	508	0.92	20700	
56	254	0.92	20700	

Note: The superscript symbols o and i are used to distinguish between outer and inner walls connecting the same two booms.

Since the wing section is loaded by a pure torque the presence of the booms has no effect on the analysis.

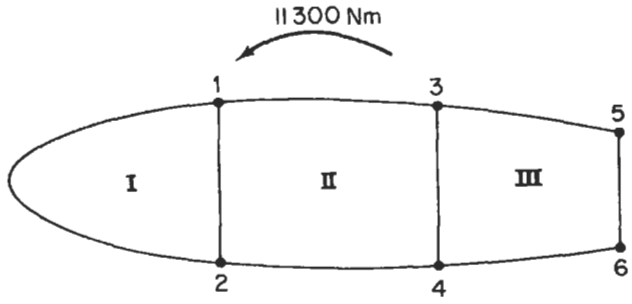

Fig. 10.20 Wing section of Example 10.7.

Choosing $G_{REF} = 27\,600\,N/mm^2$ then, from Eq. (10.27)

$$t^*_{12^o} = \frac{24\,200}{27\,600} \times 1.22 = 1.07\,mm$$

Similarly

$$t^*_{13} = t^*_{24} = 1.07\,mm, \quad t^*_{35} = t^*_{46} = t^*_{56} = 0.69\,mm$$

Hence

$$\delta_{12^o} = \int_{12^o} \frac{ds}{t^*} = \frac{1650}{1.07} = 1542$$

Similarly

$$\delta_{12^i} = 250, \quad \delta_{13} = \delta_{24} = 725, \quad \delta_{34} = 233, \quad \delta_{35} = \delta_{46} = 736, \quad \delta_{56} = 368$$

Substituting the appropriate values of δ in Eq. (10.24) for each cell in turn gives the following.

For cell I

$$\frac{d\theta}{dz} = \frac{1}{2 \times 258\,000 G_{REF}}[q_I(1542 + 250) - 250q_{II}] \tag{i}$$

For cell II

$$\frac{d\theta}{dz} = \frac{1}{2 \times 355\,000 G_{REF}}[-250q_I + q_{II}(250 + 725 + 233 + 725) - 233q_{III}] \tag{ii}$$

For cell III

$$\frac{d\theta}{dz} = \frac{1}{2 \times 161\,000 G_{REF}}[-233q_{II} + q_{III}(736 + 233 + 736 + 368)] \tag{iii}$$

In addition, from Eq. (10.22)

$$11.3 \times 10^6 = 2(258\,000q_I + 355\,000q_{II} + 161\,000q_{III}) \tag{iv}$$

Solving Eqs (i) to (iv) simultaneously gives

$$q_I = 7.1\,N/mm, \quad q_{II} = 8.9\,N/mm, \quad q_{III} = 4.2\,N/mm$$

The shear stress in any wall is obtained by dividing the shear flow by the *actual* wall thickness. Hence the shear stress distribution is as shown in Fig. 10.21.

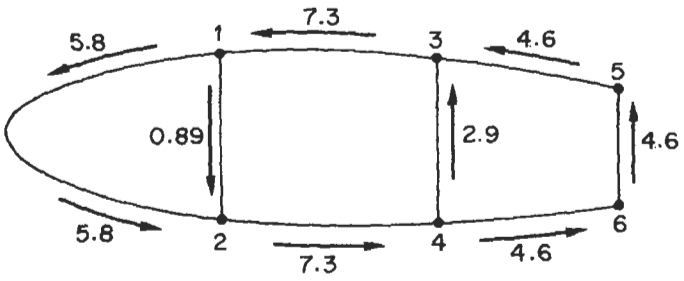

Fig. 10.21 Shear stress (N/mm^2) distribution in wing section of Example 10.7.

10.3.3 Shear

Initially we shall consider the general case of an N-cell wing section comprising booms and skin panels, the latter being capable of resisting both direct and shear stresses. The wing section is subjected to shear loads S_x and S_y whose lines of action do not necessarily pass through the shear centre S (see Fig. 10.22); the resulting shear flow distribution is therefore due to the combined effects of shear and torsion.

The method for determining the shear flow distribution and the rate of twist is based on a simple extension of the analysis of a single cell beam subjected to shear loads (Sections 9.4 and 9.9). Such a beam is statically indeterminate, the single redundancy being selected as the value of shear flow at an arbitrarily positioned 'cut'. Thus, the N-cell wing section of Fig. 10.22 may be made statically determinate by 'cutting' a skin panel in each cell as shown. While the actual position of these 'cuts' is theoretically immaterial there are advantages to be gained from a numerical point of view if the 'cuts' are made near the centre of the top or bottom skin panel in each cell. Generally, at these points, the redundant shear flows ($q_{s,0}$) are small so that the final shear flows differ only slightly from those of the determinate structure. The system of simultaneous equations from which the final shear flows are found will then be 'well conditioned' and will produce reliable results. The solution of an 'ill conditioned' system of equations would probably involve the subtraction of large numbers of a similar size which would therefore need to be expressed to a large number of significant figures for reasonable accuracy. Although this reasoning does not apply to a completely idealized wing section since the calculated values of shear flow are constant between the booms, it is again advantageous to 'cut' either the top or bottom skin panels for, in the special case of a wing section having a horizontal axis of symmetry, a 'cut' in, say, the top skin panels will result in the 'open section' shear flows (q_b) being zero in the bottom skin panels. This decreases the arithmetical labour and simplifies the derivation of the moment equation, as will become obvious in Example 10.8.

The above remarks regarding the 'cutting' of multicell wing sections are applicable only to this method of analysis. In the approximate analysis of multicell wing sections

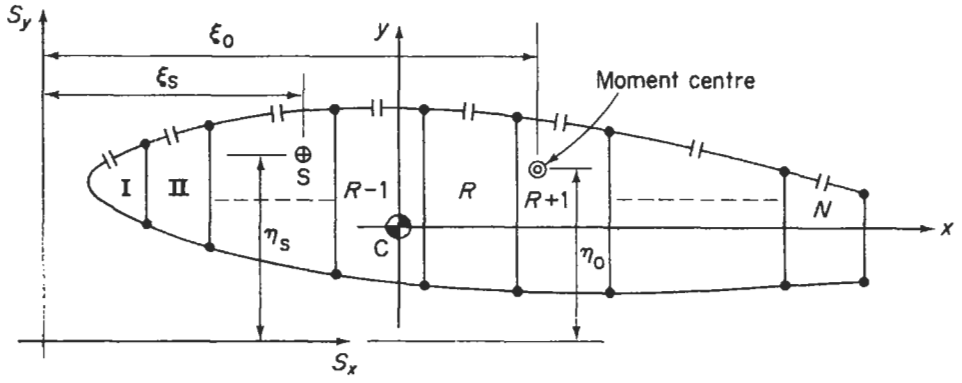

Fig. 10.22 N-cell wing section subjected to shear loads.

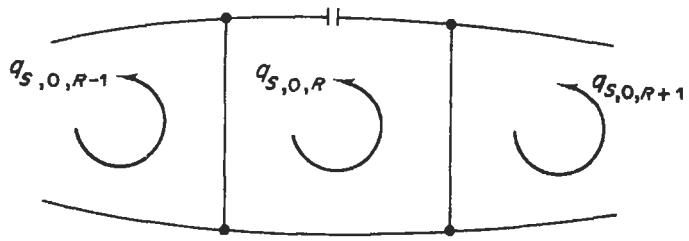

Fig. 10.23 Redundant shear flow in the Rth cell of an N-cell wing section subjected to shear.

by the method of successive approximations 'cuts' are sometimes made in the spar webs although in some cases 'cutting' the top or bottom skin panels produces a more rapid convergence in the numerical iteration process. This approximate method is extremely useful when the number of cells is large since, in the above approach, it is clear that the greater the number of cells the greater the number of simultaneous equations requiring solution.

The 'open section' shear flow q_b in the wing section of Fig. 10.22 is given by Eq. (9.75), i.e.

$$q_b = -\left(\frac{S_x I_{xx} - S_y I_{xy}}{I_{xx} I_{yy} - I_{xy}^2}\right)\left(\int_0^s t_D x \, ds + \sum_{r=1}^{n} B_r x_r\right)$$
$$-\left(\frac{S_y I_{yy} - S_x I_{xy}}{I_{xx} I_{yy} - I_{xy}^2}\right)\left(\int_0^s t_D y \, ds + \sum_{r=1}^{n} B_r y_r\right)$$

We are left with an unknown value of shear flow at each of the 'cuts', i.e. $q_{s,0,I}$, $q_{s,0,II}, \ldots, q_{s,0,N}$ plus the unknown rate of twist $d\theta/dz$ which, from the assumption of an undistorted cross-section, is the same for each cell. Therefore, as in the torsion case, there are $N + 1$ unknowns requiring $N + 1$ equations for a solution.

Consider the Rth cell shown in Fig. 10.23. The complete distribution of shear flow around the cell is given by the summation of the 'open section' shear flow q_b and the value of shear flow at the 'cut', $q_{s,0,R}$. We may therefore regard $q_{s,0,R}$ as a constant shear flow acting around the cell. The rate of twist is again given by Eq. (9.42); thus

$$\frac{d\theta}{dz} = \frac{1}{2A_R G}\oint_R q\frac{ds}{t} = \frac{1}{2A_R G}\oint_R (q_b + q_{s,0,R})\frac{ds}{t}$$

By comparison with the pure torsion case we deduce that

$$\frac{d\theta}{dz} = \frac{1}{2A_R G}\left(-q_{s,0,R-1}\delta_{R-1,R} + q_{s,0,R}\delta_R - q_{s,0,R+1}\delta_{R+1,R} + \oint_R q_b\frac{ds}{t}\right) \qquad (10.28)$$

in which q_b has previously been determined. There are N equations of the type (10.28) so that a further equation is required to solve for the $N + 1$ unknowns. This is obtained by considering the moment equilibrium of the Rth cell in Fig. 10.24.

The moment $M_{q,R}$ produced by the total shear flow about any convenient moment centre O is given by

$$M_{q,R} = \oint q_R p_0 \, ds \quad \text{(see Section 9.5)}$$

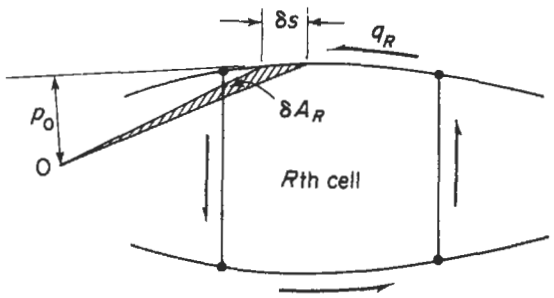

Fig. 10.24 Moment equilibrium of Rth cell.

Substituting for q_R in terms of the 'open section' shear flow q_b and the redundant shear flow $q_{s,0,R}$, we have

$$M_{q,R} = \oint_R q_b p_0 \, ds + q_{s,0,R} \oint_R p_0 \, ds$$

or

$$M_{q,R} = \oint_R q_b p_0 \, ds + 2A_R q_{s,0,R}$$

The sum of the moments from the individual cells is equivalent to the moment of the externally applied loads about the same point. Thus, for the wing section of Fig. 10.22

$$S_x \eta_0 - S_y \xi_0 = \sum_{R=1}^{N} M_{q,R} = \sum_{R=1}^{N} \oint_R q_b p_0 \, ds + \sum_{R=1}^{N} 2A_R q_{s,0,R} \tag{10.29}$$

If the moment centre is chosen to coincide with the point of intersection of the lines of action of S_x and S_y, Eq. (10.29) becomes

$$0 = \sum_{R=1}^{N} \oint_R q_b p_0 \, ds + \sum_{R=1}^{N} 2A_R q_{s,0,R} \tag{10.30}$$

Example 10.8

The wing section of Example 10.6 (Fig. 10.17) carries a vertically upward shear load of 86.8 kN in the plane of the web 572. The section has been idealized such that the booms resist all the direct stresses while the walls are effective only in shear. If the shear modulus of all walls is 27 600 N/mm^2 except for the wall 78 for which it is three times this value, calculate the shear flow distribution in the section and the rate of twist. Additional data are given below.

Wall	Length (mm)	Thickness (mm)	Cell area (mm^2)
12, 56	1023	1.22	$A_I = 265\,000$
23	1274	1.63	$A_{II} = 213\,000$
34	2200	2.03	$A_{III} = 413\,000$
483	400	2.64	
572	460	2.64	
61	330	1.63	
78	1270	1.22	

Choosing G_{REF} as 27 600 N/mm^2 then, from Eq. (10.27)

$$t_{78}^{*} = \frac{3 \times 27\,600}{27\,600} \times 1.22 = 3.66\,\text{mm}$$

Hence

$$\delta_{78} = \frac{1270}{3.66} = 347$$

Also

$$\delta_{12} = \delta_{56} = 840, \quad \delta_{23} = 783, \quad \delta_{34} = 1083, \quad \delta_{38} = 57, \quad \delta_{84} = 95, \quad \delta_{87} = 347,$$
$$\delta_{27} = 68, \quad \delta_{75} = 106, \quad \delta_{16} = 202$$

We now 'cut' the top skin panels in each cell and calculate the 'open section' shear flows using Eq. (9.75) which, since the wing section is idealized, singly symmetrical (as far as the direct stress carrying area is concerned) and is subjected to a vertical shear load only, reduces to

$$q_b = \frac{-S_y}{I_{xx}} \sum_{r=1}^{n} B_r y_r \tag{i}$$

where, from Example 10.6, $I_{xx} = 809 \times 10^6\,\text{mm}^4$. Thus, from Eq. (i)

$$q_b = -\frac{86.8 \times 10^3}{809 \times 10^6} \sum_{r=1}^{n} B_r y_r = -1.07 \times 10^{-4} \sum_{r=1}^{n} B_r y_r \tag{ii}$$

Since $q_b = 0$ at each 'cut', then $q_b = 0$ for the skin panels 12, 23 and 34. The remaining q_b shear flows are now calculated using Eq. (ii). Note that the order of the numerals in the subscript of q_b indicates the direction of movement from boom to boom.

$$q_{b,27} = -1.07 \times 10^{-4} \times 3880 \times 230 = -95.5\,\text{N/mm}$$
$$q_{b,16} = -1.07 \times 10^{-4} \times 2580 \times 165 = -45.5\,\text{N/mm}$$
$$q_{b,65} = -45.5 - 1.07 \times 10^{-4} \times 2580 \times (-165) = 0$$
$$q_{b,57} = -1.07 \times 10^{-4} \times 3880 \times (-230) = 95.5\,\text{N/mm}$$
$$q_{b,38} = -1.07 \times 10^{-4} \times 3230 \times 200 = -69.0\,\text{N/mm}$$
$$q_{b,48} = -1.07 \times 10^{-4} \times 3230 \times (-200) = 69.0\,\text{N/mm}$$

Therefore, as $q_{b,83} = q_{b,48}$ (or $q_{b,72} = q_{b,57}$), $q_{b,78} = 0$. The distribution of the q_b shear flows is shown in Fig. 10.25. The values of δ and q_b are now substituted in Eq. (10.28) for each cell in turn.

For cell I

$$\frac{d\theta}{dz} = \frac{1}{2 \times 265\,000 G_{REF}} [q_{s,0,I}(1083 + 95 + 57) - 57 q_{s,0,II} + 69 \times 95 + 69 \times 57] \tag{iii}$$

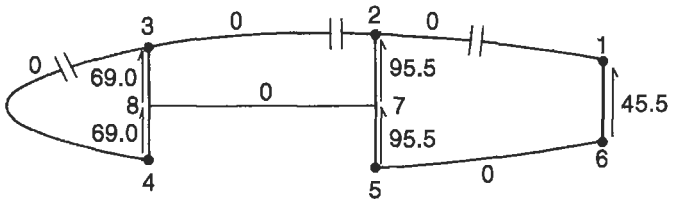

Fig. 10.25 q_b distribution (N/mm).

For cell II

$$\frac{d\theta}{dz} = \frac{1}{2 \times 213\,000 G_{REF}} [-57 q_{s,0,I} + q_{s,0,II}(783 + 57 + 347 + 68) - 68 q_{s,0,III} + 95.5 \times 68 - 69 \times 57] \quad \text{(iv)}$$

For cell III

$$\frac{d\theta}{dz} = \frac{1}{2 \times 413\,000 G_{REF}} [-68 q_{s,0,II} + q_{s,0,III}(840 + 68 + 106 + 840 + 202) + 45.5 \times 202 - 95.5 \times 68 - 95.5 \times 106] \quad \text{(v)}$$

The solely numerical terms in Eqs (iii) to (v) represent $\oint_R q_b(ds/t)$ for each cell. Care must be taken to ensure that the contribution of each q_b value to this term is interpreted correctly. The path of the integration follows the positive direction of $q_{s,0}$ in each cell, i.e. anticlockwise. Thus, the positive contribution of $q_{b,83}$ to $\oint_I q_b(ds/t)$ becomes a negative contribution to $\oint_{II} q_b(ds/t)$ and so on.

The fourth equation required for a solution is obtained from Eq. (10.30) by taking moments about the intersection of the x axis and the web 572. Thus

$$0 = -69.0 \times 250 \times 1270 - 69.0 \times 150 \times 1270 + 45.5 \times 330 \times 1020 + 2 \times 265\,000 q_{s,0,I} + 2 \times 213\,000 q_{s,0,II} + 2 \times 413\,000 q_{s,0,III} \quad \text{(vi)}$$

Simultaneous solution of Eqs (iii)–(vi) gives

$$q_{s,0,I} = 5.5\,\text{N/mm}, \quad q_{s,0,II} = 10.2\,\text{N/mm}, \quad q_{s,0,III} = 16.5\,\text{N/mm}$$

Superimposing these shear flows on the q_b distribution of Fig. 10.25, we obtain the final shear flow distribution. Thus

$$q_{34} = 5.5\,\text{N/mm}, \quad q_{23} = q_{87} = 10.2\,\text{N/mm}, \quad q_{12} = q_{56} = 16.5\,\text{N/mm}$$
$$q_{61} = 62.0\,\text{N/mm}, \quad q_{57} = 79.0\,\text{N/mm}, \quad q_{72} = 89.2\,\text{N/mm}$$
$$q_{48} = 74.5\,\text{N/mm}, \quad q_{83} = 64.3\,\text{N/mm}$$

Finally, from any of Eqs (iii)–(v)

$$\frac{d\theta}{dz} = 1.16 \times 10^{-6}\,\text{rad/mm}$$

10.3.4 Shear centre

The position of the shear centre of a wing section is found in an identical manner to that described in Section 9.4. Arbitrary shear loads S_x and S_y are applied in turn through the shear centre S, the corresponding shear flow distributions determined and moments taken about some convenient point. The shear flow distributions are obtained as described previously in the shear of multicell wing sections except that the N equations of the type (10.28) are sufficient for a solution since the rate of twist $d\theta/dz$ is zero for shear loads applied through the shear centre.

10.3.5 Tapered wings

Wings are generally tapered in both spanwise and chordwise directions. The effects on the analysis of taper in a single cell beam have been discussed in Section 10.1. In a multicell wing section the effects are dealt with in an identical manner except that the moment equation (10.16) becomes, for an N-cell wing section (see Figs 10.5 and 10.22)

$$S_x\eta_0 - S_y\xi_0 = \sum_{R=1}^{N} \oint_R q_b p_0 \, ds + \sum_{R=1}^{N} 2A_R q_{s,0,R} - \sum_{r=1}^{m} P_{x,r}\eta_r - \sum_{r=1}^{m} P_{y,r}\xi_r \qquad (10.31)$$

Example 10.9

A two-cell beam has singly symmetrical cross-sections 1.2 m apart and tapers symmetrically in the y direction about a longitudinal axis (Fig. 10.26). The beam supports loads which produce a shear force $S_y = 10\,\text{kN}$ and a bending moment

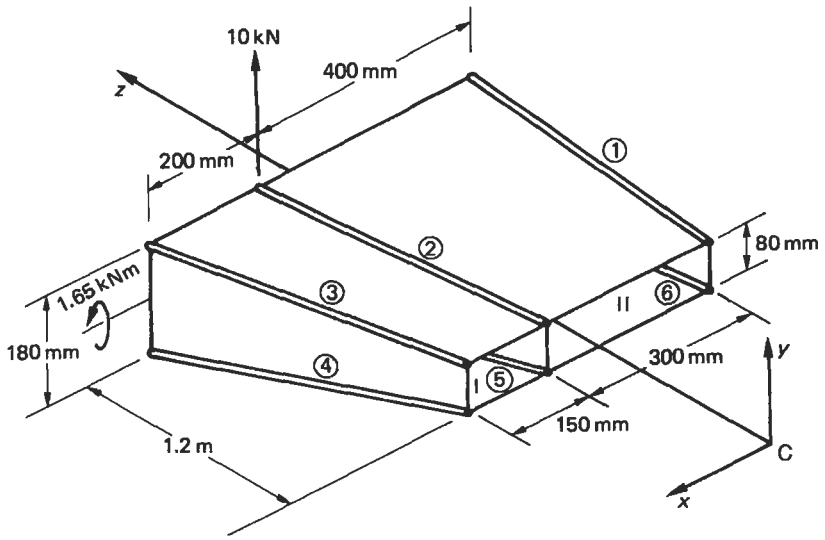

Fig. 10.26 Tapered beam of Example 10.9.

$M_x = 1.65\,\text{kN m}$ at the larger cross-section; the shear load is applied in the plane of the internal spar web. If booms 1 and 6 lie in a plane which is parallel to the yz plane calculate the forces in the booms and the shear flow distribution in the walls at the larger cross-section. The booms are assumed to resist all the direct stresses while the walls are effective only in shear. The shear modulus is constant throughout, the vertical webs are all 1.0 mm thick while the remaining walls are all 0.8 mm thick.

$$\text{Boom areas: } B_1 = B_3 = B_4 = B_6 = 600\,\text{mm}^2,\ B_2 = B_5 = 900\,\text{mm}^2$$

At the larger cross-section

$$I_{xx} = 4 \times 600 \times 90^2 + 2 \times 900 \times 90^2 = 34.02 \times 10^6\,\text{mm}^4$$

The direct stress in a boom is given by Eq. (9.6) in which $I_{xy} = 0$ and $M_y = 0$, i.e.

$$\sigma_{z,r} = \frac{M_x y_r}{I_{xx}}$$

whence

$$P_{z,r} = \frac{M_x y_r}{I_{xx}} B_r$$

or

$$P_{z,r} = \frac{1.65 \times 10^6 y_r B_r}{34.02 \times 10^6} = 0.08 y_r B_r \qquad \text{(i)}$$

The value of $P_{z,r}$ is calculated from Eq. (i) in column ② of Table 10.5; $P_{x,r}$ and $P_{y,r}$ follow from Eqs (10.10) and (10.9) respectively in columns ⑤ and ⑥. The axial load P_r is given by $[②^2 + ⑤^2 + ⑥^2]^{1/2}$ in column ⑦ and has the same sign as $P_{z,r}$ (see Eq. (10.12)). The moments of $P_{x,r}$ and $P_{y,r}$, columns ⑩ and ⑪, are calculated for a moment centre at the mid-point of the internal web taking anticlockwise moments as positive.

From column ⑤

$$\sum_{r=1}^{6} P_{x,r} = 0$$

(as would be expected from symmetry).

Table 10.5

① Boom	② $P_{z,r}$ (N)	③ δ_{x_r}/δ_z	④ δ_{y_r}/δ_z	⑤ $P_{x,r}$ (N)	⑥ $P_{y,r}$ (N)	⑦ P_r (N)	⑧ ξ_r (mm)	⑨ η_r (mm)	⑩ $P_{x,r}\eta_r$ (N mm)	⑪ $P_{y,r}\xi_r$ (N mm)
1	2619.0	0	0.0417	0	109.2	2621.3	400	90	0	43 680
2	3928.6	0.0833	0.0417	327.3	163.8	3945.6	0	90	−29 457	0
3	2619.0	0.1250	0.0417	327.4	109.2	2641.6	200	90	−29 466	21 840
4	−2619.0	0.1250	−0.0417	−327.4	109.2	−2641.6	200	90	−29 466	21 840
5	−3928.6	0.0833	−0.0417	−327.3	163.8	−3945.6	0	90	−29 457	0
6	−2619.0	0	−0.0417	0	109.2	−2621.3	400	90	0	−43 680

From column ⑥

$$\sum_{r=1}^{6} P_{y,r} = 764.4\,\text{N}$$

From column ⑩

$$\sum_{r=1}^{6} P_{x,r}\eta_r = -117\,846\,\text{N mm}$$

From column ⑪

$$\sum_{r=1}^{6} P_{y,r}\xi_r = -43\,680\,\text{N mm}$$

From Eqs (10.15)

$$S_{x,w} = 0, \quad S_{y,w} = 10 \times 10^3 - 764.4 = 9235.6\,\text{N}$$

Also, since Cx is an axis of symmetry, $I_{xy} = 0$ and Eq. (9.75) for the 'open section' shear flow reduces to

$$q_b = -\frac{S_{y,w}}{I_{xx}} \sum_{r=1}^{n} B_r y_r$$

or

$$q_b = -\frac{9235.6}{34.02 \times 10^6} \sum_{r=1}^{n} B_r y_r = -2.715 \times 10^{-4} \sum_{r=1}^{n} B_r y_r \qquad \text{(ii)}$$

'Cutting' the top walls of each cell and using Eq. (ii), we obtain the q_b distribution shown in Fig. 10.27. Evaluating δ for each wall and substituting in Eq. (10.28) gives

for cell I

$$\frac{d\theta}{dz} = \frac{1}{2 \times 36\,000G}(760q_{s,0,\text{I}} - 180q_{s,0,\text{II}} - 1314) \qquad \text{(iii)}$$

for cell II

$$\frac{d\theta}{dz} = \frac{1}{2 \times 72\,000G}(-180q_{s,0,\text{I}} + 1160q_{s,0,\text{II}} + 1314) \qquad \text{(iv)}$$

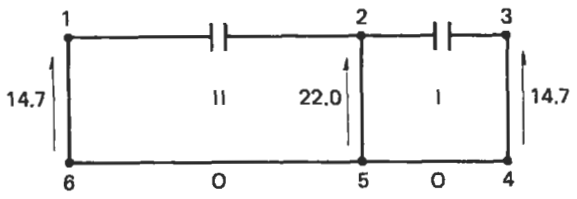

Fig. 10.27 q_b (N/mm) distribution in beam section of Example 10.9 (view along z axis towards C).

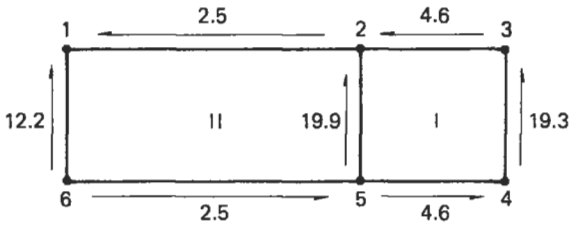

Fig. 10.28 Shear flow (N/mm) distribution in tapered beam of Example 10.9.

Taking moments about the mid-point of web 25 we have, using Eq. (10.31)

$$0 = -14.7 \times 180 \times 400 + 14.7 \times 180 \times 200 + 2 \times 36\,000 q_{s,0,\mathrm{I}} + 2 \times 72\,000 q_{s,0.\mathrm{II}} - 117\,846 - 43\,680$$

or

$$0 = -690\,726 + 72\,000 q_{s,0,\mathrm{I}} + 144\,000 q_{s,0,\mathrm{II}} \qquad \text{(v)}$$

Solving Eqs (iii)–(v) gives

$$q_{s,0,\mathrm{I}} = 4.6\,\mathrm{N/mm}, \quad q_{s,0,\mathrm{II}} = 2.5\,\mathrm{N/mm}$$

and the resulting shear flow distribution is shown in Fig. 10.28.

10.3.6 Method of successive approximations – torsion

It is clear from the torsion and shear loading of multicell wing sections that the greater the number of cells the greater the number of simultaneous equations requiring solution. Some modern aircraft have wings comprising a relatively large number of cells, for example, the Harrier wing shown in Fig. 7.8, so that the arithmetical labour involved becomes extremely tedious unless a computer is used; an approximate but much more rapid method may therefore be preferable. The method of successive approximations provides a simple and rapid method for calculating the shear flow in many-celled wing sections and may be used with slight differences of treatment for both the pure torsion and shear loading cases. Initially we shall consider a wing section subjected to a pure torque.

The mechanics of the method may be illustrated by considering the simple two-cell wing section shown in Fig. 10.29 and which carries a pure torque T. First we assume

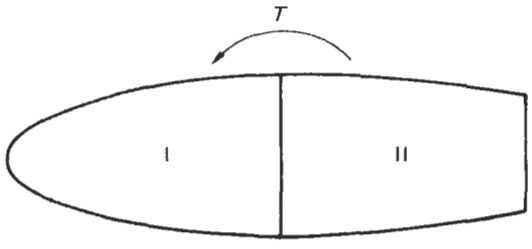

Fig. 10.29 Method of successive approximations applied to a two-cell wing section.

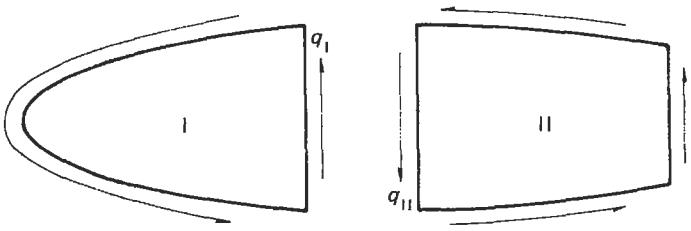

Fig. 10.30 Shear flows giving $G(\mathrm{d}\theta/\mathrm{d}z) = 1$ for the separated cells of a two-cell wing section.

that each cell acts independently and that cell I is subjected to a constant shear flow q_I such that $G(\mathrm{d}\theta/\mathrm{d}z)$ for cell I is equal to unity. From Eqs (9.49) and (9.52)

$$G\left(\frac{\mathrm{d}\theta}{\mathrm{d}z}\right)_I = \frac{q_I}{2A_I}\delta_I = 1$$

where

$$\delta_I = \oint_I \mathrm{d}s/t$$

Hence

$$q_I = \frac{2A_I}{\delta_I}$$

Similarly, for $G(\mathrm{d}\theta/\mathrm{d}z)$ to be unity for cell II

$$q_{II} = \frac{2A_{II}}{\delta_{II}}$$

We now have the situation shown in Fig. 10.30 where the two cells are separate and

$$G\left(\frac{\mathrm{d}\theta}{\mathrm{d}z}\right)_I = G\left(\frac{\mathrm{d}\theta}{\mathrm{d}z}\right)_{II} = 1$$

Imagine now that the two cells are rejoined with the interior web as a common part of both cells. The action of q_{II} is to reduce the rate of twist in cell I by applying, in effect, a clockwise torque to cell I opposing the anticlockwise torque corresponding to q_I. Thus, $G(\mathrm{d}\theta/\mathrm{d}z)_I$ is not now equal to $G(\mathrm{d}\theta/\mathrm{d}z)_{II}$ so that the assumption of an undistorted cross-section is invalidated and the shear flows q_I and q_{II} are therefore not the true shear flows.

To correct this situation we again suppose that the cells are separated and apply constant shear flows q_I' and q_{II}' around cells I and II respectively to counteract the effect of q_{II} (shown dotted) on cell I and q_I on cell II. The total shear flows now acting on each cell are shown in Fig. 10.31. Note that the effect of a shear flow acting on one wall of a cell, e.g. q_{II} applied to the internal web and acting on cell I, is counteracted by a constant shear flow applied around the complete cell. Thus

$$\frac{q_I'}{2A_I}\delta_I - \frac{q_{II}}{2A_I}\delta_{I,II} = 0$$

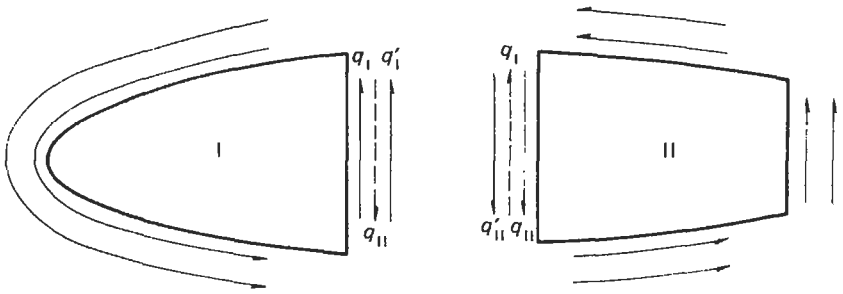

Fig. 10.31 First correction shear flows applied to give $G(\mathrm{d}\theta/\mathrm{d}z) = 1$ for the separated cells of a two-cell wing section.

where $\delta_{I,II} = \int \mathrm{d}s/t$ for the wall common to cells I and II. Hence

$$q'_I = q_{II}\frac{\delta_{I,II}}{\delta_I} \tag{10.32}$$

Similarly

$$q'_{II} = q_I\frac{\delta_{I,II}}{\delta_{II}} \tag{10.33}$$

Since q'_I and q'_{II} are expressed in terms of the shear flows in adjacent cells they are referred to as *correction carry over shear flows*. The factors $\delta_{I,II}/\delta_I$ and $\delta_{I,II}/\delta_{II}$ are known as *correction carry over factors* and may be written as

$$C_{I,II} = \frac{\delta_{I,II}}{\delta_{II}}, \quad C_{II,I} = \frac{\delta_{I,II}}{\delta_I} \tag{10.34}$$

We are now in a similar position to that at the beginning of the example with the wing section divided into two separate cells in which $G(\mathrm{d}\theta/\mathrm{d}z) = 1$ but which are now subjected to shear flows of, in cell I, q_I, q_{II} (on the internal web) and q'_I and, in cell II, q_{II}, q_I (on the internal web) and q'_{II}. On rejoining the cells we see that q'_{II} from cell II acts on the internal web wall of cell I and q'_I from cell I acts on the internal web wall of cell II thereby destroying the equality and unit value of $G(\mathrm{d}\theta/\mathrm{d}z)$ for each cell. We therefore apply second correction shear flows q''_I and q''_{II} completely around the separated cells I and II respectively where, from Eqs (10.32), (10.33) and (10.34)

$$q''_I = q'_{II}C_{II,I}, \quad q''_{II} = q'_I C_{I,II}$$

Clearly the second correction shear flows are smaller than the first so that if the procedure is repeated a number of times the correction carry over shear flows rapidly become negligible. In practice, the number of corrections made depends on the accuracy required. The final shear flows in each cell corresponding to $G(\mathrm{d}\theta/\mathrm{d}z) \approx 1$ are then

$$q_{I(\text{final})} = q_I + q'_I + q''_I + q'''_I + \cdots$$

$$q_{II(\text{final})} = q_{II} + q'_{II} + q''_{II} + q'''_{II} + \cdots$$

The actual shear flows are obtained by factoring the final shear flows by the ratio of the applied torque to the torque corresponding to the final shear flows, i.e.

$$q_{\text{actual}} = \left(\sum_{r=1}^{N} 2A_R q_{R(\text{final})} / T \right) q_{(\text{final})}$$

Example 10.10

Solve Example 10.7 using the method of successive approximations.

From Example 10.7

$$\delta_{\text{I}} = 1542 + 250 = 1792$$

$$\delta_{\text{II}} = 250 + 725 + 233 + 725 = 1933$$

$$\delta_{\text{III}} = 736 + 233 + 736 + 368 = 2073$$

$$\delta_{\text{I,II}} = 250$$

$$\delta_{\text{II,III}} = 233$$

Hence, from Eqs (10.34)

$$C_{\text{I,II}} = \frac{250}{1933} = 0.129$$

$$C_{\text{II,I}} = \frac{250}{1792} = 0.140$$

$$C_{\text{II,III}} = \frac{233}{2073} = 0.112$$

$$C_{\text{III,II}} = \frac{233}{1933} = 0.121$$

Also

$$q_{\text{I}} = \frac{2 \times 258\,000}{1792} = 287.9\,\text{N/mm}$$

$$q_{\text{II}} = \frac{2 \times 355\,000}{1933} = 367.3\,\text{N/mm}$$

$$q_{\text{III}} = \frac{2 \times 161\,000}{2073} = 155.3\,\text{N/mm}$$

The remainder of the solution is completed in Table 10.6. Note that the assumed values of q_{I}, q_{II} and q_{III} are rounded off since the method is approximate.

The solution is virtually identical to that of Example 10.7. Note that the variation in shear modulus is treated in the same way as that in Example 10.7, i.e. a reference value is chosen and the actual thicknesses converted to modulus weighted thicknesses t^*; δ is then $\int \mathrm{d}s/t^*$.

Table 10.6

	Cell I	Cell II	Cell III
Cs	0.129	0.149 0.112	0.121
Assumed q (N/mm)	288	367	155
COq	51.38	37.15 18.76	41.10
COq	5.20	6.63 4.97	2.10
COq	0.93	0.67 0.25	0.56
COq	0.09	0.12 0.07	0.03
Final q (N/mm)	345.6	435.6	198.8
$2Aq$ (N mm)	1.78×10^8	3.09×10^8	0.64×10^8
Total T (N mm)		5.51×10^8	
Actual q (N/mm) ($T = 11.3$ kN m)	7.1	8.9	4.1

10.3.7 Method of successive approximations – shear

The method is restricted to shear loads applied through the shear centre of the wing section so that the rate of twist in each cell is zero. Having determined the position of the shear centre from the resulting shear flow distribution, the case of a wing section subjected to shear loads not applied through the shear centre is solved by replacing the actual loading system by shear loads acting through the shear centre together with a pure torque; the two separate solutions are then superimposed.

Consider the three-cell wing section subjected to a shear load S_y applied through its shear centre shown in Fig. 10.32; the section comprises booms and direct stress carrying skin. The first step is to 'cut' each cell to produce an 'open section' beam (Fig. 10.33). While it is theoretically immaterial where the 'cuts' are made a more rapid convergence in the solution is obtained if the top or bottom skin panels are

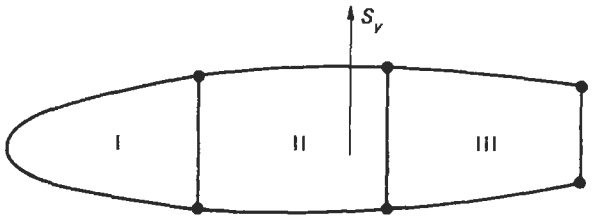

Fig. 10.32 Three-cell wing section subjected to a shear load through its shear centre.

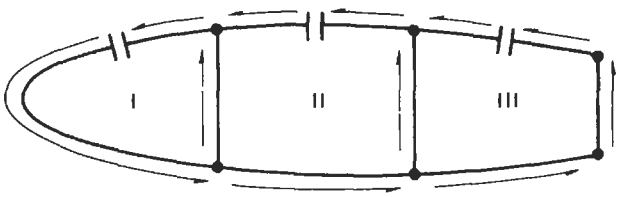

Fig. 10.33 'Open section' shear flows (q_b).

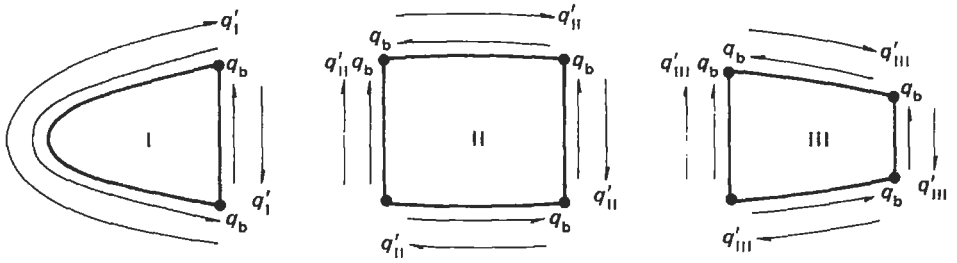

Fig. 10.34 Constant shear flows applied to each cell to counteract the twisting effect of q_b shear flows.

'cut'. This is due to the fact that, in a section carrying a shear load without twist, the spar webs carry the greater shear flows so that the 'open section' shear flows in the webs will be closer to the final values than if the webs were 'cut', giving a more rapid convergence in the successive approximation procedure. Clearly the reverse is the case if a horizontal shear load is applied. The 'open section' shear flow distribution is obtained using Eq. (9.75) in which $S_x = 0$, i.e.

$$q_b = \frac{S_y I_{xy}}{I_{xx} I_{yy} - I_{xy}^2} \left(\int_0^s t_D x \, ds + \sum_{r=1}^{n} B_r x_r \right) - \frac{S_y I_{yy}}{I_{xx} I_{yy} - I_{xy}^2} \times \left(\int_0^s t_D y \, ds + \sum_{r=1}^{n} B_r y_r \right) \tag{10.35}$$

If we now imagine that each cell is separate and closed, the above q_b shear flows will cause each cell to twist. We therefore apply constant shear flows q'_I, q'_{II} and q'_{III} to cells I, II and III respectively to reduce this twist to zero (Fig. 10.34). On rejoining the cells it is clear that q'_{II} will cause twist in cell I by its action on the web common to cells I and II, that q'_I will cause twist in cell II and so on. We therefore apply a second system of corrective shear flows q''_I, q''_{II}, q''_{III} to the separated cells I, II and III respectively. However, since the cells are not separate these additional shear flows cause twist in adjacent cells so that a third system of constant corrective shear flows is required. This procedure is repeated until the corrective shear flows become negligibly small. The totals q_I, q_{II} and q_{III} of the corrective shear flows are then given by

$$q_I = q'_I + q''_I + q'''_I + \cdots$$
$$q_{II} = q'_{II} + q''_{II} + q'''_{II} + \cdots$$
$$q_{III} = q'_{III} + q''_{III} + q'''_{III} + \cdots$$

so that the final shear flow distribution is

$$q_{(\text{final})} = q_b + q_I + q_{II} + q_{III} \tag{10.36}$$

It should be noted that all the shear flows in Eq. (10.36) do not act on every wall of the wing section. For example, on the spar web common to cells I and II the final shear flow is the sum of q_b, q_I and q_{II}.

The equations from which the actual values of q_I, q_{II} and q_{III} are obtained are derived as follows. Consider cell II, with its final shear flow acting as shown in

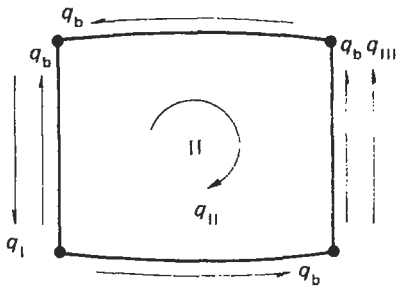

Fig. 10.35 Final shear flow system in Cell II.

Fig. 10.35. Since the cell does not twist then, from Eq. (9.42)

$$\frac{d\theta}{dz} = \frac{1}{2A_{II}G}\oint_{II} q\frac{ds}{t} = 0$$

or

$$\oint_{II} q\frac{ds}{t} = 0$$

Hence, from Fig. 10.35 and taking anticlockwise torques as positive

$$\oint_{II} q_b\frac{ds}{t} - q_{II}\delta_{II} + q_I\delta_{I,II} + q_{III}\delta_{III,II} = 0$$

giving

$$q_{II} = \frac{\oint_{II} q_b(ds/t)}{\delta_{II}} + q_I\frac{\delta_{I,II}}{\delta_{II}} + q_{III}\frac{\delta_{III,II}}{\delta_{II}} \tag{10.37}$$

The first term on the right-hand side of Eq. (10.37) represents the proportion of the 'open section' shear flow q_b which acts as a constant shear flow around the cell to cancel out the twist due to q_b; the second and third terms counteract the twist due to q_I and q_{III}. Rewriting Eq. (10.37)

$$q_{II} = q'_{II} + C_{I,II}q_I + C_{III,II}q_{III} \tag{10.38}$$

in which $C_{I,II}$ is the correction carry over factor from cell I to cell II and $C_{III,II}$ is the correction carry over factor from cell III to cell II.

As a first approximation in the solution we neglect the effect of the shear flows in adjacent cells so that

$$q_{II} \approx q'_{II}$$

Similarly

$$q_I \approx q'_I, \quad q_{III} \approx q'_{III}$$

Substituting these values in Eq. (10.38) we have

$$q_{II} = q'_{II} + C_{I,II}q'_I + C_{III,II}q'_{III} \tag{10.39}$$

or

$$q_{II} = q'_{II} + q''_{II} \tag{10.40}$$

Similarly and simultaneously, corrections q_{I}'' and q_{III}'' are applied to the approximations for q_{I} and q_{III} which in turn affect q_{II}. Thus, when the corrective shear flows become negligibly small we have

$$q_{\mathrm{II}} = q_{\mathrm{II}}' + C_{\mathrm{I,II}}(q_{\mathrm{I}}' + q_{\mathrm{I}}'' + \cdots) + C_{\mathrm{III,II}}(q_{\mathrm{III}}' + q_{\mathrm{III}}'' + \cdots)$$

Similar expressions are derived for q_{I} and q_{III}.

Example 10.11

Determine the shear flow distribution in the singly symmetrical three-cell wing section shown in Fig. 10.36 when it carries a shear load of 100 kN applied through its shear centre and hence find the distance of the shear centre from the spar web 34. Assume that all direct stresses are resisted by the booms while the skin is effective only in shear. The shear modulus G is constant throughout

Boom areas: $B_1 = B_6 = 2500\,\mathrm{mm}^2$, $B_2 = B_5 = 3800\,\mathrm{mm}^2$, $B_3 = B_4 = 3200\,\mathrm{mm}^2$

Cell areas: $A_{\mathrm{I}} = 265\,000\,\mathrm{mm}^2$, $A_{\mathrm{II}} = 580\,000\,\mathrm{mm}^2$, $A_{\mathrm{III}} = 410\,000\,\mathrm{mm}^2$

Wall	12, 56	23, 45	34°	16	25	34[i]
Length (mm)	1025	1275	2200	330	460	400
Thickness (mm)	1.25	1.65	2.25	1.65	2.65	2.65

Initially we calculate δ_{I}, δ_{II} etc. and the correction carry over factors $C_{\mathrm{I,II}}$, $C_{\mathrm{II,I}}$ etc.

$$\delta_{\mathrm{I}} = \frac{2200}{2.25} + \frac{400}{2.65} = 1128.7$$

Similarly

$$\delta_{\mathrm{II}} = 1870.0, \delta_{\mathrm{III}} = 2013.6, \delta_{\mathrm{I,II}} = \delta_{\mathrm{II,I}} = 150.9$$

$$\delta_{\mathrm{II,III}} = \delta_{\mathrm{III,II}} = 173.6$$

$$C_{\mathrm{I,II}} = \frac{150.9}{1870.0} = 0.081$$

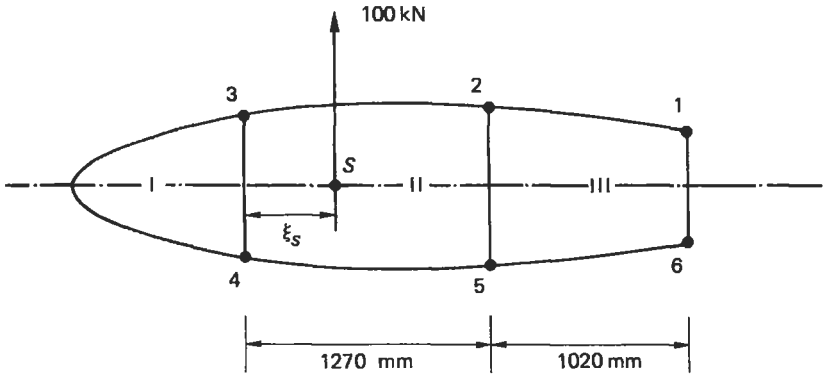

Fig. 10.36 Three-cell wing section of Example 10.11.

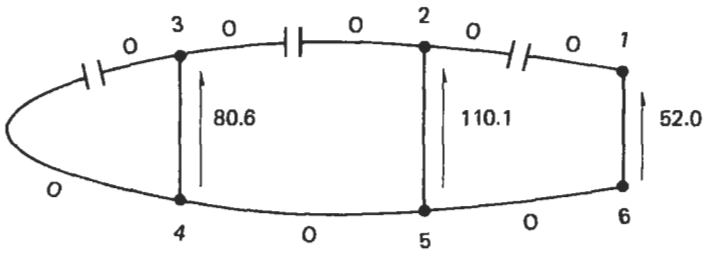

Fig. 10.37 Open section shear flow (N/mm) distribution in wing section of Example 10.11.

Similarly

$$C_{\mathrm{II,I}} = 0.134, C_{\mathrm{II,III}} = 0.086, C_{\mathrm{III,II}} = 0.093$$

The wing section has the x axis as an axis of symmetry, is completely idealized and carries a vertical shear load only so that Eq. (10.35) reduces to

$$q_{\mathrm{b}} = -\frac{S_y}{I_{xx}} \sum_{r=1}^{n} B_r y_r$$

in which

$$I_x = 2 \times 2500 \times 165^2 + 2 \times 3800 \times 230^2 + 2 \times 3200 \times 200^2 = 7.94 \times 10^8 \,\mathrm{mm}^4$$

Thus

$$q_{\mathrm{b}} = \frac{-100 \times 10^3}{7.94 \times 10^8} \sum_{r=1}^{n} B_r y_r = -1.26 \times 10^{-4} \sum_{r=1}^{n} B_r y_r \qquad \text{(i)}$$

'Cutting' the top skin panel in each cell, we obtain, using Eq. (i), the q_{b} shear flow distribution shown in Fig. 10.37. From Fig. 10.37

$$\oint_{\mathrm{I}} q_{\mathrm{b}} \frac{\mathrm{d}s}{t} = \frac{80.6 \times 400}{2.65} = 12\,166.0 \,\mathrm{N/mm}$$

$$\oint_{\mathrm{II}} q_{\mathrm{b}} \frac{\mathrm{d}s}{t} = 6945.7 \,\mathrm{N/mm}$$

$$\oint_{\mathrm{III}} q_{\mathrm{b}} \frac{\mathrm{d}s}{t} = -6218.9 \,\mathrm{N/mm}$$

The solution is now completed in Table 10.7.

Note that in Table 10.7 a negative sign is used to indicate that q_{I}' etc. are in the opposite sense to q_{b}. The final shear flow distribution is shown in Fig. 10.38.

A check on the vertical equilibrium of the wing section gives

$$(11.4 \times 400 + 73.6 \times 400 + 2 \times 4.4 \times 30 + 103.0 \times 460 + 2 \times 2.7 \times 65$$
$$+54.7 \times 330)/10^3 = 100 \,\mathrm{kN}$$

Now taking moments about the centre of spar web 34

$$100 \times 10^3 \xi_s = 2A_{\mathrm{I}} q_{\mathrm{I}} + 2A_{\mathrm{II}} q_{\mathrm{II}} + 2A_{\mathrm{III}} q_{\mathrm{III}} + 110.1 \times 460 \times 1270 + 52 \times 330 \times 2290$$

which gives $\xi_s = 946.8 \,\mathrm{mm}$.

Table 10.7

	Cell I	Cell II	Cell III
$\oint q_b\,ds/t$	12 166.0	6945.7	−6218.9
δ	1128.7	1870.0	2013.6
Cs	0.08	0.134 0.086	0.093
$q'[=-(\oint q_b\,ds/t)/\delta]$	−10.78	−3.71	3.09
COq	−0.50	−0.86 0.29	−0.32
COq	−0.08	−0.04 −0.03	−0.05
COq	−0.01	−0.01 0	0
Corrective shear flows	−11.37	−4.36	2.73

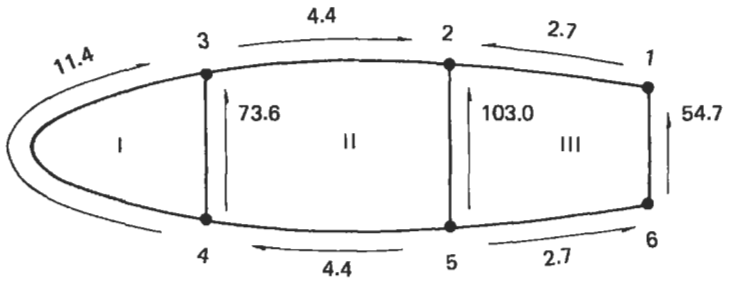

Fig. 10.38 Final shear flow (N/mm) distribution in wing section of Example 10.11.

Note that for convenience of calculation, the moments due to the 'open section' shear flows and the corrective shear flows are computed separately.

10.3.8 Deflections

Deflections of multicell wings may be calculated by the unit load method in an identical manner to that described in Section 9.10 for open and single cell beams.

Example 10.12

Calculate the deflection at the free end of the two-cell beam shown in Fig. 10.39 allowing for both bending and shear effects. The booms carry all the direct stresses while the skin panels, of constant thickness throughout, are effective only in shear.

$$\text{Take } E = 69\,000\ \text{N/mm}^2 \text{ and } G = 25\,900\ \text{N/mm}^2$$

$$\text{Boom areas: } -B_1 = B_3 = B_4 = B_6 = 650\ \text{mm}^2,\ B_2 = B_5 = 1300\ \text{mm}^2$$

The beam cross-section is symmetrical about a horizontal axis and carries a vertical load at its free end through the shear centre. The deflection Δ at the free end is then, from Eqs (9.86) and (9.88)

$$\Delta = \int_0^{2000} \frac{M_{x,0}M_{x,1}}{EI_{xx}}\,dz + \int_0^{2000} \left(\int_{\text{section}} \frac{q_0 q_1}{Gt}\,ds \right) dz \qquad \text{(i)}$$

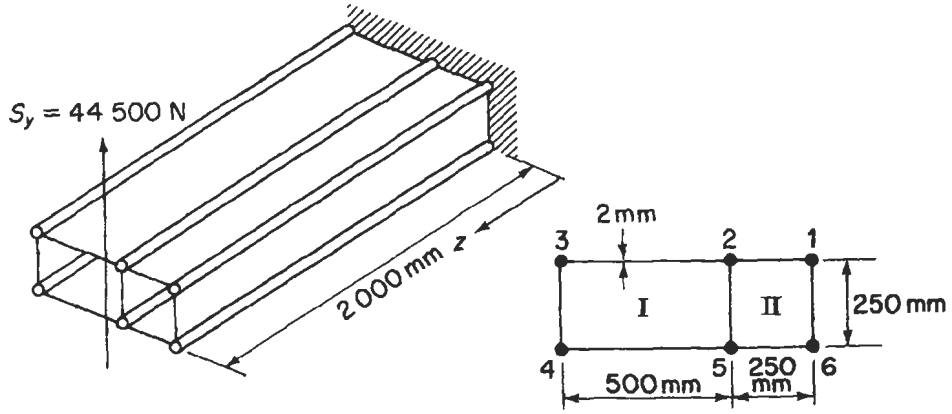

Fig. 10.39 Deflection of two-cell wing section.

where

$$M_{x,0} = -44.5 \times 10^3(2000 - z), \quad M_{x,1} = -(2000 - z)$$

and

$$I_{xx} = 4 \times 650 \times 125^2 + 2 \times 1300 \times 125^2 = 81.3 \times 10^6\,\text{mm}^4$$

also

$$S_{y,0} = 44.5 \times 10^3\,\text{N}, \quad S_{y,1} = 1$$

The q_0 and q_1 shear flow distributions are obtained as previously described (note $d\theta/dz = 0$ for a shear load through the shear centre) and are

$$q_{0,12} = 9.6\,\text{N/mm}, \quad q_{0,23} = -5.8\,\text{N/mm}, \quad q_{0,43} = 50.3\,\text{N/mm}$$

$$q_{0,45} = -5.8\,\text{N/mm}, \quad q_{0,56} = 9.6\,\text{N/mm}, \quad q_{0,61} = 54.1\,\text{N/mm}$$

$q_{0,52} = 73.6\,\text{N/mm}$ at all sections of the beam

The q_1 shear flows in this case are given by $q_0/44.5 \times 10^3$. Thus

$$\int_{\text{section}} \frac{q_0 q_1}{Gt}\,ds = \frac{1}{25\,900 \times 2 \times 44.5 \times 10^3}(9.6^2 \times 250 \times 2 + 5.8^2 \times 500 \times 2 + 50.3^2 \times 250 + 54.1^2 \times 250 + 73.6^2 \times 250)$$

$$= 1.22 \times 10^{-3}$$

Hence, from Eq. (i)

$$\Delta = \int_0^{2000} \frac{44.5 \times 10^3(2000 - z)^2}{69\,000 \times 81.3 \times 10^6}\,dz + \int_0^{2000} 1.22 \times 10^{-3}\,dz$$

giving

$$\Delta = 23.5\,\text{mm}$$

10.4 Fuselage frames and wing ribs

Aircraft are constructed primarily from thin metal skins which are capable of resisting in-plane tension and shear loads but buckle under comparatively low values of in-plane compressive loads. The skins are therefore stiffened by longitudinal stringers which resist the in-plane compressive loads and, at the same time, resist small distributed loads normal to the plane of the skin. The effective length in compression of the stringers is reduced, in the case of fuselages, by transverse frames or bulkheads or, in the case of wings, by ribs. In addition, the frames and ribs resist concentrated loads in transverse planes and transmit them to the stringers and the plane of the skin. Thus, cantilever wings may be bolted to fuselage frames at the spar caps while undercarriage loads are transmitted to the wing through spar and rib attachment points.

Generally, frames and ribs are themselves fabricated from thin sheets of metal and therefore require stiffening members to distribute the concentrated loads to the thin webs. If the load is applied in the plane of a web the stiffeners must be aligned with the direction of the load. Alternatively, if this is not possible, the load should be applied at the intersection of two stiffeners so that each stiffener resists the component of load in its direction. The basic principles of stiffener/web construction are illustrated in Example 10.13.

Example 10.13

A cantilever beam (Fig. 10.40) carries concentrated loads as shown. Calculate the distribution of stiffener loads and the shear flow distribution in the web panels assuming that the latter are effective only in shear.

We note that stiffeners HKD and JK are required at the point of application of the 4000 N load to resist its vertical and horizontal components. A further transverse stiffener GJC is positioned at the unloaded end J of the stiffener JK since stress

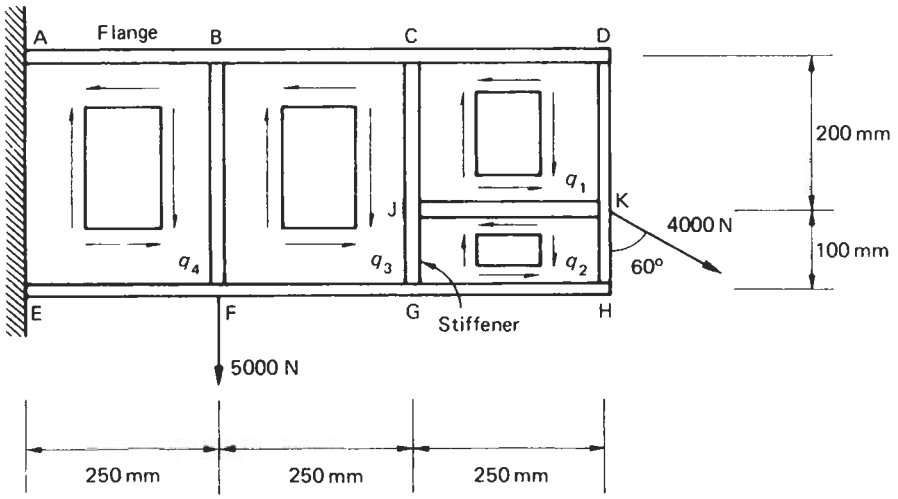

Fig. 10.40 Cantilever beam of Example 10.13.

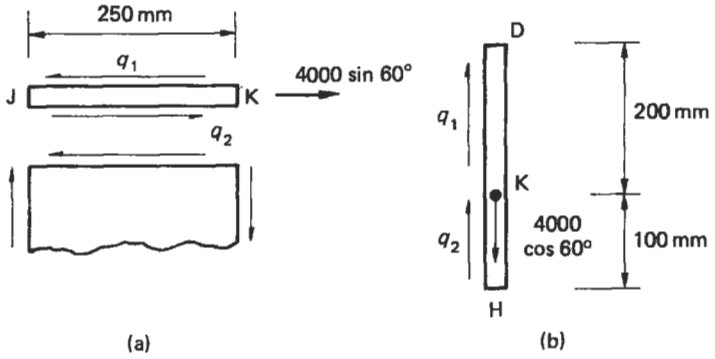

Fig. 10.41 Free body diagrams of stiffeners JK and HKD in the beam of Example 10.13.

concentrations are produced if a stiffener ends in the centre of a web panel. We note also that the web panels are only effective in shear so that the shear flow is constant throughout a particular web panel; the assumed directions of the shear flows are shown in Fig. 10.40.

It is instructive at this stage to examine the physical role of the different structural components in supporting the applied loads. Generally, stiffeners are assumed to withstand axial forces only so that the horizontal component of the load at K is equilibrated locally by the axial load in the stiffener JK and not by the bending of stiffener HKD. By the same argument the vertical component of the load at K is resisted by the axial load in the stiffener HKD. These axial stiffener loads are equilibrated in turn by the resultants of the shear flows q_1 and q_2 in the web panels CDKJ and JKHG. Thus we see that the web panels resist the shear component of the externally applied load and at the same time transmit the bending and axial load of the externally applied load to the beam flanges; subsequently, the flange loads are reacted at the support points A and E.

Consider the free body diagrams of the stiffeners JK and HKD shown in Figs 10.41(a) and (b).

From the equilibrium of stiffener JK we have

$$(q_1 - q_2) \times 250 = 4000 \sin 60° = 3464.1\,\text{N} \tag{i}$$

and from the equilibrium of stiffener HKD

$$200q_1 + 100q_2 = 4000 \cos 60° = 2000\,\text{N} \tag{ii}$$

Solving Eqs (i) and (ii) we obtain

$$q_1 = 11.3\,\text{N/mm}, \quad q_2 = -2.6\,\text{N/mm}$$

The vertical shear force in the panel BCGF is equilibrated by the vertical resultant of the shear flow q_3. Thus

$$300q_3 = 4000 \cos 60° = 2000\,\text{N}$$

whence

$$q_3 = 6.7\,\text{N/mm}$$

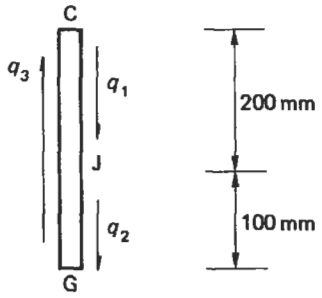

Fig. 10.42 Equilibrium of stiffener CJG in the beam of Example 10.13.

Alternatively, q_3 may be found by considering the equilibrium of the stiffener CJG. From Fig. 10.42

$$300q_3 = 200q_1 + 100q_2$$

or

$$300q_3 = 200 \times 11.3 - 100 \times 2.6$$

from which

$$q_3 = 6.7\,\text{N/mm}$$

The shear flow q_4 in the panel ABFE may be found using either of the above methods. Thus, considering the vertical shear force in the panel

$$300q_4 = 4000\cos 60° + 5000 = 7000\,\text{N}$$

whence

$$q_4 = 23.3\,\text{N/mm}$$

Alternatively, from the equilibrium of stiffener BF

$$300q_4 - 300q_3 = 5000\,\text{N}$$

whence

$$q_4 = 23.3\,\text{N/mm}$$

The flange and stiffener load distributions are calculated in the same way and are obtained from the algebraic summation of the shear flows along their lengths. For example, the axial load P_A at A in the flange ABCD is given by

$$P_A = 250q_1 + 250q_3 + 250q_4$$

or

$$P_A = 250 \times 11.3 + 250 \times 6.7 + 250 \times 23.3 = 10\,325\,\text{N (Tension)}$$

Similarly

$$P_E = -250q_2 - 250q_3 - 250q_4$$

i.e.

$$P_E = 250 \times 2.6 - 250 \times 6.7 - 250 \times 23.3 = -6850\,\text{N (Compression)}$$

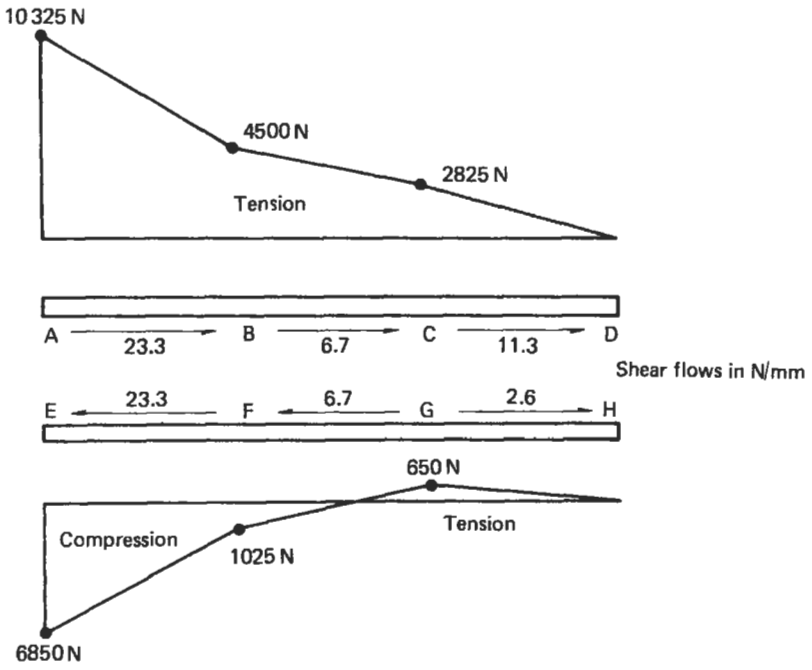

Fig. 10.43 Load distributions in flanges of the beam of Example 10.13.

The complete load distribution in each flange is shown in Fig. 10.43. The stiffener load distributions are calculated in the same way and are shown in Fig. 10.44.

The distribution of flange load in the bays ABFE and BCGF could have been obtained by considering the bending and axial loads on the beam at any section. For example, at the section AE we can replace the actual loading system by a bending moment

$$M_{AE} = 5000 \times 250 + 2000 \times 750 - 3464.1 \times 50 = 2\,576\,800\ \text{N mm}$$

and an axial load acting midway between the flanges (irrespective of whether or not the flange areas are symmetrical about this point) of

$$P = 3464.1\ \text{N}$$

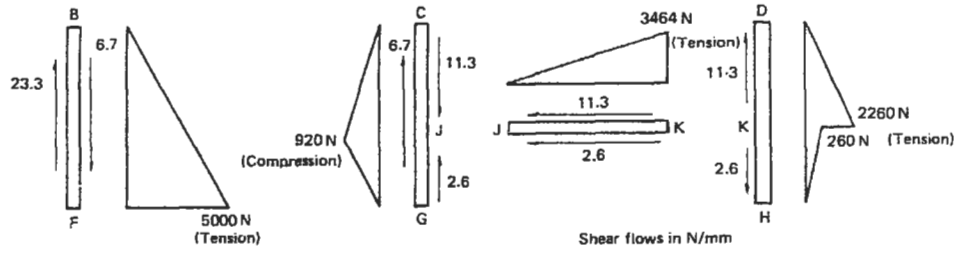

Fig. 10.44 Load distributions in stiffeners of the beam of Example 10.13.

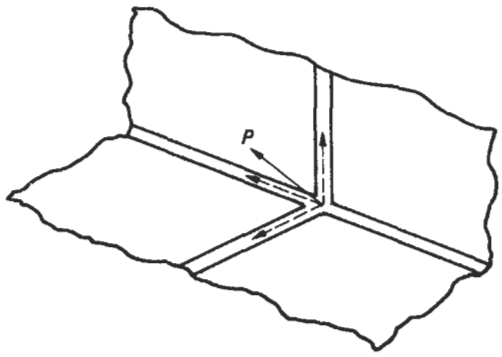

Fig. 10.45 Structural arrangement for an out of plane load.

Thus

$$P_A = \frac{2\,576\,800}{300} + \frac{3464.1}{2} = 10\,321\text{ N (Tension)}$$

and

$$P_E = \frac{-2\,576\,800}{300} + \frac{3464.1}{2} = -6857\text{ N (Compression)}$$

This approach cannot be used in the bay CDHG except at the section CJG since the axial load in the stiffener JK introduces an additional unknown.

The above analysis assumes that the web panels in beams of the type shown in Fig. 10.40 resist pure shear along their boundaries. In Section 6.13 we saw that thin webs may buckle under the action of such shear loads producing tension field stresses which, in turn, induce additional loads in the stiffeners and flanges of beams. The tension field stresses may be calculated separately by the methods described in Section 6.13 and then superimposed on the stresses determined as described above.

So far we have been concerned with web/stiffener arrangements in which the loads have been applied in the plane of the web so that two stiffeners were sufficient to resist the components of a concentrated load. Frequently, loads have an out-of-plane component in which case the structure should be arranged so that two webs meet at the point of load application with stiffeners aligned with the three component directions (Fig. 10.45). In some situations it is not practicable to have two webs meeting at the point of load application so that a component normal to a web exists. If this component is small it may be resisted in bending by an in-plane stiffener, otherwise an additional member must be provided spanning between adjacent frames or ribs, as shown in Fig. 10.46. In general, no normal loads should be applied to an unsupported web no matter how small their magnitude.

10.4.1 Fuselage frames

We have noted that fuselage frames transfer loads to the fuselage shell and provide column support for the longitudinal stringers. The frames generally take the form

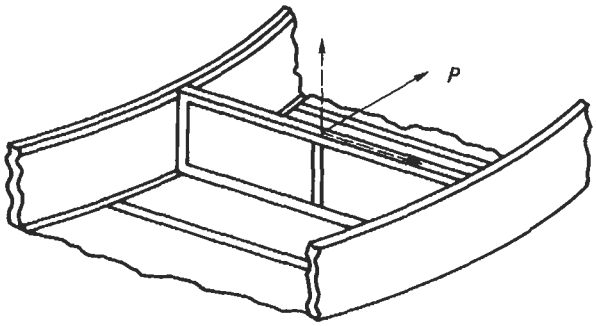

Fig. 10.46 Support of load having a component normal to a web.

of open rings so that the interior of the fuselage is not obstructed. They are connected continuously around their peripheries to the fuselage shell and are not necessarily circular in form but will usually be symmetrical about a vertical axis.

A fuselage frame is in equilibrium under the action of any external loads and the reaction shear flows from the fuselage shell. Suppose that a fuselage frame has a vertical axis of symmetry and carries a vertical external load W, as shown in Fig. 10.47(a) and (b). The fuselage shell/stringer section has been idealized such that the fuselage skin is effective only in shear. Suppose also that the shear force in the fuselage immediately to the left of the frame is $S_{y,1}$ and that the shear force in the fuselage immediately to the right of the frame is $S_{y,2}$; clearly, $S_{y,2} = S_{y,1} - W$. $S_{y,1}$ and $S_{y,2}$ generate shear flow distributions q_1 and q_2 respectively in the fuselage skin, each given by Eq. (10.17) in which $S_{x,1} = S_{x,2} = 0$ and $I_{xy} = 0$ (Cy is an axis of symmetry). The shear flow q_f transmitted to the periphery of the frame is equal to the algebraic sum of q_1 and q_2, i.e.

$$q_f = q_1 - q_2$$

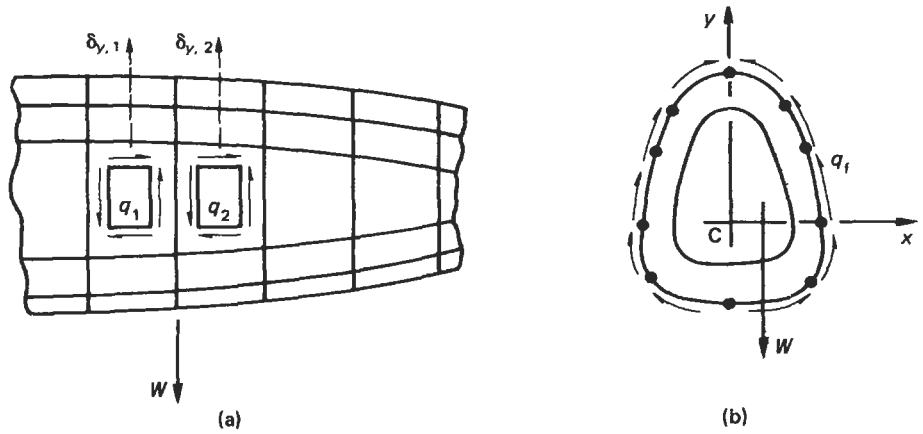

Fig. 10.47 Loads on a fuselage frame.

Thus, substituting for q_1 and q_2 obtained from Eq. (10.17) and noting that $S_{y,2} = S_{y,1} - W$, we have

$$q_f = \frac{-W}{I_{xx}} \sum_{r=1}^{n} B_r y_r + q_{s,0}$$

in which $q_{s,0}$ is calculated using Eq. (9.37) where the shear load is W and

$$q_b = \frac{-W}{I_{xx}} \sum_{r=1}^{n} B_r y_r$$

The method of determining the shear flow distribution applied to the periphery of a fuselage frame is identical to the method of solution (or the alternative method) of Example 10.5.

Having determined the shear flow distribution around the periphery of the frame, the frame itself may be analysed for distributions of bending moment, shear force and normal force, as described in Section 4.7.

10.4.2 Wing ribs

Wing ribs perform similar functions to those performed by fuselage frames. They maintain the shape of the wing section, assist in transmitting external loads to the wing skin and reduce the column length of the stringers. Their geometry, however, is usually different in that they are frequently of unsymmetrical shape and possess webs which are continuous except for lightness holes and openings for control runs.

Wing ribs are subjected to loading systems which are similar to those applied to fuselage frames. External loads applied in the plane of the rib produce a change in shear force in the wing across the rib; this induces reaction shear flows around its periphery. These are calculated using the methods described in Chapter 9 and in Section 10.3. To illustrate the method of rib analysis we shall use the example of a three-flange wing section in which, as we noted in Section 10.3, the shear flow distribution is statically determinate.

Example 10.14

Calculate the shear flows in the web panels and the axial loads in the flanges of the wing rib shown in Fig. 10.48. Assume that the web of the rib is effective only in shear while the resistance of the wing to bending moments is provided entirely by the three flanges 1, 2 and 3.

Since the wing bending moments are resisted entirely by the flanges 1, 2 and 3, the shear flows developed in the wing skin are constant between the flanges. Using the method described in Section 10.3 for a three-flange wing section we have, resolving forces horizontally

$$600q_{12} - 600q_{23} = 12\,000\,\text{N} \qquad \text{(i)}$$

Resolving vertically

$$300q_{31} - 300q_{23} = 15\,000\,\text{N} \qquad \text{(ii)}$$

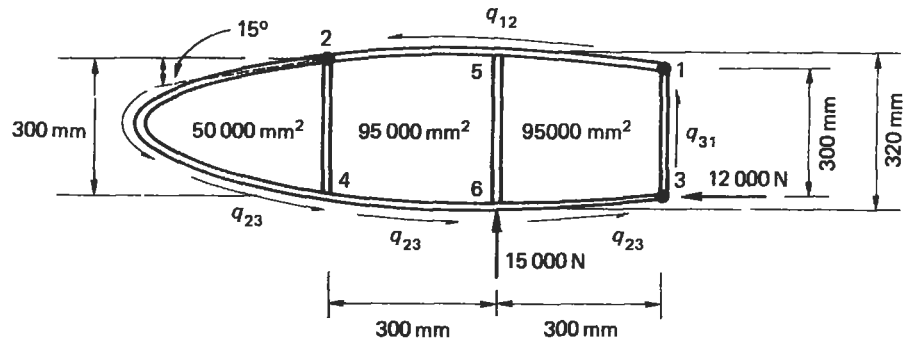

Fig. 10.48 Wing rib of Example 10.14.

Taking moments about flange 3

$$2(50\,000 + 95\,000)q_{23} + 2 \times 95\,000 q_{12} = -15\,000 \times 300\,\text{N mm} \qquad \text{(iii)}$$

Solution of Eqs (i), (ii) and (iii) gives

$$q_{12} = 13.0\,\text{N/mm}, \quad q_{23} = -7.0\,\text{N/mm}, \quad q_{31} = 43.0\,\text{N/mm}$$

Consider now the nose portion of the rib shown in Fig. 10.49 and suppose that the shear flow in the web immediately to the left of the stiffener 24 is q_1. The total vertical shear force $S_{y,1}$ at this section is given by

$$S_{y,1} = 7.0 \times 300 = 2100\,\text{N}$$

The horizontal components of the rib flange loads resist the bending moment at this section. Thus

$$P_{x,4} = P_{x,2} = \frac{2 \times 50\,000 \times 7.0}{300} = 2333.3\,\text{N}$$

The corresponding vertical components are then

$$P_{y,2} = P_{y,4} = 2333.3 \tan 15° = 625.2\,\text{N}$$

Thus the shear force carried by the web is $2100 - 2 \times 625.2 = 849.6\,\text{N}$. Hence

$$q_1 = \frac{849.6}{300} = 2.8\,\text{N/mm}$$

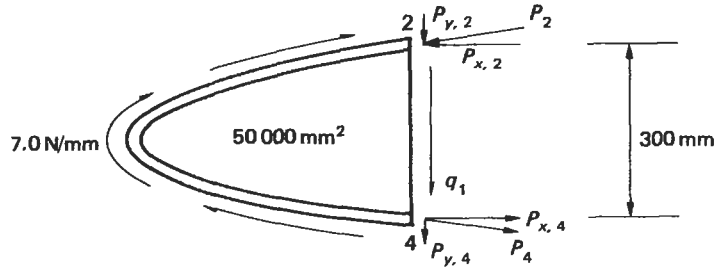

Fig. 10.49 Equilibrium of nose portion of the rib.

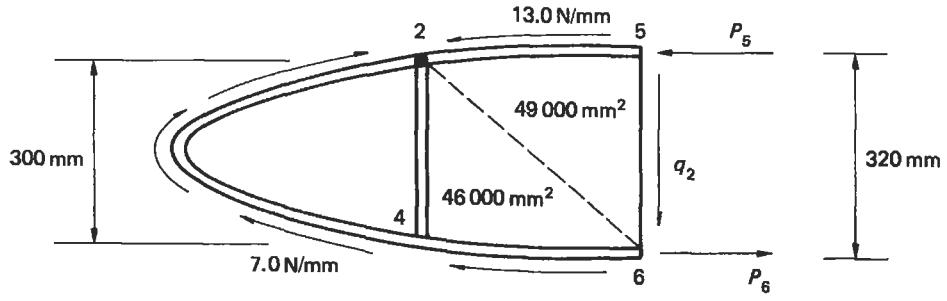

Fig. 10.50 Equilibrium of rib forward of intermediate stiffener 56.

The axial loads in the rib flanges at this section are given by

$$P_2 = P_4 = (2333.3^2 + 625.2^2)^{1/2} = 2415.6\,\text{N}$$

The rib flange loads and web panel shear flows, at a vertical section immediately to the left of the intermediate web stiffener 56, are found by considering the free body diagram shown in Fig. 10.50. At this section the rib flanges have zero slope so that the flange loads P_5 and P_6 are obtained directly from the value of bending moment at this section. Thus

$$P_5 = P_6 = 2[(50\,000 + 46\,000) \times 7.0 - 49\,000 \times 13.0]/320 = 218.8\,\text{N}$$

The shear force at this section is resisted solely by the web. Hence

$$320q_2 = 7.0 \times 300 + 7.0 \times 10 - 13.0 \times 10 = 2040\,\text{N}$$

so that

$$q_2 = 6.4\,\text{N/mm}$$

The shear flow in the rib immediately to the right of stiffener 56 is found most simply by considering the vertical equilibrium of stiffener 56 as shown in Fig. 10.51. Thus

$$320q_3 = 6.4 \times 320 + 15\,000$$

which gives

$$q_3 = 53.3\,\text{N/mm}$$

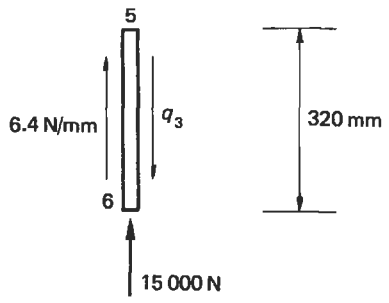

Fig. 10.51 Equilibrium of stiffener 56.

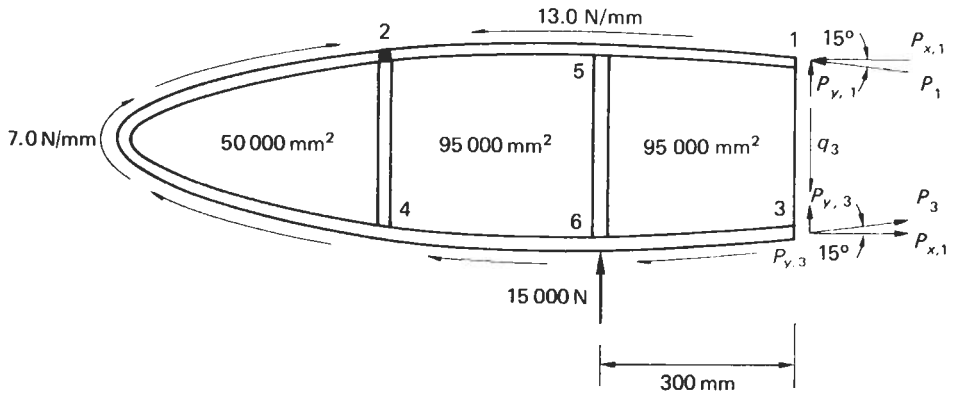

Fig. 10.52 Equilibrium of the rib forward of stiffener 31.

Finally, we shall consider the rib flange loads and the web shear flow at a section immediately forward of stiffener 31. From Fig. 10.52, in which we take moments about the point 3

$$M_3 = 2[(50\,000 + 95\,000) \times 7.0 - 95\,000 \times 13.0] + 15\,000 \times 300 = 4.06 \times 10^6 \text{ N mm}$$

The horizontal components of the flange loads at this section are then

$$P_{x,1} = P_{x,3} = \frac{4.06 \times 10^6}{300} = 13\,533.3 \text{ N}$$

and the vertical components are

$$P_{y,1} = P_{y,3} = 3626.2 \text{ N}$$

Hence

$$P_1 = P_3 = \sqrt{13\,533.3^2 + 3626.2^2} = 14\,010.7 \text{ N}$$

The total shear force at this section is $15\,000 + 300 \times 7.0 = 17\,100$ N. Therefore, the shear force resisted by the web is $17\,100 - 2 \times 3626.2 = 9847.6$ N so that the shear flow q_3 in the web at this section is

$$q_3 = \frac{9847.6}{300} = 32.8 \text{ N/mm}$$

10.5 Cut-outs in wings and fuselages

So far we have considered wings and fuselages to be closed boxes stiffened by transverse ribs or frames and longitudinal stringers. In practice it is necessary to provide openings in these closed stiffened shells. Thus, wings may have openings on their undersurfaces to accommodate retractable undercarriages; other openings might be required for fuel tanks, engine nacelles and weapon installations. Fuselage structures have openings for doors, cockpits, bomb bays, windows in passenger cabins etc. Other openings provide means of access for inspection and maintenance. These openings or 'cut-outs' produce discontinuities in the otherwise continuous shell

structure so that loads are redistributed in the vicinity of the cut-out affecting loads in the skin, stringers, ribs and frames of the wing and fuselage. Frequently these regions must be heavily reinforced resulting in unavoidable weight increases.

10.5.1 Cut-outs in wings

Initially we shall consider the case of a wing subjected to a pure torque in which one bay of the wing has the skin on its undersurface removed. The method is best illustrated by a numerical example.

Example 10.15

The structural portion of a wing consists of a three-bay rectangular section box which may be assumed to be firmly attached at all points around its periphery to the aircraft fuselage at its inboard end. The skin on the undersurface of the central bay has been removed and the wing is subjected to a torque of 10 kN m at its tip (Fig. 10.53). Calculate the shear flows in the skin panels and spar webs, the loads in the corner flanges and the forces in the ribs on each side of the cut-out assuming that the spar flanges carry all the direct loads while the skin panels and spar webs are effective only in shear.

If the wing structure were continuous and the effects of restrained warping at the built-in end ignored, the shear flows in the skin panels would be given by Eq. (9.49), i.e.

$$q = \frac{T}{2A} = \frac{10 \times 10^6}{2 \times 200 \times 800} = 31.3\,\text{N/mm}$$

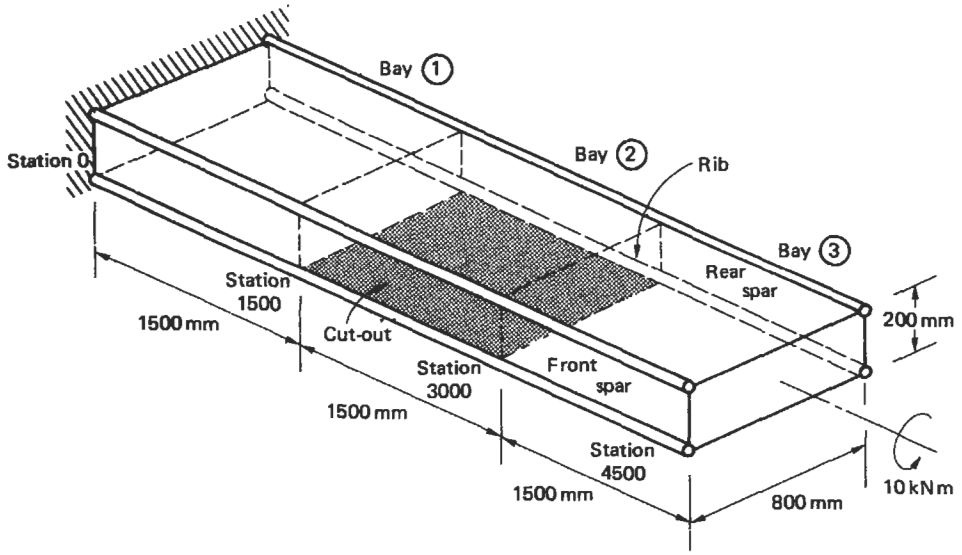

Fig. 10.53 Three-bay wing structure with cut-out of Example 10.15.

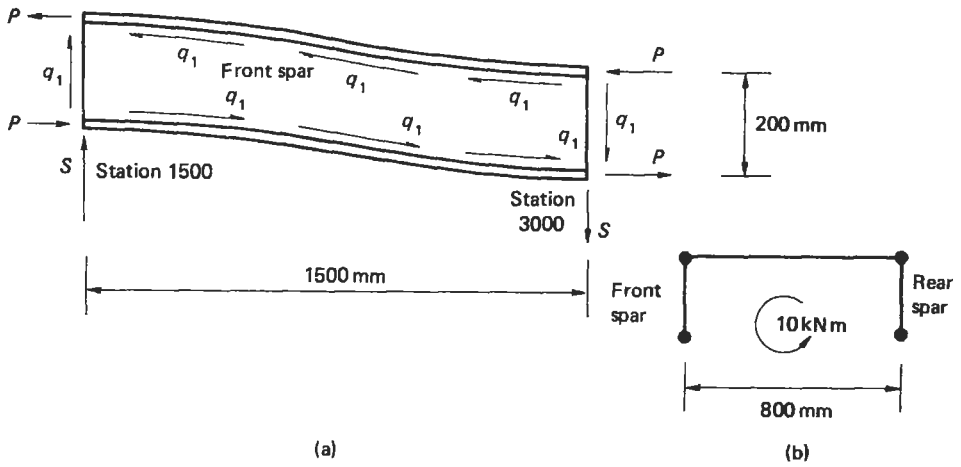

Fig. 10.54 Differential bending of front spar.

and the flanges would be unloaded. However, the removal of the lower skin panel in bay ② results in a torsionally weak channel section for the length of bay ② which must in any case still transmit the applied torque to bay ① and subsequently to the wing support points. Although open section beams are inherently weak in torsion (see Section 9.6), the channel section in this case is attached at its inboard and outboard ends to torsionally stiff closed boxes so that, in effect, it is built-in at both ends. We shall examine the effect of axial constraint on open section beams subjected to torsion in Chapter 11. An alternative approach is to assume that the torque is transmitted across bay ② by the differential bending of the front and rear spars. The bending moment in each spar is resisted by the flange loads P as shown, for the front spar, in Fig. 10.54(a). The shear loads in the front and rear spars form a couple at any station in bay ② which is equivalent to the applied torque. Thus, from Fig. 10.54(b)

$$800S = 10 \times 10^6 \text{ N mm}$$

i.e.

$$S = 12\,500 \text{ N}$$

The shear flow q_1 in Fig. 10.54(a) is given by

$$q_1 = \frac{12\,500}{200} = 62.5 \text{ N/mm}$$

Midway between stations 1500 and 3000 a point of contraflexure occurs in the front and rear spars so that at this point the bending moment is zero. Hence

$$200P = 12\,500 \times 750 \text{ N mm}$$

so that

$$P = 46\,875 \text{ N}$$

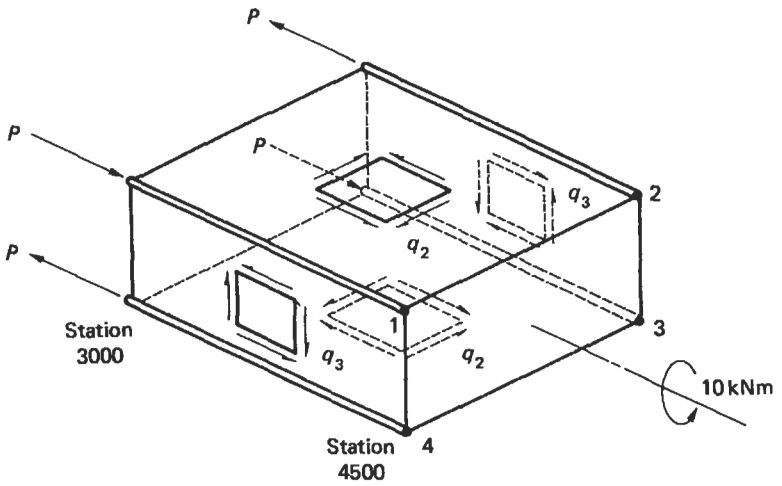

Fig. 10.55 Loads on bay ③ of the wing of Example 10.15.

Alternatively, P may be found by considering the equilibrium of either of the spar flanges. Thus

$$2P = 1500q_1 = 1500 \times 62.5\,\text{N}$$

whence

$$P = 46\,875\,\text{N}$$

The flange loads P are reacted by loads in the flanges of bays ① and ③. These flange loads are transmitted to the adjacent spar webs and skin panels as shown in Fig. 10.55 for bay ③ and modify the shear flow distribution given by Eq. (9.49). For equilibrium of flange 1

$$1500q_2 - 1500q_3 = P = 46\,875\,\text{N}$$

or

$$q_2 - q_3 = 31.3 \qquad \text{(i)}$$

The resultant of the shear flows q_2 and q_3 must be equivalent to the applied torque. Hence, for moments about the centre of symmetry at any section in bay ③ and using Eq. (9.79)

$$200 \times 800q_2 + 200 \times 800q_3 = 10 \times 10^6\,\text{N mm}$$

or

$$q_2 + q_3 = 62.5 \qquad \text{(ii)}$$

Solving Eqs (i) and (ii) we obtain

$$q_2 = 46.9\,\text{N/mm}, \quad q_3 = 15.6\,\text{N/mm}$$

Comparison with the results of Eq. (9.49) shows that the shear flows are increased by a factor of 1.5 in the upper and lower skin panels and decreased by a factor of 0.5 in the spar webs.

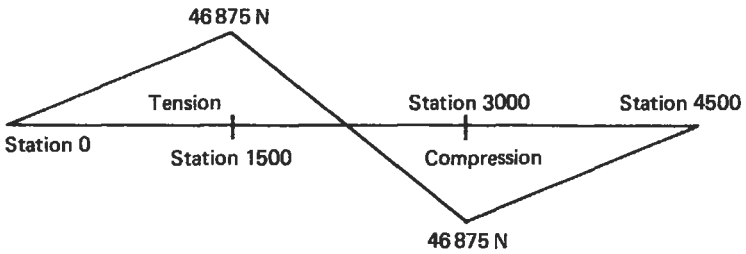

Fig. 10.56 Distribution of load in the top flange of the front spar of the wing of Example 10.15.

The flange loads are in equilibrium with the resultants of the shear flows in the adjacent skin panels and spar webs. Thus, for example, in the top flange of the front spar

$$P(\text{st.}4500) = 0$$

$$P(\text{st.}3000) = 1500q_2 - 1500q_3 = 46\,875\,\text{N (Compression)}$$

$$P(\text{st.}2250) = 1500q_2 - 1500q_3 - 750q_1 = 0$$

The loads along the remainder of the flange follow from antisymmetry giving the distribution shown in Fig. 10.56. The load distribution in the bottom flange of the rear spar will be identical to that shown in Fig. 10.56 while the distributions in the bottom flange of the front spar and the top flange of the rear spar will be reversed. We note that the flange loads are zero at the built-in end of the wing (station 0). Generally, however, additional stresses are induced by the warping restraint at the built-in end; these are investigated in Chapter 11. The loads on the wing ribs on either the inboard or outboard end of the cut-out are found by considering the shear flows in the skin panels and spar webs immediately inboard and outboard of the rib. Thus, for the rib at station 3000 we obtain the shear flow distribution shown in Fig. 10.57. The shear flows in the wing rib panels and the loads in the flanges and stiffeners are found as previously described in Section 10.4.

In Example 10.15 we implicitly assumed in the analysis that the local effects of the cut-out were completely dissipated within the length of the adjoining bays which were equal in length to the cut-out bay. The validity of this assumption relies on St. Venant's principle (Section 2.4). It may generally be assumed therefore that the effects of a cut-out are restricted to spanwise lengths of the wing equal to the length of the cut-out on both inboard and outboard ends of the cut-out bay.

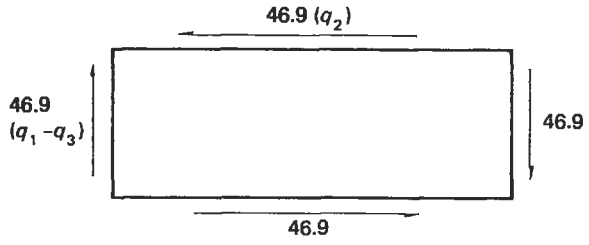

Fig. 10.57 Shear flows (N/mm) on wing rib at station 3000 in the wing of Example 10.15.

We shall now consider the more complex case of a wing having a cut-out and subjected to shear loads which produce both bending and torsion. Again the method is illustrated by a numerical example.

Example 10.16

A wing box has the skin panel on its undersurface removed between stations 2000 and 3000 and carries lift and drag loads which are constant between stations 1000 and 4000 as shown in Fig. 10.58(a). Determine the shear flows in the skin panels and spar webs and also the loads in the wing ribs at the inboard and outboard ends of the cut-out bay. Assume that all bending moments are resisted by the spar flanges while the skin panels and spar webs are effective only in shear.

The simplest approach is first to determine the shear flows in the skin panels and spar webs as though the wing box were continuous and then to apply an equal and opposite shear flow to that calculated around the edges of the cut-out. The shear flows in the wing box without the cut-out will be the same in each bay and are calculated using the method described in Section 9.9 and illustrated in Example 9.14. This gives the shear flow distribution shown in Fig. 10.59.

We now consider bay ② and apply a shear flow of 75.9 N/mm in the wall 34 in the opposite sense to that shown in Fig. 10.59. This reduces the shear flow in the wall 34 to zero and, in effect, restores the cut-out to bay ②. The shear flows in the remaining walls of the cut-out bay will no longer be equivalent to the externally applied shear

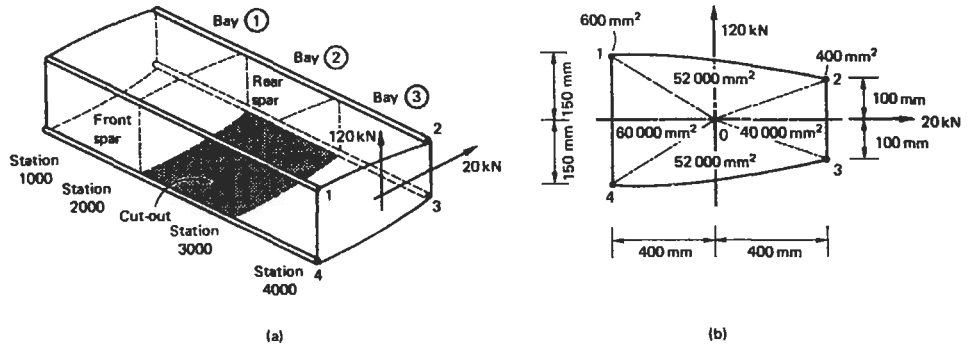

Fig. 10.58 Wing box of Example 10.16.

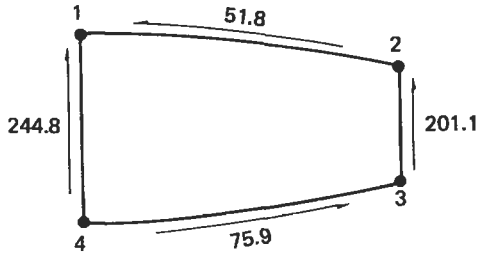

Fig. 10.59 Shear flow (N/mm) distribution at any station in the wing box of Example 10.16 without cut-out.

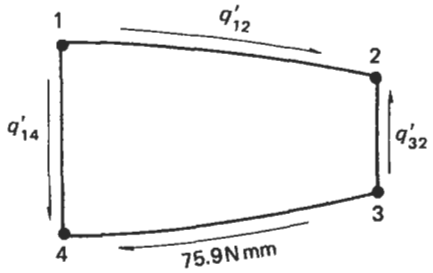

Fig. 10.60 Correction shear flows in the cut-out bay of the wing box of Example 10.16.

loads so that corrections are required. Consider the cut-out bay (Fig. 10.60) with the shear flow of 75.9 N/mm applied in the opposite sense to that shown in Fig. 10.59. The correction shear flows q'_{12}, q'_{32} and q'_{14} may be found using statics. Thus, resolving forces horizontally we have

$$800q'_{12} = 800 \times 75.9\,\text{N}$$

whence

$$q'_{12} = 75.9\,\text{N/mm}$$

Resolving forces vertically

$$200q'_{32} = 50q'_{12} - 50 \times 75.9 - 300q'_{14} = 0 \qquad \text{(i)}$$

and taking moments about O in Fig. 10.58(b) we obtain

$$2 \times 52\,000q'_{12} - 2 \times 40\,000q'_{32} + 2 \times 52\,000 \times 75.9 - 2 \times 60\,000q'_{14} = 0 \qquad \text{(ii)}$$

Solving Eqs (i) and (ii) gives

$$q'_{32} = 117.6\,\text{N/mm}, \quad q'_{14} = 53.1\,\text{N/mm}$$

The final shear flows in bay ② are found by superimposing q'_{12}, q'_{32} and q'_{14} on the shear flows in Fig. 10.59, giving the distribution shown in Fig. 10.61. Alternatively, these shear flows could have been found directly by considering the equilibrium of the cut-out bay under the action of the applied shear loads.

The correction shear flows in bay ② (Fig. 10.60) will also modify the shear flow distributions in bays ① and ③. The correction shear flows to be applied to those shown in Fig. 10.59 for bay ③ (those in bay ① will be identical) may be found by determining the flange loads corresponding to the correction shear flows in bay ②.

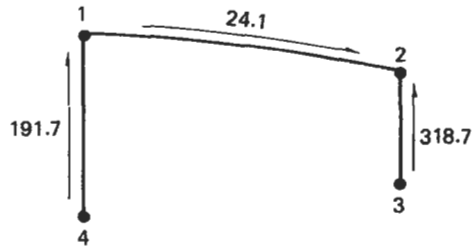

Fig. 10.61 Final shear flows (N/mm) in the cut-out bay of the wing box of Example 10.16.

It can be seen from the magnitudes and directions of these correction shear flows (Fig. 10.60) that at any section in bay ② the loads in the upper and lower flanges of the front spar are equal in magnitude but opposite in direction; similarly for the rear spar. Thus, the correction shear flows in bay ② produce an identical system of flange loads to that shown in Fig. 10.54 for the cut-out bays in the wing structure of Example 10.15. It follows that these correction shear flows produce differential bending of the front and rear spars in bay ② and that the spar bending moments and hence the flange loads are zero at the mid-bay points. Thus, at station 3000 the flange loads are

$$P_1 = (75.9 + 53.1) \times 500 = 64\,500\,\text{N (Compression)}$$

$$P_4 = 64\,500\,\text{N (Tension)}$$

$$P_2 = (75.9 + 117.6) \times 500 = 96\,750\,\text{N (Tension)}$$

$$P_3 = 96\,750\,\text{N (Tension)}$$

These flange loads produce correction shear flows q''_{21}, q''_{43}, q''_{23} and q''_{41} in the skin panels and spar webs of bay ③ as shown in Fig. 10.62. Thus for equilibrium of flange 1

$$1000q''_{41} + 1000q''_{21} = 64\,500\,\text{N} \tag{iii}$$

and for equilibrium of flange 2

$$1000q''_{21} + 1000q''_{23} = 96\,750\,\text{N} \tag{iv}$$

For equilibrium in the chordwise direction at any section in bay ③

$$800q''_{21} = 800q''_{43}$$

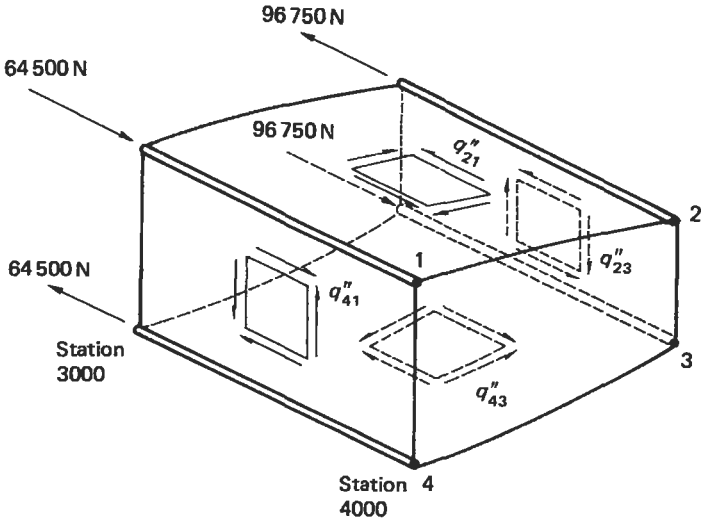

Fig. 10.62 Correction shear flows in bay ③ of the wing box of Example 10.16.

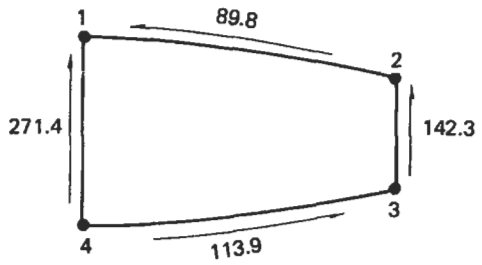

Fig. 10.63 Final shear flows in bay ③ (and bay ①) of the wing box of Example 10.16.

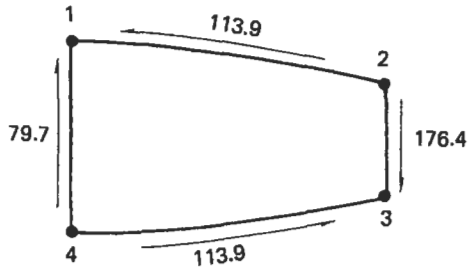

Fig. 10.64 Shear flows (N/mm) applied to the wing rib at station 3000 in the wing box of Example 10.16.

or

$$q''_{21} = q''_{43} \tag{v}$$

Finally, for vertical equilibrium at any section in bay ③

$$300q''_{41} + 50q''_{43} + 50q''_{21} - 200q''_{23} = 0 \tag{vi}$$

Simultaneous solution of Eqs (iii)–(vi) gives

$$q''_{21} = q''_{43} = 38.0\,\text{N/mm}, \quad q''_{23} = 58.8\,\text{N/mm}, \quad q''_{41} = 26.6\,\text{N/mm}$$

Superimposing these correction shear flows on those shown in Fig. 10.59 gives the final shear flow distribution in bay ③ as shown in Fig. 10.63. The rib loads at stations 2000 and 3000 are found as before by adding algebraically the shear flows in the skin panels and spar webs on each side of the rib. Thus, at station 3000 we obtain the shear flows acting around the periphery of the rib as shown in Fig. 10.64. The shear flows applied to the rib at the inboard end of the cut-out bay will be equal in magnitude but opposite in direction.

Note that in this example only the shear loads on the wing box between stations 1000 and 4000 are given. We cannot therefore determine the final values of the loads in the spar flanges since we do not know the values of the bending moments at these positions caused by loads acting on other parts of the wing.

10.5.2 Cut-outs in fuselages

Large openings in fuselage structures such as those required for cockpits, bomb bays and doors are treated in the same way as cut-outs in wing structures. In some

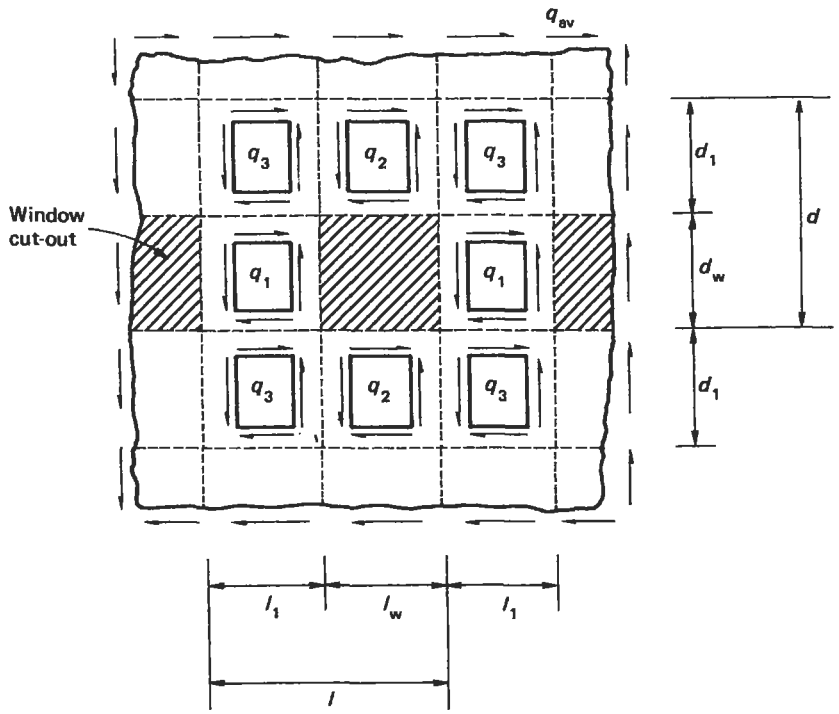

Fig. 10.65 Fuselage panel with windows.

situations, for example door openings in passenger aircraft, it is not possible to provide rigid frames on either side of the opening because the cabin space must not be restricted. In these cases a rigid frame is inserted to resist the shear loads and transmit loads around the opening.

The effects of smaller cut-outs, such as those required for rows of windows in passenger aircraft, may be found approximately as follows. Figure 10.65 shows a fuselage panel provided with cut-outs for windows which are spaced a distance l apart. The panel is subjected to an average shear flow q_{av} which would be the value of the shear flow in the panel without cut-outs. Considering a horizontal length of the panel through the cut-outs we see that

$$q_1 l_1 = q_{av} l$$

or

$$q_1 = \frac{l}{l_1} q_{av} \tag{10.41}$$

Now considering a vertical length of the panel through the cut-outs

$$q_2 d_1 = q_{av} d$$

or

$$q_2 = \frac{d}{d_1} q_{av} \tag{10.42}$$

The shear flows q_3 may be obtained by considering either vertical or horizontal sections not containing the cut-out. Thus

$$q_3 l_1 + q_2 l_w = q_{av} l$$

Substituting for q_2 from Eq. (10.42) and noting that $l = l_1 + l_w$ and $d = d_1 + d_w$, we obtain

$$q_3 = \left(1 - \frac{d_w}{d_1}\frac{l_w}{l_1}\right) q_{av} \tag{10.43}$$

10.6 Laminated composite structures

An increasingly large proportion of the structures of many modern aircraft are fabricated from composite materials. These, as we saw in Chapter 7, consist of laminas in which a stiff, high strength filament, for example carbon fibre, is embedded in a matrix such as epoxy, polyester etc. The use of composites can lead to considerable savings in weight over conventional metallic structures. They also have the advantage that the direction of the filaments in a multi-lamina structure may be aligned with the direction of the major loads at a particular point resulting in a more efficient design. In this section we shall derive expressions for the elastic constants of a composite and consider the analysis of a simple lamina subjected to transverse and in-plane loads.

10.6.1 Elastic constants

A simple lamina of a composite structure can be considered as orthotropic with two principal material directions in its own plane: one parallel, the other perpendicular to the direction of the filaments; we shall designate the former the longitudinal direction (l), the latter the transverse direction (t).

In Fig. 10.66 a portion of a lamina containing a single filament is subjected to a stress, σ_l, in the longitudinal direction which produces an extension Δl. If it is assumed that plane sections remain plane during deformation then the strain ε_l

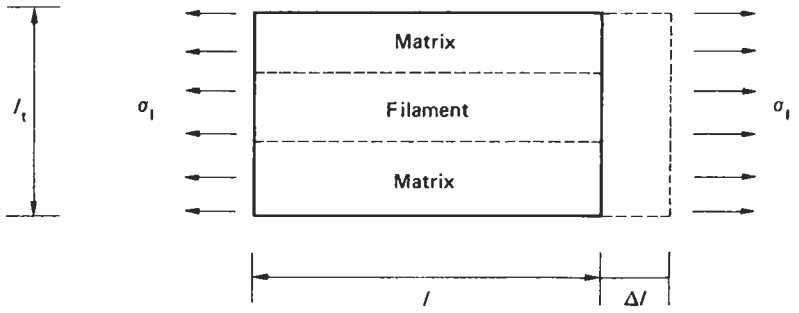

Fig. 10.66 Determination of E_l.

corresponding to σ_l is given by

$$\varepsilon_l = \frac{\Delta l}{l} \tag{10.44}$$

and

$$\sigma_l = E_l \varepsilon_l \tag{10.45}$$

where E_l is the modulus of elasticity of the lamina in the direction of the filament. Also, using the suffixes f and m to designate filament and matrix parameters, we have

$$\sigma_f = E_f \varepsilon_l, \quad \sigma_m = E_m \varepsilon_l \tag{10.46}$$

Further, if A is the total area of cross-section of the lamina in Fig. 10.66, A_f is the cross-sectional area of the filament and A_m the cross-sectional area of the matrix then, for equilibrium in the direction of the filament

$$\sigma_l A = \sigma_f A_f + \sigma_m A_m$$

or, substituting for σ_l, σ_f and σ_m from Eqs (10.45) and (10.46)

$$E_l \varepsilon_l A = E_f \varepsilon_f A_f + E_m \varepsilon_l A_m$$

so that

$$E_l = E_f \frac{A_f}{A} + E_m \frac{A_m}{A} \tag{10.47}$$

Writing $A_f/A = v_f$ and $A_m/A = v_m$, Eq. (10.47) becomes

$$E_l = v_f E_f + v_m E_m \tag{10.48}$$

Equation (10.48) is generally referred to as the *law of mixtures.*

A similar approach may be used to determine the modulus of elasticity in the transverse direction (E_t). In Fig. 10.67 the total extension in the transverse direction is produced by σ_t and is given by

$$\varepsilon_t l_t = \varepsilon_m l_m + \varepsilon_f l_f$$

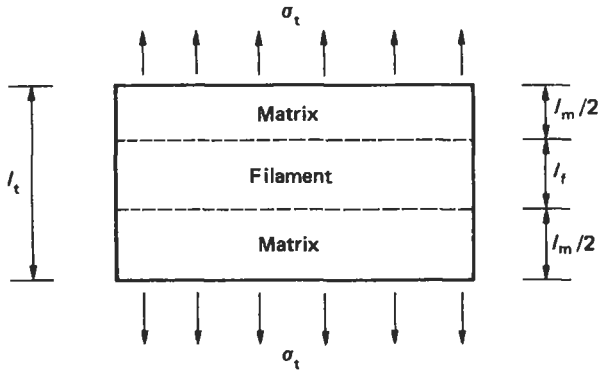

Fig. 10.67 Determination of E_t.

or

$$\frac{\sigma_t}{E_t} l_t = \frac{\sigma_t}{E_m} l_m + \frac{\sigma_t}{E_f} l_f$$

which gives

$$\frac{1}{E_t} = \frac{v_m}{E_m} + \frac{v_f}{E_f}$$

Rearranging this we obtain

$$E_t = \frac{E_m E_f}{v_m E_f + v_f E_m} \tag{10.49}$$

The major Poisson's ratio ν_{lt} may be found by referring to the stress system of Fig. 10.66 and the dimensions given in Fig. 10.67. The total displacement in the transverse direction produced by σ_l is given by

$$\Delta_t = \nu_{lt} \varepsilon_l l_t$$

i.e.

$$\Delta_t = \nu_{lt} \varepsilon_l l_t = \nu_m \varepsilon_l l_m + \nu_f \varepsilon_l l_f$$

from which

$$\nu_{lt} = v_m \nu_m + v_f \nu_f \tag{10.50}$$

The minor Poisson's ratio ν_{tl} is found by referring to Fig. 10.67. The strain in the longitudinal direction produced by the transverse stress σ_t is given by

$$\nu_{tl} \frac{\sigma_t}{E_t} = \nu_m \frac{\sigma_t}{E_t} = \nu_f \frac{\sigma_t}{E_f} \tag{10.51}$$

From the last two of Eqs (10.51)

$$\nu_f = \frac{E_f}{E_m} \nu_m$$

Substituting in Eq. (10.50)

$$\nu_{lt} = \nu_m \left(v_m + \frac{E_f}{E_m} v_f \right) = \frac{\nu_m}{E_m} (v_m E_m + v_f E_f)$$

or, from Eq. (10.48)

$$\nu_{lt} = \nu_m \frac{E_l}{E_m}$$

Now substituting for ν_m in the first two of Eqs (10.51)

$$\frac{\nu_{tl}}{E_t} = \frac{\nu_{lt}}{E_t}$$

or

$$\nu_{tl} = \frac{E_t}{E_l} \nu_{lt} = \frac{E_t}{E_l} (v_m \nu_m + v_f \nu_f) \tag{10.52}$$

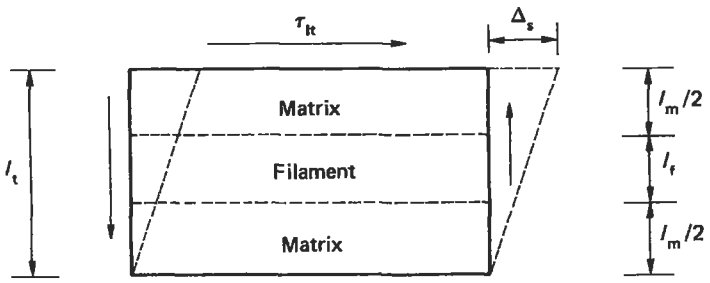

Fig. 10.68 Determination of G_{lt}.

Finally, the shear modulus $G_{lt}(= G_{tl})$ is determined by assuming that the constituent materials are subjected to the same shear stress τ_{lt} as shown in Fig. 10.68. The displacement Δ_s produced by shear is

$$\Delta_s = \frac{\tau_{lt}}{G_{lt}} l_t = \frac{\tau_{lt}}{G_m} l_m + \frac{\tau_{lt}}{G_f} l_f$$

in which G_m and G_f are the shear moduli of the matrix and filament respectively. Thus

$$\frac{l_t}{G_{lt}} = \frac{l_m}{G_m} + \frac{l_f}{G_f}$$

whence

$$G_{lt} = \frac{G_m G_f}{v_m G_f + v_f G_m} \tag{10.53}$$

Example 10.17

A laminated bar whose cross-section is shown in Fig. 10.69 is 500 mm long and comprises an epoxy resin matrix reinforced by a carbon filament having moduli equal to 5000 N/mm^2 and 200 000 N/mm^2 respectively; the corresponding values of Poisson's ratio are 0.2 and 0.3. If the bar is subjected to an axial tensile load of 100 kN, determine the lengthening of the bar and the reduction in its thickness. Calculate also the stresses in the epoxy resin and the carbon filament.

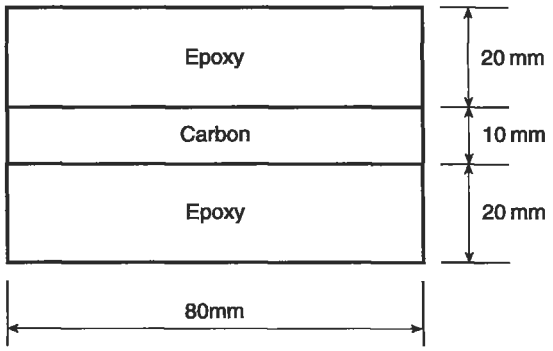

Fig. 10.69 Cross-section of the bar of Example 10.17.

From Eq. (10.48) the modulus of the bar is given by

$$E_l = 200\,000 \times \frac{80 \times 10}{80 \times 50} + 5000 \times \frac{80 \times 40}{80 \times 50}$$

i.e.

$$E_l = 44\,000\,\text{N/mm}^2$$

The direct stress, σ_l, in the longitudinal direction is given by

$$\sigma_l = \frac{100 \times 10^3}{80 \times 50} = 25.0\,\text{N/mm}^2$$

Therefore, from Eq. (10.45), the longitudinal strain in the bar is

$$\varepsilon_l = \frac{25.0}{44\,000} = 5.68 \times 10^{-4}$$

The lengthening, Δ_l, of the bar is then

$$\Delta_l = 5.68 \times 10^{-4} \times 500$$

i.e.

$$\Delta_l = 0.284\,\text{mm}$$

The major Poisson's ratio for the bar is found from Eq. (10.50). Thus

$$\nu_{lt} = \frac{80 \times 40}{80 \times 50} \times 0.2 + \frac{80 \times 10}{80 \times 50} \times 0.3 = 0.22$$

Hence the strain in the bar across its thickness is

$$\varepsilon_t = -0.22 \times 5.68 \times 10^{-4} = -1.25 \times 10^{-4}$$

The reduction in thickness, Δ_t, of the bar is then

$$\Delta_t = 1.25 \times 10^{-4} \times 50$$

i.e.

$$\Delta_t = 0.006\,\text{mm}$$

The stresses in the epoxy and the carbon are found using Eqs (10.46). Thus

$$\sigma_m\,(\text{epoxy}) = 5000 \times 5.68 \times 10^{-4} = 2.84\,\text{N/mm}^2$$

$$\sigma_f\,(\text{carbon}) = 200\,000 \times 5.68 \times 10^{-4} = 113.6\,\text{N/mm}^2$$

10.6.2 Composite plates

In Chapter 5 we considered thin plates subjected to a variety of loading conditions. We shall now extend the analysis to a lamina comprising a filament and matrix of the type shown in Fig. 10.66.

Suppose the lamina of Fig. 10.66 is subjected to stresses σ_l, σ_t and τ_{lt} acting simultaneously. From Eqs (1.42) and (1.46)

$$\left.\begin{aligned} \varepsilon_l &= \frac{\sigma_l}{E_l} - \nu_{tl}\frac{\sigma_t}{E_t} \\ \varepsilon_t &= \frac{\sigma_t}{E_t} - \nu_{lt}\frac{\sigma_l}{E_l} \\ \gamma_{lt} &= \frac{\tau_{lt}}{G_{lt}} \end{aligned}\right\} \tag{10.54}$$

Solving the first two of Eqs (10.54), we obtain

$$\left.\begin{aligned} \sigma_l &= \frac{E_l}{1-\nu_{lt}\nu_{tl}}(\varepsilon_l + \nu_{tl}\varepsilon_t) \\ \sigma_t &= \frac{E_t}{1-\nu_{lt}\nu_{tl}}(\varepsilon_t + \nu_{lt}\varepsilon_l) \end{aligned}\right\} \tag{10.55}$$

Also $\tau_{lt} = G_{lt}\gamma_{lt}$

Equations (10.55) may be written in matrix form as

$$\begin{Bmatrix} \sigma_l \\ \sigma_t \\ \tau_{lt} \end{Bmatrix} = \begin{bmatrix} C_{11} & C_{12} & 0 \\ C_{21} & C_{22} & 0 \\ 0 & 0 & C_{33} \end{bmatrix} \begin{Bmatrix} \varepsilon_l \\ \varepsilon_t \\ \gamma_{lt} \end{Bmatrix} \tag{10.56}$$

in which

$$C_{11} = \frac{E_l}{1-\nu_{lt}\nu_{tl}}$$

$$C_{12} = \frac{E_l\nu_{tl}}{1-\nu_{lt}\nu_{tl}}$$

$$C_{21} = \frac{E_l\nu_{lt}}{1-\nu_{lt}\nu_{tl}} \quad (= C_{12}, \text{ see Eq. (10.52)})$$

$$C_{22} = \frac{E_t}{1-\nu_{lt}\nu_{tl}}$$

$$C_{33} = G_{lt}$$

Suppose now that the longitudinal and transverse directions coincide with the x and y axes respectively of the plates in Chapter 5. Equations (10.56) then become

$$\begin{Bmatrix} \sigma_x \\ \sigma_y \\ \tau_{xy} \end{Bmatrix} = \begin{bmatrix} C_{11} & C_{12} & 0 \\ C_{12} & C_{22} & 0 \\ 0 & 0 & C_{33} \end{bmatrix} \begin{Bmatrix} \varepsilon_x \\ \varepsilon_y \\ \gamma_{xy} \end{Bmatrix} \tag{10.57}$$

From Eqs (1.27), (1.28) and the derivation of Eq. (5.13) we see that

$$\varepsilon_x = -z\frac{\partial^2 w}{\partial x^2}, \quad \varepsilon_y = -z\frac{\partial^2 w}{\partial y^2}, \quad \gamma_{xy} = -2z\frac{\partial^2 w}{\partial x \partial y}$$

so that Eqs (10.57) may be rewritten as

$$\begin{Bmatrix} \sigma_x \\ \sigma_y \\ \tau_{xy} \end{Bmatrix} = -z \begin{bmatrix} C_{11} & C_{12} & 0 \\ C_{12} & C_{22} & 0 \\ 0 & 0 & 2C_{33} \end{bmatrix} \begin{Bmatrix} \dfrac{\partial^2 w}{\partial x^2} \\ \dfrac{\partial^2 w}{\partial y^2} \\ \dfrac{\partial^2 w}{\partial x \partial y} \end{Bmatrix} \tag{10.58}$$

From Section 5.3

$$M_x = \int_{-t/2}^{t/2} \sigma_x z \, dz, \quad M_y = \int_{-t/2}^{t/2} \sigma_y z \, dz, \quad M_{xy} = -\int_{-t/2}^{t/2} \tau_{xy} z \, dz$$

Substituting for σ_x, σ_y and τ_{xy} from Eqs (10.58) and integrating, we obtain

$$M_x = \frac{-t^3}{12}\left(C_{11}\frac{\partial^2 w}{\partial x^2} + C_{12}\frac{\partial^2 w}{\partial y^2}\right)$$

Writing $C_{11}t^3/12$ as D_{11}, $C_{12}t^3/12$ as D_{12}

$$M_x = -\left(D_{11}\frac{\partial^2 w}{\partial x^2} + D_{12}\frac{\partial^2 w}{\partial y^2}\right) \tag{10.59}$$

Similarly

$$M_y = -\left(D_{12}\frac{\partial^2 w}{\partial x^2} + D_{22}\frac{\partial^2 w}{\partial y^2}\right) \tag{10.60}$$

and

$$M_{xy} = 2D_{33}\frac{\partial^2 w}{\partial x \partial y} \tag{10.61}$$

For a lamina subjected to a distributed load of intensity q per unit area we see, by substituting for M_x, M_y and M_{xy} from Eqs (10.59)–(10.61) into Eq. (5.19), that

$$D_{11}\frac{\partial^4 w}{\partial x^4} + 2(D_{12} + 2D_{33})\frac{\partial^4 w}{\partial x^2 \partial y^2} + D_{22}\frac{\partial^4 w}{\partial y^4} = q \tag{10.62}$$

Further, for a lamina subjected to in-plane loads in addition to q we obtain, by a comparison of Eq. (10.62) with Eq. (5.33)

$$D_{11}\frac{\partial^4 w}{\partial x^4} + 2(D_{12} + 2D_{33})\frac{\partial^4 w}{\partial x^2 \partial y^2} + D_{22}\frac{\partial^4 w}{\partial y^4} = q + N_x\frac{\partial^2 w}{\partial x^2} + 2N_y\frac{\partial^2 w}{\partial y^2} + N_{xy}\frac{\partial^2 w}{\partial x \partial y} \tag{10.63}$$

Problems involving laminated plates are solved in a similar manner to those included in Chapter 5 after the calculation of the modified flexural rigidities D_{11}, D_{12}, D_{22} etc. If the principal material directions l and t do not coincide with the x and y directions in the above equations, in-plane shear effects are introduced which modify Eqs (10.62)

and (10.63) (Ref. 1). The resulting equations are complex and require numerical methods of solution.

Generally, composite structures consist of several laminas with the direction of the filaments arranged so that they lie in the directions of the major loads. Thus, for a loading system which comprises two mutually perpendicular loads, it is necessary to build or *lay-up* a laminate with sufficient *plies* in both directions to withstand each load. Such an arrangement is known as a *cross-ply laminate*. The analysis of multi-ply laminates is complex and is normally carried out using finite difference or finite element methods.

Reference

1 Calcote, L. R., *The Analysis of Laminated Composite Structures*, Van Nostrand Reinhold Co., New York, 1969.

Further reading

Datoo, M. H., *Mechanics of Fibrous Composites*, Elsevier Applied Science, London, 1991.

Problems

P.10.1 A wing spar has the dimensions shown in Fig. P.10.1 and carries a uniformly distributed load of 15 kN/m along its complete length. Each flange has a cross-sectional area of 500 mm^2 with the top flange being horizontal. If the flanges are assumed to resist all direct loads while the spar web is effective only in shear, determine the flange loads and the shear flows in the web at sections 1 m and 2 m from the free end.

Ans. 1 m from free end: $P_U = 25$ kN (tension), $P_L = 25.1$ kN (compression), $q = 41.7$ N/mm.

2 m from free end: $P_U = 75$ kN (tension), $P_L = 75.4$ kN (compression), $q = 56.3$ N/mm.

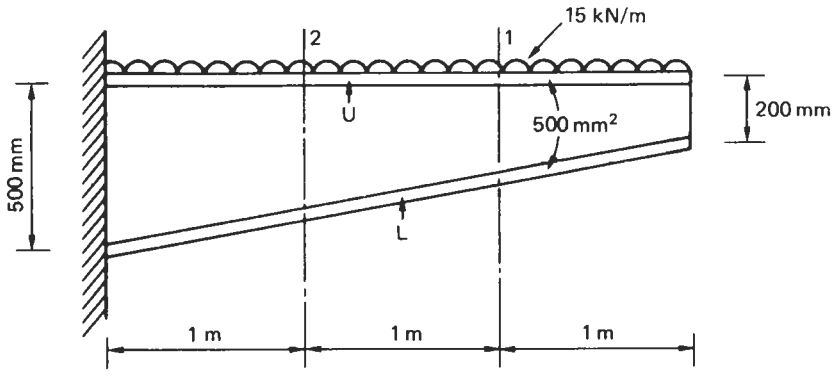

Fig. P.10.1

P.10.2 If the web in the wing spar of P.10.1 has a thickness of 2 mm and is fully effective in resisting direct stresses, calculate the maximum value of shear flow in the web at a section 1 m from the free end of the beam.

Ans. 46.8 N/mm.

P.10.3 Calculate the shear flow distribution and the stringer and flange loads in the beam shown in Fig. P.10.3 at a section 1.5 m from the built-in end. Assume that the skin and web panels are effective in resisting shear stress only; the beam tapers symmetrically in a vertical direction about its longitudinal axis.

Ans. $q_{13} = q_{42} = 36.9\,\text{N/mm}$, $q_{35} = q_{64} = 7.3\,\text{N/mm}$, $q_{21} = 96.2\,\text{N/mm}$, $q_{65} = 22.3\,\text{N/mm}$.

$$P_2 = -P_1 = 133.3\,\text{kN},\ P_4 = P_6 = -P_3 = -P_5 = 66.7\,\text{kN}$$

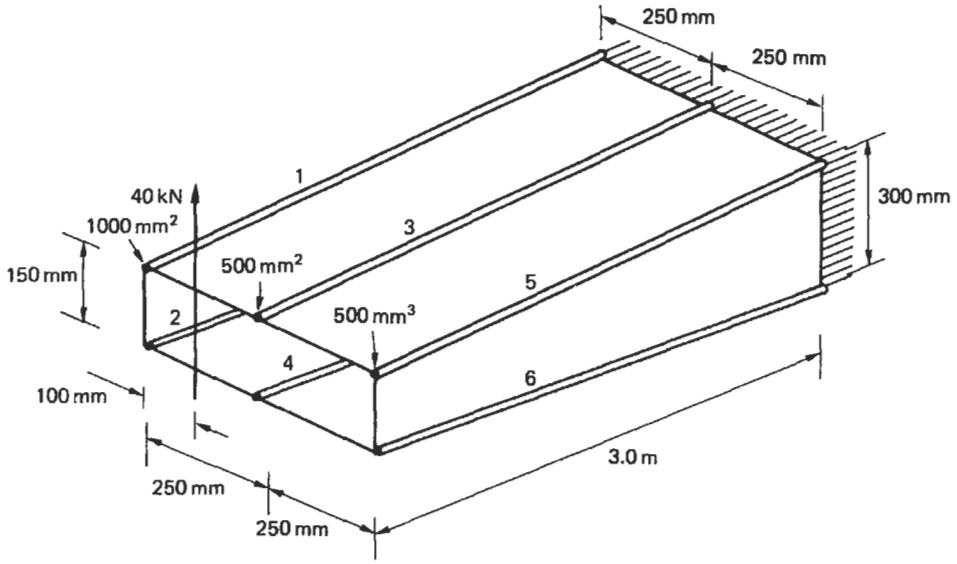

Fig. P.10.3

P.10.4 The doubly symmetrical fuselage section shown in Fig. P.10.4 has been idealized into an arrangement of direct stress carrying booms and shear stress carrying skin panels; the boom areas are all 150 mm^2. Calculate the direct stresses in the booms and the shear flows in the panels when the section is subjected to a shear load of 50 kN and a bending moment of 100 kN m.

Ans. $\sigma_{z,1} = -\sigma_{z,6} = 180\,\text{N/mm}^2$, $\sigma_{z,2} = \sigma_{z,10} = -\sigma_{z,5} = -\sigma_{z,7} = 144.9\,\text{N/mm}^2$, $\sigma_{z,3} = \sigma_{z,9} = -\sigma_{z,4} = -\sigma_{z,8} = 60\,\text{N/mm}^2$.

$q_{21} = q_{65} = 1.9\,\text{N/mm}$, $q_{32} = q_{54} = 12.8\,\text{N/mm}$, $q_{43} = 17.3\,\text{N/mm}$,

$q_{67} = q_{101} = 11.6\,\text{N/mm}$, $q_{78} = q_{910} = 22.5\,\text{N/mm}$, $q_{89} = 27.0\,\text{N/mm}$

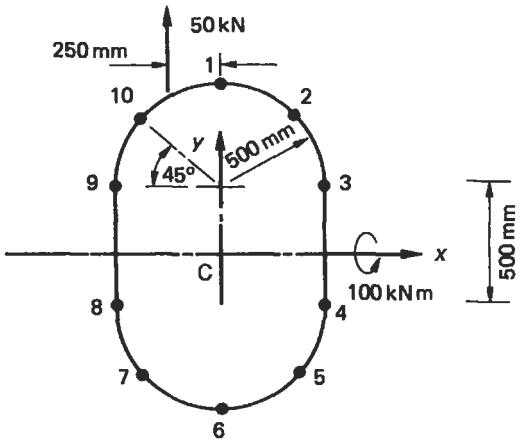

Fig. P.10.4

P.10.5 Determine the shear flow distribution in the fuselage section of P.10.4 by replacing the applied load by a shear load through the shear centre together with a pure torque.

P.10.6 The central cell of a wing has the idealized section shown in Fig. P.10.6. If the lift and drag loads on the wing produce bending moments of $-120\,000$ N m and $-30\,000$ N m respectively at the section shown, calculate the direct stresses in the booms. Neglect axial constraint effects and assume that the lift and drag vectors are in vertical and horizontal planes

$$\text{Boom areas: } B_1 = B_4 = B_5 = B_8 = 1000\,\text{mm}^2$$
$$B_2 = B_3 = B_6 = B_7 = 600\,\text{mm}^2$$

Ans. $\sigma_1 = -190.7\,\text{N/mm}^2$, $\sigma_2 = -181.7\,\text{N/mm}^2$, $\sigma_3 = -172.8\,\text{N/mm}^2$,
$\sigma_4 = -163.8\,\text{N/mm}^2$, $\sigma_5 = 140\,\text{N/mm}^2$, $\sigma_6 = 164.8\,\text{N/mm}^2$,
$\sigma_7 = 189.6\,\text{N/mm}^2$, $\sigma_8 = 214.4\,\text{N/mm}^2$

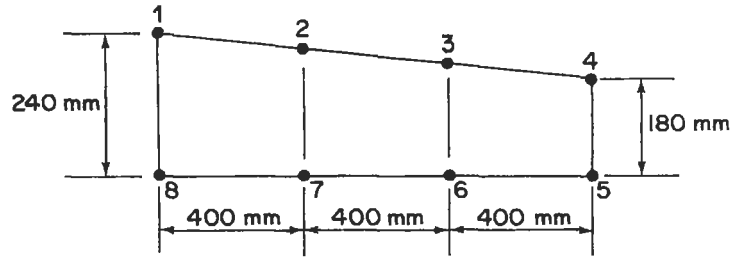

Fig. P.10.6

P.10.7 Figure P.10.7 shows the cross-section of a two-cell torque box. If the shear stress in any wall must not exceed 140 N/mm^2, find the maximum torque which can be applied to the box.

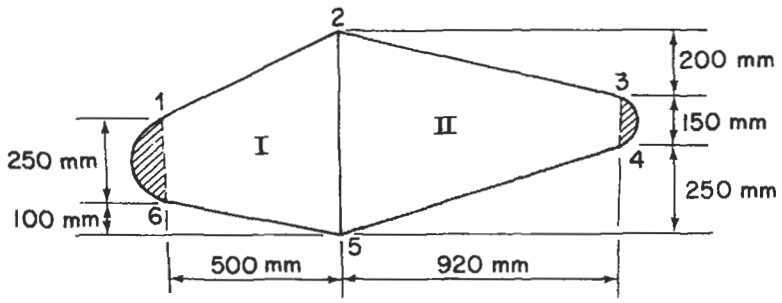

Fig. P.10.7

If this torque were applied at one end and resisted at the other end of such a box of span 2500 mm, find the twist in degrees of one end relative to the other and the torsional rigidity of the box. The shear modulus $G = 26\,600\,\text{N/mm}^2$ for all walls.

Data:

Shaded areas:	$A_{34} = 6450\,\text{mm}^2$, $A_{16} = 7750\,\text{mm}^2$
Wall lengths:	$s_{34} = 250\,\text{mm}$, $s_{16} = 300\,\text{mm}$
Wall thickness:	$t_{12} = 1.63\,\text{mm}$, $t_{34} = 0.56\,\text{mm}$
	$t_{23} = t_{45} = t_{56} = 0.92\,\text{mm}$
	$t_{61} = 2.03\,\text{mm}$
	$t_{25} = 2.54\,\text{mm}$

Ans. $T = 102\,417\,\text{N m}$, $\theta = 1.46°$, $GJ = 10 \times 10^{12}\,\text{N mm}^2/\text{rad}$.

P.10.8 Determine the torsional stiffness of the four-cell wing section shown in Fig. P.10.8.

Data:

Wall	12	23	34					
	78	67	56	45°	45^{i}	36	27	18
Peripheral length (mm)	762	812	812	1525	356	406	356	254
Thickness (mm)	0.915	0.915	0.915	0.711	1.220	1.625	1.220	0.915

Cell areas (mm^2) $A_{\text{I}} = 161\,500$, $A_{\text{II}} = 291\,000$

$A_{\text{III}} = 291\,000$, $A_{\text{IV}} = 226\,000$

Ans. $522.5 \times 10^6 G\,\text{N mm}^2/\text{rad}$.

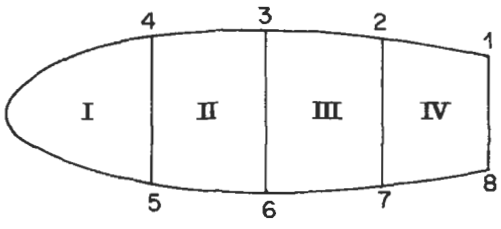

Fig. P.10.8

P.10.9 Determine the shear flow distribution for a torque of 56 500 N m for the three cell section shown in Fig. P.10.9. The section has a constant shear modulus throughout.

Wall	Length (mm)	Thickness (mm)	Cell	Area (mm^2)
12^U	1084	1.220	I	108 400
12^L	2160	1.625	II	202 500
14, 23	127	0.915	III	528 000
34^U	797	0.915		
34^L	797	0.915		

Ans. $q_{12^U} = 25.4\,\text{N/mm}$, $q_{21^L} = 33.5\,\text{N/mm}$, $q_{14} = q_{32} = 8.1\,\text{N/mm}$,
$q_{43^U} = 13.4\,\text{N/mm}$, $q_{34^L} = 5.3\,\text{N/mm}$

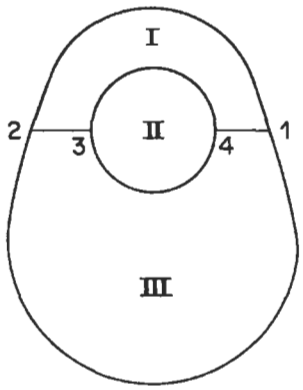

Fig. P.10.9

P.10.10 The idealized cross-section of a two-cell thin-walled wing box is shown in Fig. P.10.10. If the wing box supports a load of 44 500 N acting along the web 25, calculate the shear flow distribution. The shear modulus G is the same for all walls of the wing box.

Wall	Length (mm)	Thickness (mm)	Boom	Area (mm^2)
16	254	1.625	1, 6	1290
25	406	2.032	2, 5	1936
34	202	1.220	3, 4	645
12, 56	647	0.915		
23, 45	775	0.559		
Cell areas: $A_I = 232\,000\,mm^2$, $A_{II} = 258\,000\,mm^2$				

Ans. $q_{16} = 33.9\,\text{N/mm}$, $q_{65} = q_{21} = 1.1\,\text{N/mm}$,
$q_{45} = q_{23} = 7.2\,\text{N/mm}$, $q_{34} = 20.8\,\text{N/mm}$,
$q_{25} = 73.4\,\text{N/mm}$

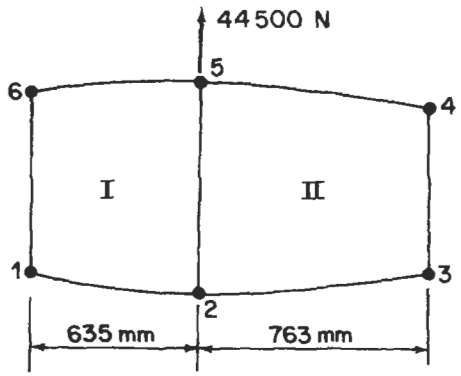

Fig. P.10.10

P.10.11 Figure P.10.11 shows a singly symmetric, two-cell wing section in which all direct stresses are carried by the booms, shear stresses alone being carried by the walls. All walls are flat with the exception of the nose portion 45. Find the position of the shear centre S and the shear flow distribution for a load of $S_y = 66\,750$ N through S. Tabulated below are lengths, thicknesses and shear moduli of the shear carrying walls. Note that dotted line 45 is not a wall.

Wall	Length (mm)	Thickness (mm)	G (N/mm^2)	Boom	Area (mm^2)
34, 56	380	0.915	20 700	1, 3, 6, 8	1290
12, 23, 67, 78	356	0.915	24 200	2, 4, 5, 7	645
36, 81	306	1.220	24 800		
45	610	1.220	24 800		
Nose area $N_1 = 51\,500$ mm^2					

Ans. $x_S = 160.1$ mm, $q_{12} = q_{78} = 17.8$ N/mm, $q_{32} = q_{76} = 18.5$ N/mm, $q_{63} = 88.2$ N/mm, $q_{43} = q_{65} = 2.9$ N/mm, $q_{54} = 39.2$ N/mm, $q_{81} = 90.4$ N/mm

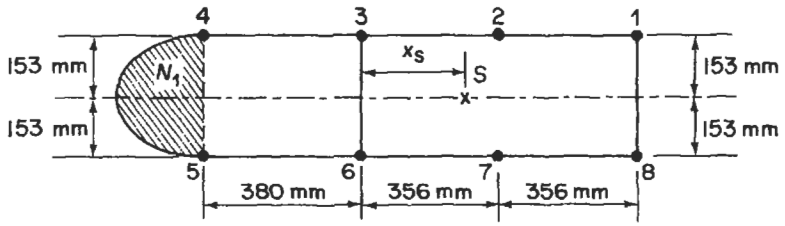

Fig. P.10.11

P.10.12 A singly symmetric wing section consists of two closed cells and one open cell (see Fig. P.10.12). The webs 25, 34 and the walls 12, 56 are straight, while all other walls are curved. All walls of the section are assumed to be effective in carrying shear stresses only, direct stresses being carried by booms 1 to 6. Calculate

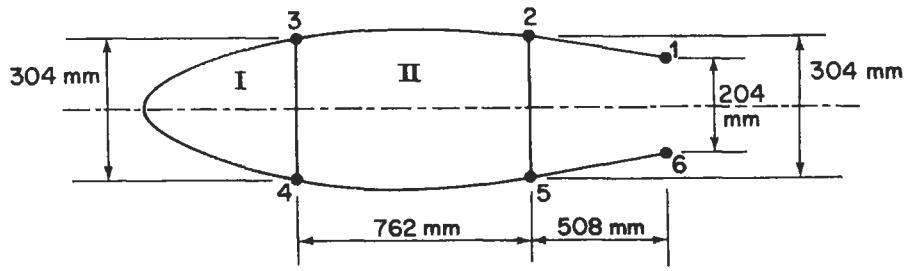

Fig. P.10.12

the distance x_S of the shear centre S aft of the web 34. The shear modulus G is the same for all walls.

Wall	Length (mm)	Thickness (mm)	Boom	Area (mm^2)	Cell	Area (mm^2)
12, 56	510	0.559	1, 6	645	I	93 000
23, 45	765	0.915	2, 5	1290	II	258 000
34^o	1015	0.559	3, 4	1935		
34^i	304	2.030				
25	304	1.625				

Ans. 241.4 mm.

P.10.13 A portion of a tapered, three-cell wing has singly symmetrical idealized cross-sections 1000 mm apart as shown in Fig. P.10.13. A bending moment $M_x = 1800$ N m and a shear load $S_y = 12\,000$ N in the plane of the web 52 are applied at the larger cross-section. Calculate the forces in the booms and the shear flow distribution at this cross-section. The modulus G is constant throughout. Section dimensions at the larger cross-section are given below.

Wall	Length (mm)	Thickness (mm)	Boom	Area (mm^2)	Cell	Area (mm^2)
12, 56	600	1.0	1, 6	600	I	100 000
23, 45	800	1.0	2, 5	800	II	260 000
34^o	1200	0.6	3, 4	800	III	180 000
34^i	320	2.0				
25	320	2.0				
16	210	1.5				

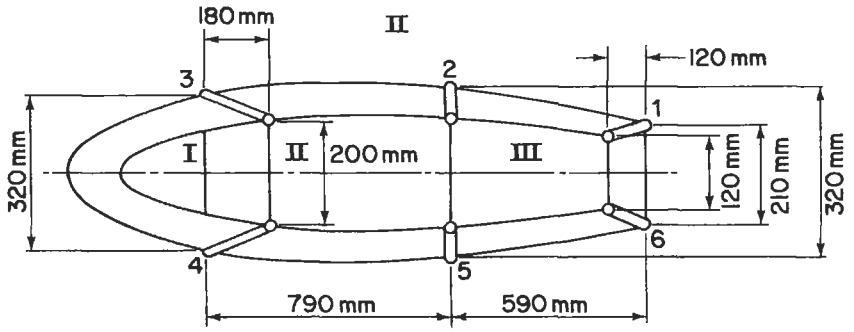

Fig. P.10.13

Ans. $P_1 = -P_6 = 1200\,\text{N}$, $P_2 = -P_5 = 2424\,\text{N}$, $P_3 = -P_4 = 2462\,\text{N}$,

$q_{12} = q_{56} = 3.74\,\text{N/mm}$, $q_{23} = q_{45} = 3.11\,\text{N/mm}$, $q_{34^o} = 0.06\,\text{N/mm}$,

$q_{43^i} = 12.16\,\text{N/mm}$, $q_{52} = 14.58\,\text{N/mm}$, $q_{61} = 11.22\,\text{N/mm}$

P.10.14 Solve P.10.8 using the method of successive approximations.

P.10.15 A multispar wing has the singly symmetrical cross-section shown in Fig. P.10.15 and carries a vertical shear load of 100 kN through its shear centre. If the booms resist all the direct stresses and the skin panels and spar webs are effective only in shear, determine the shear flow distribution in the section and the distance of the shear centre from the spar web 47. The shear modulus G is constant throughout and all booms have a cross-sectional area of $2000\,\text{mm}^2$.

Cell areas (mm^2):

	I	II	III	IV	V
	120 000	215 000	250 000	215 000	155 000
Wall	56°	45, 67	43, 78	32, 89	12, 910
Lengths (mm)	1500	605	603	605	605
Thickness (mm)	2.5	3.0	3.0	3.0	2.5

All spar webs have a thickness of 3.0 mm.

Ans. $q_{65^o} = 9.1\,\text{N/mm}$, $q_{65^i} = 54.6\,\text{N/mm}$, $q_{54} = q_{76} = 8.2\,\text{N/mm}$,

$q_{74} = 65.9\,\text{N/mm}$, $q_{43} = q_{87} = 0.1\,\text{N/mm}$, $q_{83} = 66.2\,\text{N/mm}$,

$q_{23} = q_{89} = 7.7\,\text{N/mm}$, $q_{92} = 57.3\,\text{N/mm}$,

$q_{12} = q_{9\,10} = q_{10\,1} = 5.9\,\text{N/mm}$

404.5 mm in cell III

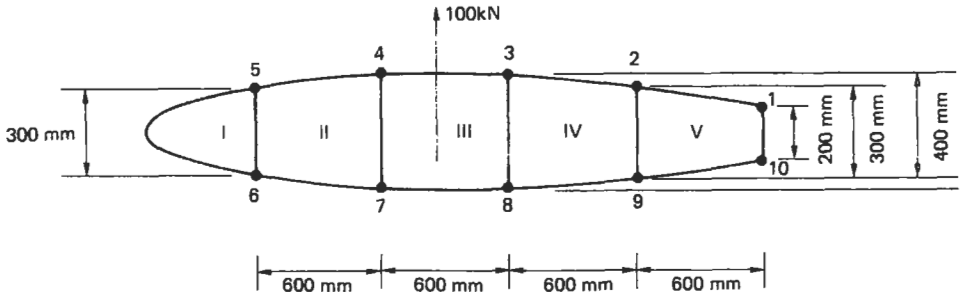

Fig. P.10.15

P.10.16 The beam shown in Fig. P.10.16 is simply supported at each end and carries a load of 6000 N. If all direct stresses are resisted by the flanges and stiffeners and the web panels are effective only in shear, calculate the distribution of axial load in the flange ABC and the stiffener BE and the shear flows in the panels.

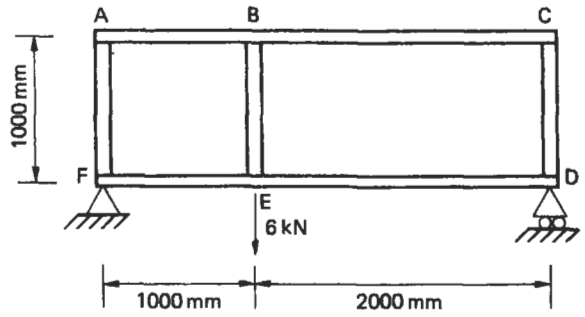

Fig. P.10.16

Ans. $q(\text{ABEF}) = 4\,\text{N/mm}$, $q(\text{BCDE}) = 2\,\text{N/mm}$.

P_{BE} increases linearly from zero at B to 6000 N (tension) at E

P_{AB} and P_{CB} increase linearly from zero at A and C to 4000 N (compression) at B

P.10.17 Calculate the shear flows in the web panels and direct load in the flanges and stiffeners of the beam shown in Fig. P.10.17 if the web panels resist shear stresses only.

Ans. $q_1 = 21.6\,\text{N/mm}$, $q_2 = -1.6\,\text{N/mm}$, $q_3 = 10\,\text{N/mm}$.

$P_C = 0$, $P_B = 6480\,\text{N}$ (tension), $P_A = 9480\,\text{N}$ (tension)

$P_F = 0$, $P_G = 480\,\text{N}$ (tension), $P_H = 2520\,\text{N}$ (compression)

P_E in BEG $= 2320\,\text{N}$ (compression), P_D in ED $= 6928\,\text{N}$ (tension)

P_D in CD $= 4320\,\text{N}$ (tension), P_D in DF $= 320\,\text{N}$ (tension)

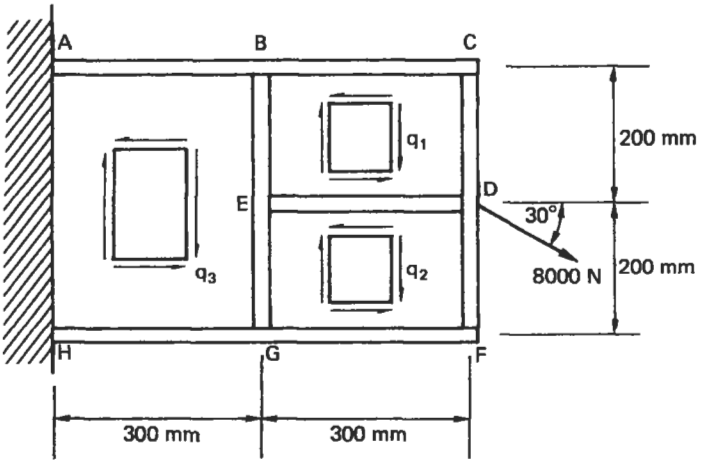

Fig. P.10.17

P.10.18 A three-flange wing section is stiffened by the wing rib shown in Fig. P.10.18. If the rib flanges and stiffeners carry all the direct loads while the rib panels are effective only in shear, calculate the shear flows in the panels and the direct loads in the rib flanges and stiffeners.

Ans. $q_1 = 4.0\,\text{N/mm}$, $q_2 = 26.0\,\text{N/mm}$, $q_3 = 6.0\,\text{N/mm}$.

P_2 in $12 = -P_3$ in $43 = 1200\,\text{N}$ (tension), P_5 in $154 = 2000\,\text{N}$ (tension),

P_3 in $263 = 8000\,\text{N}$ (compression), P_5 in $56 = 12\,000\,\text{N}$ (tension),

P_6 in $263 = 6000\,\text{N}$ (compression)

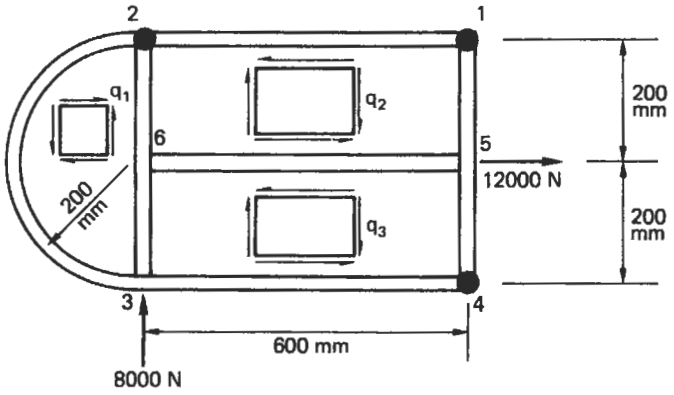

Fig. P.10.18

P.10.19 A portion of a wing box is built-in at one end and carries a shear load of 2000 N through its shear centre and a torque of 1000 N m as shown in Fig. P.10.19. If the skin panel in the upper surface of the inboard bay is removed, calculate the

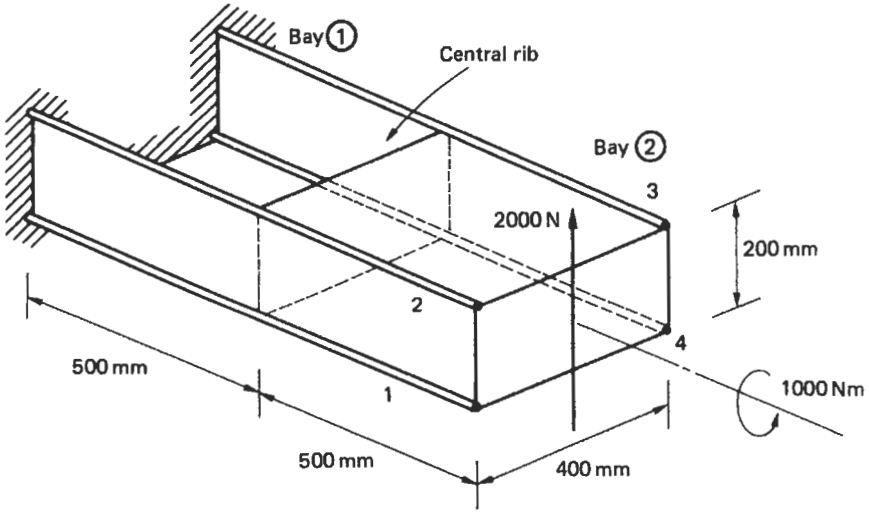

Fig. P.10.19

shear flows in the spar webs and remaining skin panels, the distribution of load in the spar flanges and the loading on the central rib. Assume that the spar webs and skin panels are effective in resisting shear stresses only.

Ans. Bay ①: q in spar webs = 7.5 N/mm

Bay ②: q in spar webs = 1.9 N/mm, in skin panels = 9.4 N/mm

Flange loads (2): at built-in end = 1875 N (compression)

at central rib = 5625 N (compression)

Rib loads: q (horizontal edges) = 9.4 N/mm,

q (vertical edges) = 9.4 N/mm

P.10.20 A bar, whose cross-section is shown in Fig. P.10.20, comprises a polyester matrix and Kevlar filaments; the respective moduli are 3000 N/mm^2 and 140 000 N/mm^2 with corresponding Poisson's ratios of 0.16 and 0.28. If the bar is 1 m long and is subjected to a compressive axial load of 500 kN, determine the shortening of the bar, the increase in its thickness and the stresses in the polyester and Kevlar.

Ans. 3.26 mm, 0.032 mm, 9.78 N/mm^2, 456.4 N/mm^2

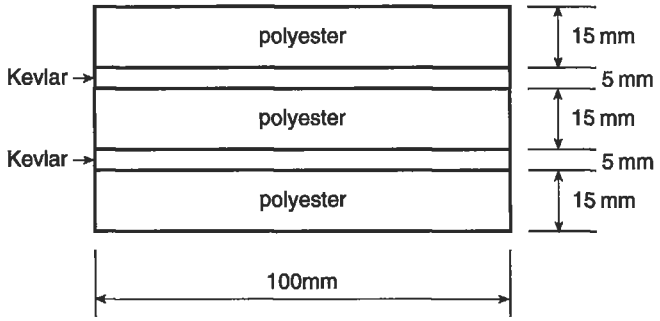

Fig. P.10.20.